92PC92104-TPR-8

ADVANCED THERMALLY STABLE JET FUELS

Technical Progress Report
April 1994 - June 1994

H.H. Schobert, S. Eser, C. Song, P.G. Hatcher, P.M. Walsh, M.M. Coleman

Contributions from:

R. Arumugan, J. Bortiatynski, D. Clifford, R. Dutta, K. Gergova, W.-C. Lai, J. Li, D. McKinney, M. Sobkowiak, J. Stallman, and J. Yu

July 1994

Prepared for U.S. Department of Energy
under
Contract No. DE-FG22-92PC92104

DISCLAIMER

Portions of this document may be illegible in electronic image products. Images are produced from the best available original document.

OBJECTIVES

The Penn State program in advanced thermally stable coal-based jet fuels has five objectives: 1) development of mechanisms of degradation and solids formation; 2) quantitative measurement of growth of sub-micrometer and micrometer-sized particles suspended in fuels during thermal stressing; 3) characterization of carbonaceous deposits by various instrumental and microscopic methods; 4) elucidation of the role of additives in retarding the formation of carbonaceous solids; and 5) assessment of the potential of production of high yields of cycloalkanes and hydroaromatics by direct liquefaction of coal.

SUMMARY

Significant progress has been made on the detection of polycyclic aromatic hydrocarbons present in highly stressed fuels, using high-performance liquid chromatography (HPLC) with diode-array detection. Gas chromatography is not able to detect compounds with ≥6 fused aromatic rings, but such compounds can be identified using the HPLC method. The concentration of such compounds is low in comparison to aromatics of 1–3 rings, but the role of the large compounds in the formation of solid deposits may be crucial in determining the thermal stability of a fuel.

The unusual properties of fluid fuels in the near-critical region appear to have significant effects on their thermal decomposition reactions. This issue has been investigated in the present reporting period using *n*-tetradecane as a model compound for fuel decomposition.

Temperature-programmed retention indices are very useful for gas chromatographic and gas chromatography/mass spectrometric analysis of coal- and petroleum-derived jet fuels. We have demonstrated this in the identification of components in two JP-8 fuels and their liquid chromatographic fractions. Over 100 fuel components were identified in detail.

The role of activated carbon surfaces as catalysts in the thermal stressing of jet fuel was investigated using *n*-dodecane and *n*-octane as model compounds. In some cases the reactions were spiked with addition of 5% decalin to test the ability of the carbon to catalyze the transformation of decalin to naphthalene.

We have previously shown that benzyl alcohol and 1,4-benzenedimethanol are effective stabilizers at temperatures ≥400°C for jet fuels and the model compound dodecane. The addition of ethanol to hydrocarbon/benzyl alcohol mixtures has a significant effect on the thermal stabilization of jet fuels above 400°C. Ethanol appears to function by reducing the benzaldehyde formed during the degradation of the benzyl alcohol. This reduction regenerates the benzyl alcohol. Thus in the presence of ethanol less benzyl alcohol is required for thermal stabilization of jet fuel.

We have clearly shown that cycloalkanes and hydroaromatics are desirable components of advanced jet fuels because of their high thermal stabilities. Therefore materials that are predominantly cycloparaffinic could be ideal potential feedstocks for advanced fuels. As part of the exploratory research in this area, we have examined the hydrogenation, dehydrogenation, and cracking of rosin, and the hydrocracking reactions of dammar.

Task 1. Investigation of the Quantitative Degradation Chemistry of Fuels

1. Detection of Polycyclic Aromatic Hydrocarbons Present in Highly Stressed Jet Fuel by High Performance Liquid Chromatography (HPLC) Using Normal-phase Separation with Diode Arraty Detection (Contributed by Daniel E. McKinney, David J. Clifford, Jacqueline M. Bortiatynski and Patrick G. Hatcher)

Introduction:

The future high-Mach aircraft requires advanced jet fuel with high stability in rigorous thermal environments (Song et al. 1993). To test a fuel's thermal stability, jet fuels are normally stressed at severe temperatures in closed reactor systems (Song et al. 1993) or flow reactors, and their subsequent complex liquids analyzed by either gas chromatography (GC), gas chromatography/mass spectrometry (GC/MS) or ^{1}H and ^{13}C liquids NMR to reveal structural changes that have taken place within the fuel (Song et al. 1993, McKinney et al. 1993). These analytical techniques can, to a certain point, provide valuable information on the relative stability of a given fuel and chemical transformations that occur within that fuel. However, the build-up of large polycyclic aromatic hydrocarbons (PAHs) in thermally stressed jet fuel leads to problems when it comes to GC and GC/MS analysis. Only PAHs with ≤6 fused rings are amenable to GC and GC/MS analysis. Therefore, a percentage of highly stressed jet fuel in the form of large PAHs may go undetected using GC analysis; a percentage that may be significant to the onset of solid deposit formations which are detrimental to the fuel's overall performance.

Since its introduction as an analytical method in the late 1960's and early 1970's, high performance liquid chromatography (HPLC) has become widely used in environmental studies, especially for the analysis of PAHs (Wise et al., 1993; Fetzer and Biggs, 1993). PAHs are widespread environmental contaminants and much effort has been devoted to the development of liquid chromatographic columns which are sensitive to PAH separation. Schmit *et al.* (1971) first described the separation of PAHs by liquid chromatography using a reverse-phase column consisting of a chemically bonded C_{18} stationary phase. Since then, reverse-phase HPLC on chemically bonded C_{18} has become the method of choice for the separation of PAHs (Bartle et al., 1981; Wise, 1983; Wise, 1985; Fetzer, 1989), and a review by Wise *et al.* (1993) has described general protocols for the separation of PAHs using reverse-phase HPLC. These general procedures have been applied to studies of PAHs in a variety of fuel-related materials including coal tar mixtures (Wise et al., 1988), petroleum (Boduszynski, 1988; Sullivan et al. 1989; Packham and Fielden, 1991; Hsu and Qian, 1993), shale oil (Hertz et al. 1980), lubricating oils (Palmentier et al. 1989) and crude oils (Akhlaq 1993). However, in many of these studies, direct

analysis of PAHs in fuels using reverse-phase HPLC is complicated as sample preparations have become elaborate, due in large part to the fact that most complex fuel-related materials contain compounds that are not usually miscible in acetonitrile, the solvent of choice for reverse-phase HPLC separations of PAHs. These materials routinely are fractionated first into general compound class categories (Akhlaq, 1993) (*i.e.* aliphatics, polar compounds, aromatics, resins, and asphaltenes) before separation of PAHs can be performed, and usually normal-phase HPLC is relegated to general cleanup and isolation of the total PAH fraction.

Another problem associated with HPLC analysis of complex fuel mixtures and other extracts of natural samples is that, in the past, normal-phase and reverse-phase HPLC have depended upon either fluorescence detection or monochromatic UV absorbance detection. Fetzer and Biggs (1993) have pointed out that these detection methods are too selective and many compounds go unobserved due to varying optimal wavelengths for different compounds. Recent developments in the last fifteen years of a full spectrum UV absorbance detector (*i.e.* diode array detector or DAD) enable full spectrum detection of HPLC eluates. A distinct advantage of the diode array HPLC technique, which provides UV spectra of separated fractions as a function of time, is its ability to identify, by spectral comparisons, the molecular components of the eluates, including the isomers of PAHs. In a previous study of decant-oils (acetonitrile-soluble, highly aromatic bottoms from fluid catalytic cracking of petroleum feed stocks), using the diode array detection with reverse-phase HPLC, distinctions were made between phenanthrene and anthracene, pyrene and fluoranthene, and their substituted homologues (Liu et al. 1992). PAH's with more than five condensed rings were also separated by HPLC.

The reverse-phase HPLC technique, however, is not applicable to more complex fuel mixtures such as highly stressed jet fuel, because these are only sparingly soluble in polar solvents required for reverse-phase HPLC. In a recent report by Clifford *et al.* (1993), samples of coal liquefaction process streams, known to contain large amounts of PAHs, were analyzed using normal-phase separation with diode array detection. PAHs consisting of two-to nine rings, along with their corresponding isomers and alkylated derivatives, were separated and quantified using this method. Clear differences were observed among liquefaction process streams due, in large part, to differences in feed coals and process conditions. The development of "charge-transfer" stationary phases for separation of π-electron rich PAHs (Nondek and Malek, 1978; Holstein, 1981; Grizzle and Thomson, 1982) allows for the separation of PAHs and their isomers in the normal-phase using solvents which are generally miscible with complex fossil fuel systems. In this section, we demonstrate a more sensitive method for detection of the build-up of large ring PAHs which can lead to the onset of solid deposit formations inherent to severe stressing of jet fuel. This is accomplished by the normal-phase separation of PAHs and their alkylated derivatives, present in highly stressed jet fuel, using a tetrachlorophthalimidopropyl (TCPP)-modified silica column

(Hypersil Green PAH-2) (Holstein, 1981). This column, in combination with UV-diode array detector, allows for a more sensitive detection of large PAHs (compared to normal GC and GC/MS analysis) and efficient separation of multi-ring PAHs and their isomers without elaborate sample preparations or on-line coupling of a reverse-phase HPLC system.

Experimental:

The dilute stressed jet fuel samples were analyzed and separated using a Waters 600E HPLC and Waters 991 photodiode array detector. The column used for HPLC separations was a Hypersil Green PAH-2 column purchased from Keystone Scientific, Inc.(Bellefonte, PA).

Samples for this study were prepared from an essentially additive-free Jet A fuel supplied by the Air Force/ WRDC Aero Propulsion Laboratory (No. 90-POSF-2747).

Pyrolyses were performed in 25 mL tubing bomb reactors at 450°C for heating periods of 0-12 hours under an initial pressure of 100 psi of air. The details of the tubing bomb reactors were described elsewhere (Song et al. 1993) The reactor was loaded with 10 mL of sample and pressure tested for leaks with 1000 psi of N_2. To provide an inert pyrolysis environment and minimize oxidation reactions, the sealed reactor was purged (5 times) with 1000 psi of N_2 to remove oxygen/air dissolved in the sample. After the desired reaction time, the bomb was removed from the sand bath and quenched in a cool water bath. The liquid products were collected and diluted approximately 5:1 in methylene chloride.

The mixtures are then filtered through 0.2 μm filters (Supelco brand ISO-DISC N-32 3mm diameter, nylon membrane, 0.2 μm pore size filters) in order to remove any insoluble material. The column, equilibrated with 100% hexane, was operated in the gradient elution mode. Samples are injected onto the PAH-2 column, and following an initial 10 minute isocratic period, a linear gradient from 100% hexane to 100% dichloromethane is used up to 80 minutes followed by a final hold for 5 minutes.

Results and Discussion:

The column used in this study is capable of separating polynuclear aromatic hydrocarbons due to the inherent capabilities of the bonded phase. TCPP-modified silica (Structure I) belongs to the family of π-acidic phases which separate π-electron-rich PAHs and have been used for some time (Lochmuller, 1980). Holstein (1981) developed the TCPP-modified silica and determined capacity ratios for up to sixty different PAHs including heteroaromatics and also demonstrated its usefulness on coal liquids and other aromatic mixtures. Even recently, Herren *et al.* (1993) have reported the use of TCPP-modified silica in the separation of higher fullerenes. This stationary phase reacts strongly with electron-rich species by a mechanism which involves the delocalization

of electrons between the support material and the analyte. The analyte and support material form a reversible complex by electron

Structure I

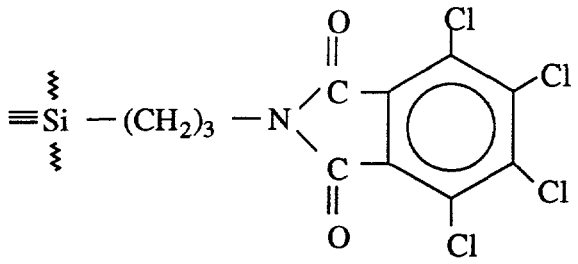

tetrachlorophthalimidopropyl bonded to silica

transfer, which results from a p-p interaction mechanism inherent in polynuclear aromatic species. The extent to which this donor (analyte) and acceptor (bonded phase) form a complex is dictated by solvent polarity. Retention times decrease as the polarity of the mobile phase increases.

The chromatogram at maximum UV absorbance for a standard mix of PAHs is shown in Figure 1. Co-elution of several PAHs is obvious, but it demonstrates the use of the TCPP-modified silica phase in separating PAHs. Identification of the elution order of PAHs is described in a previous report (Clifford et al. 1993). The use of a maximum absorbance plot (maxiplot) is an ideal method of insuring that the peak intensities in the 1-D plot are at maximum UV absorbance and, therefore, at maximum intensity.

Knowing that highly stressed jet fuel contains numerous amounts of polynuclear aromatic hydrocarbons and that the PAH-2 column successfully separated PAHs in a known standard, we had reason to be optimistic about its use for stressed jet fuel samples. Figure 2 shows a max-plot of the three samples analyzed by 2-D HPLC (0 hrs., 6 hrs., and 12 hrs.). From these chromatograms, it is obvious that as the stressing time at 450°C is increased, the fuel is being degraded and an increase of PAHs is being observed. Figure 3, a 254 nm cut across the UV absorbance region, identifies the number of fused aromatic rings present in Jet A stressed at 450°C for 12 hrs. and a general map of where these ring numbers would fall in the chromatogram.

With the use of the UV-diode array detector, contour plots and 3-D plots could be obtained for each sample which enhance significantly the ability of the user to detect and identify components that may not be well separated at one specific wavelength. The added dimension for the display of HPLC data provides an additional perspective which aids in the identification of compounds that might otherwise go undetected. For example, Figures 4 and 5 show two different wavelength cuts across the UV absorbance range which tend to highlight specific regions of the

chromatogram. The 335 nm cut (Figure 4) highlights pyrene derivatives and their alkylated isomers and minimizes any interferences from other compounds. After 6 hrs., it is obvious that a significant amount of pyrene and alkylated pyrenes is present and that their relative concentrations change very little between 6 and 12 hours. The 375 nm cut (Figure 5) highlights the increase in the concentration of PAHs greater than six rings; PAH build-ups that would otherwise go undetected by normal GC analyses. There is an overall increase in the relative concentrations of large fused ring PAHs from time 0, where there are no large PAH systems, to 12 hrs., where there is a complex hump of unresolved material representing large PAH systems.
Fetzer, J. C., Biggs, W. R., *J. Chromatogr.*, **1993**, 642, 319.

Conclusions:

In general, as the time of the stressing grows, so does the complexity of the chromatograms. This indicates that a build-up of large PAHs is taking place, which is to be expected, and that solid deposit formations should also be increasing. These results could have been determined by GC and GC/MS analyses or just by physical observations. However, GC analyses would not have detected the ≥6 ring systems which can be identified using the 2-D HPLC method. Granted the concentrations of these larger ring systems is low in comparison to the 1-3 ring PAHs (Figure 3), but their significance to the formation of solid deposits during the stressing reactions may be crucial in the determination of a fuel's ability to remain stabile at high temperatures.

References:

1. Akhlaq, M. S., *J. Chromatogr.*, **1993**, 644, 253.

2. Bartle, K. D., Lee, M.L., Wise, S. A., *Chem. Soc. Rev.*, **1981**, 10, 113.

3. Boduszynski, M. M., *Energy & Fuels*, **1988**, 2, 597.

4. Clifford, D. J., McKinney, D. E., Hou, L., Hatcher, P. G., "High Performance Liquid Chromatography (HPLC) of Coal Liquefaction Process Streams Using Normal-phase Separation with UV Diode Array Detection"; Final Report, October 1993, DE-AC22-89PC89883, The Pennsylvania State University.

5. Fetzer, J. C., *Chemical Analysis of Polycyclic Aromatic Compounds*, Wiley, New York, **1989**, Ch. 5, p. 59.

6. Grizzle, P.L. and Thomson, J.S., *Anal. Letters*, **1987**, 20(8), 1171-1192.

7. Herren, D., Thilgen, C., Calzaferri, G., Diederich, F., *J. Chromatogr.*, **1993**, 644, 188.

8. Hertz, H. S., Brown, J. M., Chesler, S. N., Guenther, F. R., Hilpert, L. R., May, W. E., Parris, R. M., Wise, S. A., *Anal. Chem.*, **1980**, 52, 1650.

9. Holstein, W., *Chromatographia*, **1981**, 14, 468-477.

10. Hsu, C. S., Qian, K., *Energy & Fuels*, **1993**, 7, 268.

11. Liu, Y., Eser, S., Hatcher, P. G., *Prepr. Pap. - Am. Chem. Soc., Div. Fuel Chem.* **1992**, 37(3), 1227.

12. Lochmuller, C. H., in D. E. Leyden and W. Collins (Editors), *Silylated Surfaces*, Gordon and Breach, New York, **1980**, 231.

13. McKinney, D.E., Bortiatynski, J.M. and Hatcher, P.G., *Energy & Fuels*, **1993**, 7, 578-581.

14. Packham, A. J., Fielden, P. R., *J. Chromatogr.*, **1991**, 552, 575.

15. Palmentier, J.-P. F., Britten, A. J., Charbonneau, G. M., Karasek, F. W., *J. Chromatogr.*, **1989**, 469, 241.

16. Song, C., Eser, S., Schobert, H.H., and Hatcher, P.G., *Enerry & Fuels*, **1993**, 7, 234-243.

17. Schmit, J. A., Henry, R. A., Williams, R. C., Dieckman, J. F., *J. Chromatogr.*, **1971**, 9, 645.

18. Sullivan, R. F., Boduszynski, M. M., Fetzer, J. C., *Energy & Fuels*, **1989**, 3, 603.

19. Wise, S. A., Sander, L. C., May, W. E., *J. Chromatogr.*, **1993**, 642, 329.

20. Wise, S. A., Benner, B. A., Byrd, G. D., Chesler, S. N., Rebbert, R. E., Schantz, M. M., *Anal. Chem.*, **1988**, 60, 887.

21. Wise, S. A., *Handbook of Polycyclic Aromatic Hydrocarbons - Emission Sources and Recent Progress in Analytical Chemistry*, Vol. II, Marcel Dekker, New York, **1985**, Ch. 5, p. 113.

22. Wise, S. A., *Handbook of Polycyclic Aromatic Hydrocarbons*, vol. I, Marcel Dekker, New York, **1983**, Ch. 5, p. 183.

2. Temperature-Programmed Retention Indices for GC and GC-MS Analysis of Coal- and Petroleum-Derived Jet Fuels (Contributed by Wei-Chuan Lai and Chunshan Song)

Abstract

Retention indices are very useful in identifying components in jet fuels by gas chromatography (GC), even when GC is coupled with mass spectrometry (GC-MS). In this work, temperature-programmed retention indices of over 150 compounds were determined on an intermediately polar capillary column coated with 50% phenyl-50% methyl polysiloxane (Restek

Rtx-50) and a slightly polar column coated with 5% phenyl-95% methyl polysiloxane (J&W DB-5) at three heating rates (2, 4, and 6°C/min from 40 to 310°C). Aliphatic compounds give nearly constant indices at different heating rates. However, the retention indices of polycyclic aromatic compounds exhibit relatively large temperature dependence. The use of a short isothermal holding (5 min) prior to the programmed heat-up did not cause any significant difference in the retention indices. The column polarity can affect the retention indices significantly, depending on the compound type. The differences between the retention indices on the two columns are relatively small with aliphatic compounds but become larger with polycyclic and polar compounds. In general, retention indices as well as their sensitivity to temperature program decrease with decreasing column polarity. The usefulness of the temperature-programmed retention indices was also demonstrated in the analysis of jet fuels. Combined use of retention indices and mass spectra allows identification of many more compounds with higher confidence in petroleum- and coal-derived JP-8 jet fuels. The knowledge of the effects of temperature and column polarity can be applied for selecting appropriate column and temperature program for separation and reliable identification of compounds in given samples. In addition, the present results can be used in combination with a mass spectral library to accomplish faster and more reliable compound identification.

Introduction

Modern gas chromatography-mass spectrometry (GC-MS) has contributed greatly to analysis of various mixtures of organic compounds. However, many compounds in coal- and petroleum-derived fuels are difficult to identify just by mass spectra alone. A common phenomenon in GC-MS of fuels is that two or more GC peaks have very similar or even identical mass spectra, although they have different retention times and different chemical nature. Examples of such compounds are the isomers of some cycloalkanes; the isomers of substituted aromatics such as trimethylbenzenes (MW: 120), methylnaphthalenes (MW: 142) and dimethylnaphthalenes (MW: 156); different polyaromatics with same molecular weight but different ring structures, such as biphenyl and acenaphthene (MW: 154), and phenanthrene and anthracene (MW: 178); partially hydrogenated aromatics such as sym-octahydrophenanthrene and sym-octahydroanthracene (MW: 186). Thus using GC-MS for compound identification often requires the assistance or confirmation of GC retention time. On the other hand, in many cases highly reliable identification can not be made by using retention times alone. This is because co-elution of two or more different compounds is possible under given conditions, and whether this occurs can not be determined by GC alone for unknown samples. For these reasons, the retention times and mass spectra are complementary to each other. The combined use of retention index and mass spectra can allow the identifications of individual compounds in complex mixtures to be made with high confidence.

The present work is concerned with retention index for temperature-programmed GC and GC-MS analysis of jet fuels. The sources of the future hydrocarbon jet fuels may include petroleum, coal, and other fossil resources.[1-5] The future high-performance aircraft requires advanced thermally stable jet fuels.[6-10] Clarifying the hydrocarbon components in conventional and alternate jet fuels and identifying the thermally stable and unstable compounds are considered to be key steps in developing advanced jet fuels with high thermal stability and high density for future high-performance aircraft.[11-15] The need to characterize coal- and petroleum-derived jet fuels stems from the lack of knowledge on their molecular composition and the desire to establish the relationship between their composition/structure and thermal stability at high temperatures. Hayes and Pitzer[16,17], and Steward and Pitzer[18] have analyzed several petroleum- and shale-derived JP-4 jet fuels using capillary gas chromatography. These fuels are deceptively simple in appearance but are actually mixtures of hundreds of hydrocarbons. They indicated that, even for petroleum-derived jet fuels, the detailed hydrocarbon distribution is far too complicated to be unraveled by even the most efficient capillary column.[16] The coal-derived fuels are more complex than petroleum-derived fuels.[15] There is little published information on the detailed characterization of coal-derived jet fuels.

A common practice of qualitative GC analysis is the use of retention time. However, it is well known that retention time depends on several factors, *e.g.*, temperature and flow rate. Thus retention time itself is not an ideal parameter for identification purposes, especially for complex samples such as jet fuels; parameters that are less dependent on these factors are needed. A useful parameter is the relative retention time instead of the absolute retention time. Retention index[19,20] system is a measure of relative retention times referenced to a homologous series of organic compounds, and is one of the successful parameters used for identification purposes.[16-18,21-25] Hayes and Pitzer[16,17] have demonstrated the usefulness of determining retention indices for identifying compounds in complex mixtures. Though many GC and GC-MS analyses are carried out under isothermal conditions, temperature programming[26] is known to improve separating complex mixtures such as jet fuels whose components have widely varying vapor pressures.

Kováts index relates (interpolates) the retention time of an unknown compound to that of reference standards eluting before and after it under isothermal conditions. Any homologous series of organic compounds (for example, *n*-alkanes) can be used as the retention index reference standards. Each of the standards is assigned an index I, for example, I = 100n for a given alkane with a carbon number n. The retention index of any unknown compound is then calculated by logarithmic interpolation between the two relevant standards according to the following relationship *under isothermal conditions*

$$I_u = 100 \left[\frac{\log (t_u) - \log (t_n)}{\log (t_{n+1}) - \log (t_n)} + n \right] \quad (1)$$

where n and n+1 are the carbon numbers of the bracketing n-hydrocarbons, t_u is the absolute retention time of the unknown under isothermal conditions, t_n and t_{n+1} are the absolute retention times of the *n*-hydrocarbons, eluted just prior to and just after the unknown respectively under isothermal conditions. However, in contrast to the logarithmetric relationship under isothermal conditions, a quasi-linear relationship exists for a non-isothermal GC analysis with a linear temperature program, as shown by Van den Dool and Kratz.[27]

The present work aimed at establishing retention indices for temperature-programmed GC and GC-MS analysis on two different capillary columns at three programmed heating rates for over 150 compounds that are components of coal and petroleum-derived jet fuels. The effects of heating rate, temperature program, and polarity of the stationary phase on the retention indices as well as the relative elution order were studied. The temperature dependence and the column polarity dependence of retention indices have been examined for different compound classes. The data presented are temperature-programmed retention indices of 1-alkenes, *n*-alkanes, alkylcyclohexanes, alkylbenzenes, polycyclic aromatics, partially hydrogenated polycyclic aromatics, and N-, S-, and O-containing compounds. Also presented in this section are the retention indices on many compounds that were not used in previous studies but are generally found in coal-derived jet fuels. The usefulness of using temperature-programmed retention indices for GC and GC-MS analysis was demonstrated in the detailed identification of components in two JP-8 jet fuels including a petroleum-derived JP-8P and a coal-derived JP-8C. The results reported here are believed to be useful to researchers in the field of chromatographic analysis of jet fuels.

Experimental

1. Reagents and fuels. Reagent grade chemicals from Aldrich, Supelco, K&K Laboratories, TCI America, and Fisher Scientific were used for the determination of retention indices. Over 150 pure compounds were examined, covering aliphatic, olefinic, aromatic, and polycyclic aromatic hydrocarbons and O-, N-, and S-containing compounds that are related to coal- and petroleum-derived jet fuels. The jet fuel samples used in this work were two JP-8 fuels supplied by the Air Force Wright Laboratory/Aero Propulsion and Power Directorate. The coal-derived fuel, JP-8C, was produced by hydrotreating of tar liquids produced from the Great Plains Gasification plant.[14,28] The petroleum-derived JP-8P is a conventional military jet fuel, whose properties are usually selected to be identical to those of commercial jet fuel Jet A-1.[29] The JP-8C fuel is a blend of hydrotreated and hydrocracked stocks.[14] The chromatographic fractions of JP-8P and JP-8C

fuels were obtained using neutral alumina column and a series of elution solvents, as described elsewhere.[15]

2. Retention index. Standard mixtures of reagent grade chemicals were prepared for the determination of retention indices. The standard mixtures were analyzed on a Hewlett-Packard 5890 Series II GC coupled with HP 5971A Mass Selective Detector (MSD). The columns used were 30 m, 0.25 mm i.d., 0.25 μm film thickness, fused silica capillary columns (intermediately polar Restek Rtx-50 column coated with 50% phenyl - 50% methyl polysiloxane; slightly polar J&W DB-5 column coated with 5% phenyl - 95% methyl polysiloxane). The column temperature was programmed linearly from 40°C to 310°C at three heating rates (2, 4, and 6°C/min), unless otherwise mentioned. Index values calculated from three different heating rates can be used as cross-references to known materials and aid in identifying unknown compounds. Other chromatographic operating conditions are as follows: detector temperature, 280°C; injector temperature, 280°C; average linear velocity of carrier gas (helium) through the column, 33 cm/sec; septum purge flow rate, 13 ml/min; volumetric column flow rate, 0.98 ml/min. The capillary column's sample capacity was also taken into consideration to avoid non-Gaussian peaks (tailing or fronting), which shift slightly in retention time. Symmetric (Gaussian) peaks were obtained by injecting appropriate amount (0.01 μL) standards under split mode (split ratio at 66); the amount of each standard compound entering the column was kept in the range of 1-10 ng/component.

The temperature-programmed retention indices of over 150 compounds were determined at three heating rates using the equation established by Van den Dool and Kratz[27]. They have shown that the retention indices for a linear temperature programmed GC can be calculated by the following quasi-linear relationship:

$$I_u = 100 \left[\frac{t_u - t_n}{t_{n+1} - t_n} + n \right] \qquad (2)$$

where the absolute retention times of the compounds are determined under conditions of *linear temperature programming*.

Results and Discussion

of naphthalene calculated by interpolating between non-neighboring alkanes (*n*-tridecane and *n*-pentadecane) are 1388.2, 1403.3, and 1413.4, respectively, at 2, 4, and 6°C/min; these are comparable with those calculated from neighboring *n*-alkanes: 1386.8, 1401.2, and 1410.9.

Table 1 presents the retention indices determined using two columns at three heating rates (2, 4, and 6°C/min) for 154 compounds generally found in coal- and petroleum-derived jet fuels. For calculation of indices shown in Table 1, neighboring *n*-alkanes were used as the reference

standards (fixed points) for more accurate results. The compounds are arranged in increasing order of indices at the heating rate of 2°C/min on the Rtx-50 column. The values reported are the averages of 2-5 replicates. The retention times were reproducible to within about ±0.01 min and ±0.02 min for low- and high-boiling compounds, respectively. In general, the experimental error for the retention indices is of the order of 2 index units (i.u.). However, it is slightly larger for those low-boiling compounds eluted before *n*-octane; this can be rationalized from Equation 2 that due to the shorter retention times of these compounds a small difference in retention times can cause a larger error in the index calculation.

1. Temperature dependence. Several features can be seen from Table 1 regarding the dependence of retention indices on the column temperature experienced. First, the small temperature dependence of compounds that are analogous to the reference standards, such as branched alkanes and 1-alkenes, reflects one of the excellent characteristics of the retention index system. Table 2 gives the experimental results of retention indices and final elution temperatures for 1-alkenes (ranging from 1-hexene to 1-octadecene) at the three heating rates on the Rtx-50 column. The difference in index values at different elution temperatures is less than ±1 index unit (i.u.), which is within the experimental error (of the order of 2 index units). These data demonstrate the temperature-independent nature of the indices for these compounds (Table 2) even for a 30°C range (*e.g.*, 157.9-187.8°C for 1-octadecene, Table 1).

Second, the other compounds do show measurable linear temperature dependence as shown in Figure 7, which presents the retention index of several representative compounds as a function of elution temperature. The numerical results of the linear temperature dependence for cycloalkanes and benzenes are given in Table 3 for both Rtx-50 and DB-5 columns. The second column in Table 3 denotes the elution temperature range, which indicates the lowest (corresponding to at 2°C/min) and the highest (corresponding to at 6°C/min) elution temperatures for intermediately polar Rtx-50 column. The third column gives the corresponding indices at the lowest and the highest elution temperatures. The ΔR.I./ΔT ratios in Table 3 indicates the index change per 1°C, *i.e.*, the average temperature coefficient of retention indices. Columns 5-7 in Table 3 show the data on the slightly polar DB-5 column. In the same fashion, Table 4 presents the numerical results of the linear temperature dependence for aromatics and NSO (N-, S-, and O-containing) compounds. Take the data on Rtx-50 as an example, it can be seen that in general, alkylated cyclohexanes and benzenes displayed a ΔR.I./ΔT of about 0.33±0.05 index units/°C while benzenes with multi-substitution (such as tetramethyl-) and long side-chains (decyl- and dodecyl-) exhibit slightly higher values (ca. 0.46). Compared with alkylated cyclohexanes and benzenes, the indices for compounds with two-ring structure exhibit higher temperature dependence. For example, indan, 1- and 2-methylindan, bicyclopentyl, and trans-decalin all have values about 0.49; 4- and 5-methylindan, cis-decalin, and bicyclohexyls show even higher index temperature

dependence (ca. 0.60). Multi-ring aromatics exhibit the largest temperature dependence of the retention index among the studied compounds. The 16 alkylated (C_1~C_3) naphthalenes and 6 biphenyls in Table 4 show an average ΔR.I./ΔT of 0.94 and 0.86, respectively, with a standard deviation of about 0.08. The values for three-ring aromatics in general range from 1.20 to 1.65. Four-ring aromatics all display significant temperature dependence judging from the large values of ΔR.I./ΔT (larger than 2.0); chrysene shows a value as large as 2.88. The ΔR.I./ΔT ratios in Table 3 are quite useful in that they may be easily used to estimate the retention indices of these compounds over the studied temperature range by interpolation. On the other hand, the large temperature dependence of indices for multi-ring aromatics implies that using the ΔR.I./ΔT ratios in Table 4 to estimate their retention indices over the studied temperature range by interpolation will be less accurate. As to the NSO compounds, they in general show larger retention indices and exhibit slightly greater temperature dependence (ΔR.I./ΔT) than their corresponding hydrocarbons.

Third, an important consequence of the observed difference in the different temperature dependence (ΔR.I./ΔT) among the compounds is that compounds which co-eluted at one temperature may be separated at some other temperature(s). This means that co-elution problems occurred when using a given heating rate may be solved by using a different heating rate. For example, 1-alkenes which co-eluted with some compounds at the heating rates of 2°C/min can be easily separated from their respective co-eluting compounds at 6°C/min, *e.g.*, 1-decene and 1,2-dimethylbenzene; 1-undecene and sec-butylbenzene; 1-dodecene and 2-methylindan; 1-hexadecene and 2,7-dimethylnaphthalene. Some other examples, which can be found in Table 1, include 2-methylbiphenyl and 1-ethylnaphthalene; 1,2-dimethylnaphthalene and *n*-decylcyclohexane; acenaphthene and 1,2-diphenylethane; 9,10-dihydroanthracene and dodecylbenzene; pyrene and 9,10-dimethylanthracene.

Although the retention indices in Table 1 were measured under linear temperature programming *without* isothermal initial holding period, the results may also be applied to GC analysis *with* a short initial holding time. Table 5 presents the retention times and retention indices measured *with* 5 minutes of initial isothermal holding time at 40 °C as well as those *without* initial holding time for 60 representative (out of 154 in Table 1) compounds. The data were collected using the heating rate of 4 °C/min on the DB-5 column. The retention indices with 5-minute holding time were also approximated by Equation 2. It was found that adding a 5-minute holding time at low temperature (40 °C) has only small effects on retention indices although the retention times may differ by as many as 5 minutes. It was apparent from Table 5 that adding initial holding time only serves to delay the elution of heavier compounds which have retention indices greater than 1400 by as much time as added, for example, 5 minutes in this study. For the 154 compounds studied, the retention index was lowered, on average, by about 1 index unit when 5 minutes of holding time was added at the beginning temperature; the retention index decrement for

heavier compounds is in general negligible. Therefore, the temperature-programmed retention indices in Table 1 may also be applied with minor adjustment to the analysis which incorporates a short initial holding time.

2. Column polarity dependence. Retention indices exhibit significant dependence on column polarity as shown in Table 1. There are several characteristics to be pointed out. First, Table 1 shows that the retention indices of all the compounds studied decrease as the column polarity decreases (from Rtx-50 to DB-5). Similar to temperature dependence, the decrement of the retention indices depends on the structure of the compounds. For example, Figure 8 displays the retention index difference between Rtx-50 column and DB-5 column (Δ_{pol}R.I.) for 20 representative compounds. The retention index difference ranges from as small as 20 to over 600. Compared with other compounds, 1-alkenes, which are analogous to the reference standards (*n*-alkanes in this work), display the smallest polarity dependence. Δ_{pol}R.I. is about 20±2 for 1-alkenes ranging from 1-hexene to 1-octadecene. Alkylcyclohexanes (from methylcyclohexane to *n*-decylcyclohexane) also show small polarity dependence; Δ_{pol}R.I. is about 36±6. On the other hand, the retention indices of alkylbenzenes, aromatics, and N-, S-, and O-containing compounds are highly dependent on the column polarity. Multi-ring aromatics exhibit the largest polarity dependence of the retention index among the studied compounds. It is worth noting that the more polar column (Rtx-50) retains more polar compounds longer than less polar isomer compounds and results in larger Δ_{pol}R.I. This can be demonstrated by 2,6-dimethylnaphthalene and 1,8-dimethylnaphthalene; the latter is more polar and display larger Δ_{pol}R.I. than the former. Overall, the behavior of the polarity dependence of retention index can be summarized by the facts that the retention of polar compounds decreases, but that of non-polar compounds such as *n*-alkanes increases, when the polarity of stationary phase decreases.

Second, the change or shift of compound elution order on different columns can be observed owing to the fact that different compounds display different degrees of retention index changes with column polarity. For example, the effects of column polarity on the elution order of compounds are very evident by comparing 1-alkenes and *n*-alkanes. 1-Alkene, which eluted after the *n*-alkane with the same carbon number on Rtx-50 column, eluted before *n*-alkane on DB-5 column. More examples of the shift in elution order can be easily found in Table 1. Based on the knowledge on the shift in compound elution order, compound identification can be improved by using columns of different polarity. Another application of the knowledge on the retention indices is that they can facilitate the choice of column phase to reduce or even eliminate co-elution within complex samples.

Third, for the two capillary columns studied, in general the values of ΔR.I./ΔT are larger for Rtx-50 than for DB-5; i.e., almost all the compounds studied display higher temperature sensitivity

on the more polar column (Rtx-50) than on the less polar column (DB-5), as can be seen from Tables 3 and 4.

3. Characterization of JP-8 jet fuels. Retention indices determined in this work can be directly used in identifying compounds in complex mixtures such as jet fuels. In many cases, the unknown compounds may be identified by calculating their retention indices and comparing with standards shown in Table 1, if the match is within ± 2 index units for a given heating rate. The choice of 2 index units is based on and close to the experimental error for the retention indices. In fact, coal-derived JP-8C fuel was analyzed by GC under the same flow conditions as those for the standard compounds, and two heating rates (4 and 6 °C/min) were used for the purpose of cross references. The capillary column's sample capacity was again taken into consideration and symmetric GC peaks were obtained. Figure 9 presents the GC-MS total ion chromatogram (TIC) of coal-derived JP-8C fuel on Rtx-50 column, together with the structures of major components. Besides the *n*-alkane components, more than 50 representative compounds present in JP-8C were identified by matching retention indices, as shown in Table 6. The first column in Table 6 denotes the representative compounds identified. The second and third columns display the retention indices (at 4°C/min) of known standard compounds (denoted Std) and those of the JP-8C, respectively. Similarly, the data under 6°C/min are given in the last two columns. The reported data are the mean indices of three replicates. The deviations between $R.I._{Std}$ and $R.I._{JP\text{-}8C}$ in Table 6 are less than 1 index unit, which is within the experimental error for the retention indices (of the order of 2 index units). We also analyzed the petroleum-derived JP-8P fuel in a similar fashion. Figure 5 shows the GC-MS TIC of petroleum-derived JP-8P fuel on Rtx-50 column, together with the structures of major components.

The GC-MS analysis of the whole jet fuel also reveals that many compounds are present in trace amounts or co-eluted with other compounds, making them difficult to be identified from analyzing the whole fuels. Another approach used in this work is to separate the jet fuels into chemically similar compound classes by liquid column chromatographic separation, which also serves to concentrate the compounds present in whole fuels in very low concentrations and to eliminate (or reduce) the co-elution of different compounds from capillary GC column, followed by the GC-MS analysis of the chromatographic fractions. The fuels were separated into several fractions using a neutral alumina gel column and a series of elution solvents, as described elsewhere.[15] The identifications of compounds in JP-8P fraction 1 (*n*-pentane elute), fraction 2 (5% benzene-pentane elute), and fraction 3 (benzene elute) are described as follows.

Figure 11 shows the TIC as well as the detailed identification results of the JP-8P fraction 1 (saturates). All the identifications in Figure 11 were made by using retention indices and further confirmed by using mass spectrometry. Combined use of retention indices and mass spectra allows compound identification to be performed with higher confidence. The JP-8P saturates are highly

paraffinic in nature. In their mass spectra, straight-chain alkanes show weak molecular ions but typical and relatively strong $C_nH_{2n+1}^+$ fragment ions, and specific compounds can be accurately identified using GC-MS. Many branched alkanes exhibit very weak molecular ions, and in some cases such ions disappear from their mass spectra. It should be noted that Hayes and Pitzer[16,17] have published the retention indices of some branched alkanes and alkylated benzenes. Their data were also used to help identify several more peaks. It can be seen that the dominant constituents in fraction 1 of JP-8P are the long-chain alkanes with carbon number ranging from C_7 to C_{17} with most falling between C_9 and C_{14}. Straight-chain (normal) alkanes are predominant; many branched alkanes are also present, and the positions of the side chain are also indicated for them in Figure 11.

Figures 12 and 13 show the detailed GC-MS results for JP-8P fractions 2 and 3, respectively. Fraction 2 is composed of monoaromatics, and is free of saturates. Alkylbenzenes are the major components in this fraction, and minor components include tetralins and indans, whose concentrations are much lower than those found in coal-derived jet fuel. The analysis shows that multi-substituted alkylbenzenes (instead of long-chain n-alkylbenzenes) are the major compounds. Fraction 3 from JP-8P represents a concentrated diaromatics fraction, and consists of mainly naphthalene and alkylnaphthalenes. The identifications of ethylnaphthalenes and dimethylnaphthalenes were based on our own retention indices and GC-MS results; however, trimethylnaphthalenes were identified by comparing calculated retention indices in this study with those reported in literature for similar capillary columns.[30,31] This again demonstrates the usefulness of retention indices and that retention indices from one study may be easily applied to another study with similar columns.

The above results indicate that the coal-derived JP-8C fuel is significantly different from petroleum-based JP-8P in composition. The major compounds in JP-8P saturates are straight-chain and branched alkanes ranging from C_7 to C_{17}. However, the JP-8C saturates consist mainly of monocyclic, bicyclic and tricyclic alkanes, together with some long-chain alkanes. The aromatics in JP-8P are dominated by alkylbenzenes and alkylnaphthalenes, whereas the JP-8C aromatics are rich in hydroaromatic compounds such as tetralin, alkyltetralins, indans, cyclohexylbenzene, and some partially hydrogenated three-ring compounds, together with some alkylbenzenes and alkylnaphthalenes. These results show that jet fuels derived from different sources may have distinctly different molecular composition.

Table 7 displays the quantitative compositions of the JP-8P and JP-8C fuels based on the major hydrocarbon types found in fuels (alkanes, cyclohexanes, benzenes, decalins, tetralins, and indans) and others (such as alkylnaphthalenes). The compounds were quantified using the area percent of GC integration results coupled with the compounds' response factors determined from known amount of standard chemicals. In summary, JP-8P is a paraffinic fuel derived from

petroleum with long-chain alkanes as the dominant constituents (61%). The rest includes cyclohexanes (14%) and benzenes (15%); hydroaromatic compounds exist in small amount. On the other hand, the coal-derived fuel, JP-8C, is composed mainly of monocyclic and bicyclic alkanes, and hydroaromatic compounds. The major cyclic components are alkyl-substituted cyclohexanes (about 40%), decalin (15%), tetralin (8%), indans (6%), and about 11% alkylbenzenes. The alkanes only account for about 10% of JP-8C. The qualitative and quantitative information is useful in evaluating and explaining the thermal stability of fuels, which is significantly affected by their chemical composition.[11,14]

For comparison, the results of fractionation of these two fuels by liquid chromatographic separation on neutral alumina column[15] and by distillation[14] undertaken in previous work are also shown in Table 7. The data show that JP-8C contains more low-boiling components, as reflected by the higher content of IBP-165 °C fraction in JP-8C (27 vol %) than in JP-8P (8.3 vol %). GC-MS analysis of the distillation fractions revealed that the low-boiling and high-boiling distillate fractions of the petroleum derived JP-8P contains mainly the same type of compound classes (*i.e.*, *n*-alkanes) with different carbon numbers. In contrast, different distillate fractions of the coal-derived JP-8C showed a segregation of main compound classes. For example, the low-boiling fraction of JP-8C (IBP-165 °C) contains more alkylcyclohexanes, while the high-boiling fraction of JP-8C (185-215 °C) appears to have a higher concentration of bicyclic alkanes and hydroaromatics, principally decalin, methyldecalin, tetralin, methyltetralins and indans.

Conclusions

We have determined temperature-programmed retention indices of over 150 pure compounds using two capillary columns with different phase polarity at three different heating rates. The retention characteristics of various hydrocarbons and N-, S-, and O-containing compounds on different columns have been established. Aliphatic compounds give nearly constant indices at different heating rates, but the retention indices of polycyclic aromatic compounds exhibit relatively large temperature dependence. The use of a short isothermal holding (5 min) prior to the programmed heat-up does not cause any significant difference in the retention indices. Their dependences on the heating rates and temperature program, and on column phase polarity have been demonstrated. The column polarity can affect the retention behavior significantly, depending on the compound type. There also exist relationships between the temperature dependence (or column polarity dependence) of retention indices and the compound type. Almost all the compounds studied display higher temperature sensitivity on the more polar column (Rtx-50) than on the less polar column (DB-5), i.e., the values of ΔR.I./ΔT are larger for Rtx-50 than for DB-5. Retention indices as well as their sensitivity to temperature program decrease with decreasing column polarity.

The temperature-programmed retention indices are very useful for GC and GC-MS analysis of coal- and petroleum-derived jet fuels, as have been demonstrated in identifying components in two JP-8 jet fuels and their liquid chromatographic fractions. Over 100 fuel components were identified in detail. The results revealed that the coal-derived JP-8C fuel is significantly different from petroleum-based JP-8P in composition.

The knowledge on the effects of temperature and column polarity on retention behavior of various compounds can be applied to improving compound identification by using temperature programming or using columns of different polarity. Another application of the present results lies in the selection of appropriate column coating phase and temperature program for more efficient analysis of given samples and for eliminating or reducing co-elution of certain compounds. In addition, the present results of retention indices can be used to build a computer-assisted library of retention indices, which in combination with mass spectral library can lead to faster and more reliable automatic peak identification through computer library search.

References

1. Nowack, C. J.; Solash, J.; Delfosse, R. J. *Coal Processing Technol.* **1977**, *3*, 122-126.

2. Erwin, J.; Sefer, N. R. *Prepr. Pap.-Am. Chem. Soc., Div. Pet. Chem.* **1989**, *34(4)*, 900-904.

3. Zhou, P.-Z.; Marano, J. J.; Winschel, R. A. *Prepr. Pap.-Am. Chem. Soc., Div. Fuel Chem.* **1992**, *37(4)*, 1847-1854.

4 TeVelde, J.; Spadaccini, L. J.; Szetela, E. J.; Glickstein, M. R. *Thermal Stability of Alternative Aircraft Fuels.* AIAA-83-1143. American Institute of Aeronautics and Astronautics: New York, **1983**.

5 Sullivan, R. J.; Frumkin, H. A. *Prepr. Pap.-Am. Chem. Soc., Div. Fuel Chem.* **1986**, *31(2)*, 325-339.

6 Roquermore, W. M.; Pearce, J. A.; Harrison III, W. E.; Krazinski, J. L.; Vanka, S. P. *Prepr. Pap.-Am. Chem. Soc., Div. Pet. Chem.* **1989**, *34(4)*, 841-849.

7 Lee, C. M.; Niedzwiecki, R. W. *Prepr. Pap.-Am. Chem. Soc., Div. Pet. Chem.* **1989**, *34(4)*, 911-919.

8 Moler, J. L.; Steward, E. M. *Prepr. Pap.-Am. Chem. Soc., Div. Pet. Chem.* **1989**, *34 (4)*, 837-840.

9 Watkins, J. J.; Krukonis, V. J. *Supercritical Fluid Fractionation of JP-8*, Final Report, U.S. Air Force Aero Propulsion and Power Laboratory, WL-TR-91-2083, **1992**; 159 pp (Available from NTIS).

10 Hazlett, R. N. *Thermal Oxidation Stability of Aviation Turbine Fuels.* ASTM Monograph 1, American Society for Testing and Materials: Philadelphia, PA, **1991**; 163 pp.

11 Lai, W.-C..; Song, C.; Schobert, H. H.; Arumugam, R. *Prepr. Pap.-Am. Chem. Soc., Div. Fuel Chem.* **1992**, *37(4)*, 1671-1680.

12 Song, C.; Lai, W.-C..; Schobert, H. H. *Ind. Eng. Chem. Res.* **1994**, *33*, 534-547.

13 Song, C.; Lai, W.-C..; Schobert, H. H. *Ind. Eng. Chem. Res.* **1994**, *33*, 548-557.

14 Song, C.; Eser, S.; Schobert, H. H.; Hatcher, P. G. *Energy & Fuels* **1993**, *7*, 234-243.

15 Song, C.; Hatcher, P. G. *Prepr. Pap.-Am. Chem. Soc., Div. Petrol. Chem.* **1992**, *37(2)*, 529-539.

16 Hayes Jr., P. C.; Pitzer, E. W. *J. Chromatog.* **1982**, *253*, 179-198.

17 Hayes, P. C., Jr.; Pitzer, E. W. *Journal of High Resolution Chromatography & Chromatography Communications* **1985**, *8*, 230-242.

18 Steward, E. M.; Pitzer, E. W. *J. of Chromatographic Science* **1988**, *26*, 218-222.

19 Kováts, E. sz. *Helv. Chim. Acta.* **1958**, *41*, 1915.

20 Kováts, E. sz. In *Advances in Chromatography*, edited by J. C. Giddings and R. A. Keller. Vol. 1, **1965**, pp229-247. Marcel Dekker, Inc.: N.Y.

21 Budahegyi, M. V.; Lombosi, E. R.; Lombosi, T. S.; Mészáros, S. Y.; Nyiredy, Sz.; Tarján, G.; Timár, I.; Takács, J. M. *J. Chromatog.* **1983**, *271*, 213-307.

22 Guiochon, G. *Anal. Chem.* **1964**, *36(3)*, 661-663.

23 Habgood, H. W.; Harris, W. E. *Anal. Chem.* **1964**, *36(3)*, 663-665.

24 Lee, M. L.; Vassilaros, D. L.; White, C. M.; Novotny, M. *Anal. Chem.* **1979**, *51(6)*, 768-774.

25 Whalen-Pedersen, E. K.; Jurs, P. C. *Anal. Chem.* **1981**, *53*, 2184-2187.

26 Harris, W. E.; Habgood, H. W. *Programmed Temperature Gas Chromatography.* Wiley: New York, **1966**.

27 Ven Den Dool, H.; Kratz, P. D. *J. Chromatog.* **1963**, *11*, 463-471.

28 Furlong, M.; Fox, J.; Masin, J. *Production of Jet Fuels from Coal-Derived Liquids. Vol. IX*, Interim Report, AFWAL-TR-87-2042, 1989; 52 pp (available from NTIS).

29 Martel, C. R. *Military Jet Fuels 1944-1987.* Summary Report for period Oct. 85-Oct. 87, U.S. Air Force Aero Propulsion and Power Laboratory, AFWAL-TR-87-2062, 1987; 62 pp.

30 Rowland, S. J.; Alexander, R.; Kagi, R. I. *J. Chromatog.* **1984**, *294*, 407-412.

31 Borrett, V.; Charlesworth, J. M.; Moritz, Alan G. *Ind. Eng. Chem. Res.* **1991**, *30*, 1971-1976.

3. Product Distributions from Pyrolysis of n-Tetradecane in Near-Critical Region (Contributed by Jian Yu)

Previous studies show that initial phase behavior has a significant effect on the thermal decomposition of *n*-tetradecane (*n*-C_{14}) (Schobert et al., 1994a, 1994b). It was found that at temperatures above the critical temperature (T_c) the first-order rate constants for *n*-C_{14} decomposition exhibited large pressure dependence in the near-critical region. For example, at 425°C and 450°C, both above T_c (419.15°C for *n*-C_{14}), the first-order rate constants decrease significantly as pressure increases in the pressure region near the critical pressure P_c (1.573 MPa for *n*-C_{14}). It was also found that significant changes in the rate constants fall in the sub- and near-critical regions and will not extend to farther supercritical region. Following up previous work, this subsection presents the results of product distributions from *n*-C_{14} pyrolysis in the near-critical region.

Figures 14-22 show the change in the yield of individual paraffinic and olefinic product with loading ratio (defined as the ratio of initial sample volume to reactor volume) at 400°C and with reduced pressure P_r (P_r=P/P_c) at 425°C and 450°C. P_r was calculated at given temperature and loading ratio using Soave-Redlich-Kwong equation of state (Soave, 1972). The yields of the products were expressed as the number of moles based on 100 moles of *n*-C_{14} reacted. Under the conditions used in this study the major pyrolytic products are *n*-alkanes with carbon number from C_1 to C_{11} and 1-alkenes with carbon number from C_2 to C_{12}. While *n*-C_{12}, *n*-C_{13}, and 1-C_{13} are also present in pyrolytic products, their yields are considerably smaller than those of the major products. There are also very small amounts of minor reaction products such as branched-chain alkanes, internal alkenes, cycloalkanes, and aromatics whose relative amounts are dependent upon reaction conditions (temperature, loading ratio, and residence time). Hydrogen was detected only at 450°C. Straight-chain and branched-chain alkanes with carbon number from C_{15} to C_{23} were also detected under some reaction conditions. The amounts of these high-molecular-weight alkanes were low, especially for the branched-chain alkanes. In reality there were 50-100 liquid components eluted from GC column at the conditions employed. Since present study emphasizes the effects of near-critical conditions on product distributions from *n*-C_{14} pyrolysis, it is not necessary to include minor product distributions. With this consideration in mind, the changes in the yields of the major paraffinic and olefinic products with loading ratio or reduced pressure are presented in Figures 14-22. C_4 products were dissolved in the liquid product , but significant losses occurred before the liquid sample was analyzed. Consequently the yields of both butane and butene were not included. C_5 products also suffered from slight losses but were still presented since the prompt analysis of the sample after the reaction minimized the losses. 1-C_{12} was removed only for the clarity of the Figures.

Figures 14-16 show the changes of the product components with loading ratio r at 400°C and two different reaction time, 3 h and 5 h. From the change of the gas components with r it can be seen that the yields of propane and propylene increase with r while those of ethane and ethylene decrease with r. The yield of methane remains in a narrow range. In both cases the yields of gas components decrease in the order of propane > propylene > ethane > methane > ethylene. The low ethylene yield reveals that the reaction mechanism under the reaction conditions used in this study is different from that of low-pressure and high-temperature pyrolyses, which give very high ethylene yield. Among the liquid products the component with longer chain in the same homologous series usually has low yield (Figures 15 and 16). The yield of paraffinic component increases with r while that of olefinic component decreases with r.

When the reactions were carried out at 425°C for 0.5 h and 1 h, the yields of gas components follow the similar order but the changes of the yields with P_r exhibit unusual features in the near-critical region (Figure 17). The yields of paraffinic and olefinic components in the liquid product also decrease with increasing carbon number (Figures 18 and 19). In the near-critical region the yield of paraffinic component increases rapidly with P_r while in the farther supercritical region the yield does not change significantly with P_r. The yield of olefinic component exhibits complex pressure dependence in the near-critical region for 0.5 h run. For 1 h run the yield of olefinic component decreases with P_r with large change in the near-critical region.

At 450°C and 0.5 h the yields of gas components still exhibit similar order and pressure dependence (Figure 20). For 1 h run gas product distributions give complex pressure dependence although the yield of ethylene is still the lowest among gas products and decreases with P_r. For liquid products similar observations were obtained (Figures 21 and 22). That is, the longer the chain, the less the yield. Also, the yield of paraffinic component increases with P_r while that of olefinic component decreases with pressure. There is no large pressure dependence of the yield in the region around $P_r = 1$.

Figures 23-25 show the changes in the molar ratios of n-alkane to 1-alkene with r or P_r for selected carbon number of 7, 9, 11 under different reaction conditions. It can be found that the selectivity for paraffinic component relative to olefinic component with the same carbon number increases with pressure. At 425°C large changes in *n*-alkane/1-alkene ratios were observed in the near-critical region. At all three temperatures the product selectivities for *n*-alkanes are very high and even over the selectivities for corresponding 1-alkenes at higher pressures. These results are largely different from those obtained under typical *n*-alkane pyrolysis conditions (~atmospheric pressure, > 600°C) which usually give methane and ethane as the only paraffinic products.

The results presented above can be explained by free radical theory and transition state theory. For *n*-C_{14} the homolytic initiation reaction produces two primary radicals. These primary radicals then abstract hydrogen from surrounding reactant molecules to form various parent

radicals $C_{14}H_{29}\cdot$, of which most are secondary radicals, since the formation of a primary radical by hydrogen abstraction requires higher energy of activation. The parent radicals undergo β-scission to form a 1-alkene and a primary radical. The subsequent reactions of these primary radicals include hydrogen-abstraction, β-scission, isomerization, and addition at higher conversions. The competitions between these reactions determine the final product distribution. At high temperatures and low pressures, unimolecular radical decomposition reactions are favored because of higher activation energies than bimolecular reactions. At high pressures and lower temperatures, bimolecular reactions such as hydrogen abstraction and radical addition reactions are favored. The relative rates of hydrogen abstraction and radical decomposition can be estimated using the Arrhenius rate parameters given in the article by Song et al. (1994). Let's use the competition between the following two reactions as an example.

$$1\text{-}C_5H_{11}\cdot + n\text{-}C_6H_{14} \text{ -----> } n\text{-}C_5H_{12} + 2\text{-}C_6H_{13}\cdot \qquad (1)$$

$$1\text{-}C_5H_{11}\cdot \text{ -----> } C_2H_4 + 1\text{-}C_3H_7\cdot \qquad (2)$$

The rate parameters for the hydrogen abstraction (1) are $A = 10^{11.0}$ L/(mol.s) and E = 10.4 kcal/mol while those for the decomposition (2) are $A = 10^{13.4}$ 1/s and E = 28.8 kcal/mol. Assuming the concentration of *n*-hexane [RH] = 1.1 mol/L which corresponds to a 4 mL loading of *n*-hexane in a 28 mL reactor, the rate ratio of hydrogen abstraction and radical decomposition at 425°C is around 2500. Therefore, hydrogen abstraction is favored under the condition studied. This means that the larger free radical formed from β-scission of the parent radical would tend to be stabilized by hydrogen abstraction from a surrounding molecule rather than undergoing further decomposition. This would result in equimolar distributions between *n*-alkanes and 1-alkenes in the products. In addition the radical addition reaction between a free radical and an olefinic molecule will also be favored at high pressures and higher conversion (for example, larger than 10%). Both hydrogen abstraction and radical addition reactions increase the ratio of *n*-alkanes to 1-alkenes in the products. This explains the observed results: high ratios of *n*-alkanes to 1-alkenes, low ethylene yields, increasing *n*-alkane yields and decreasing 1-alkene yields with increasing pressure.

The large changes in the ratios of *n*-alkane to 1-alkene in the near-critical region (Figure 11) probably result from unusual properties of the fluid in this region. In the near-critical region the fluid exhibits very high compressibility and many physicochemical properties change significantly with pressure. When the reaction is carried out in the near-critical region pressure may influence the rate constant significantly. This can be explained by means of transition state theory (Laidler, 1965; Eckert, 1972).

For a bimolecular reaction the reactants A and B are assumed to be in chemical equilibrium with the transition state $M^{\neq}$.

$$A+B \Leftrightarrow M^{\neq} \Rightarrow \text{Products} \qquad (3)$$

The change of the reaction rate constant k with pressure is given by the following expression

$$\left(\frac{\partial \ln k}{\partial P}\right)_T = -\frac{\Delta V^{\neq}}{RT} \qquad (4)$$

where $\Delta V^{\neq}$, the volume of activation, is the difference in the partial molar volumes of the transition state species M, and the reactants A and B and is given by

$$\Delta V^{\neq} = \overline{V}_M - \overline{V}_A - \overline{V}_B \qquad (5)$$

$\Delta V^{\neq}$ can be either positive or negative. If $\Delta V^{\neq}$ is positive, then reaction will be retarded by pressure. Otherwise, the reaction rate will be enhanced by pressure.

In conventional liquid solutions, pressure changes in kilobars are required to affect the rate constant significantly because $\Delta V^{\neq}$ is usually in the range of –50 to +20 cm^3/mol (Eckert, 1972). However, in the highly compressible near-critical region, small pressure changes can produce substantial variations in the rate constant because the magnitude of $\Delta V^{\neq}$ is much larger. For example, Simmons and Mason (1972) found activation volumes lower than –3000 cm^3/mol for the dimerization of chlorotrifluoroethylene near its critical point. Johnston and Haynes (1987) reported activation volumes as low as –6000 cm^3/mol for the unimolecular decomposition of α-chlorobenzyl methyl ether in the near-critical region of 1,1-difluoroethane. From the results obtained in this study it can be inferred that the magnitudes of the activation volumes for elementary bimolecular reactions such as hydrogen abstraction and radical addition or for elementary radical decomposition may attain rather large values when the reaction is carried out in the near-critical region of *n*-C_{14} (425°C and initial P_r around 1). Probably the larger negative values of the activation volumes for bimolecular reactions or the large positive value of $\Delta V^{\neq}$ for the unimolecular radical decomposition reaction results in the large increases in the ratios of *n*-alkane to 1-alkene with pressure in the near-critical region of *n*-C_{14}. It is impossible to infer which reaction or reactions have large values of activation volumes because hydrogen abstraction, radical addition, and radical decomposition are competitive reactions and the existence of large value of $\Delta V^{\neq}$ for any reaction can result in large changes in the ratios of *n*-alkane to 1-alkene. Such information can be

obtained only from the study for elementary reactions. While detailed mechanism governing this unique product distributions in the near-critical region is not yet clear, it can be inferred that unusual properties of the fluid in the near-critical region may have significant effects on the thermal reactions.

References

1. Eckert, C. A. High Pressure Kinetics in Solution. *Annu. Rev. Phys. Chem.* **1972**, *23*, 239.

2. Johnston, K. P.; Haynes, C. Extreme Solvent Effects on Reaction Rate Constants at Supercritical Fluid Conditions. *AIChE J.* **1987**, *33*, 2017.

3. Laidler, K. J. *Chemical Kinetics*; McGraw-Hill: New York, **1965**, Chap. 5.

4. Schobert, H. H.; Eser, S.; Song, C.; Hatcher, P. G.; Walsh, P. M.; Coleman, M. M. *Advanced Thermally Stable Jet Fuels*. Technical Progress Report (January 1994 - March 1994), January, **1994a**, The Pennsylvania State University.

5. Schobert, H. H.; Eser, S.; Song, C.; Hatcher, P. G.; Walsh, P. M.; Coleman, M. M. *Advanced Thermally Stable Jet Fuels*. Technical Progress Report (October 1993 - December 1993), January, **1994b**, The Pennsylvania State University.

6. Simmons, G. M.; Mason, D. M. Pressure Dependency of Gas Phase Reaction Rate Coefficients. *Chem. Eng. Sci.* **1972**, *27*, 89.

7. Soave, G. Equilibrium Constants from a Modified Redlich-Kwong Equation of State. *Chem. Eng. Sci.* **1972**, *27*, 1197.

8. Song, C.; Lai, W.-C.; Schobert, H. H. Condensed-Phase Pyrolysis of n-Tetradecane at Elevated Pressures for Long Duration. Product Distribution and Reaction Mechanisms. *Ind. Eng. Chem. Res.* **1994**, *33*, 534.

Task 3. Investigation of the Quantitative Degradation Chemistry of Fuels

The Effects of High Surface Area Activated Carbon as a Catalyst during Thermal Stressing of n-Octane and n-Dodecane (Contributed by Semih Eser, Katia Gergova, Rathnamala Arumugan)

Our previous studies showed that addition of high surface area activated carbon PX-21 is effective in slowing thermal degradation reactions of jet fuel heated to a high temperature (450°C) even for a long period of time (5h) [1,2].

The main use of activated carbons is as adsorbents, but they can also promote a variety of surface reactions. Their role as a catalyst is different in different reactions. The catalytic reactions have been classified into oxidation reactions, combination reactions, decomposition reaction and elimination reactions. The performance of an activated carbon as catalyst depends on a number of factors, such as the nature of the carbon surface, the presence of carbon-oxygen surface structures, the availability of the active sites and the surface area. Spiro [3] studied the catalytic effect of carbon on reactions in solution and reported that the surface area played an important role on carbon catalytic activity. Alfelli at al. [4] reported that solid adsorbents which they called "fuel stability foam" produced from polyurethane were found to be effective in greatly improving diesel fuel instability.

For better understanding the role of activated carbon as catalyst during thermal stressing of jet fuel, we used model compounds *n*-dodecane and *n*-octane. Using model compounds instead of jet fuel simplifies the study of the details of activated carbons' catalytic reactions and their mechanisms.

The 5% decalin was added to the model compounds in order to test the ability of activated carbon PX-21 to catalyze the transformation of decalin to naphthalene. The cis/trans decalin d_{18} purchased from Cambridge Isotope Laboratories was used in a single experiment to confirm the activated carbon catalytic capabilities of hydrogen carrier. This work is a new approach to better understanding the role of activated carbons during thermal stressing of jet fuel at high temperature (450°C. In this study the samples were stressed for 1h because of the complicated mixture of compounds obtained after thermal stressing of jet fuel as well as dodecane at 450°C for 5 h, which does not allow insight into catalytic reactions of activated carbon. The influence of the amount of carbon added during pyrolysis of the compounds was also studied.

The dodecane and *n*-octane used were purchased from Aldrich Chemical Corporation; and PX-21 activated carbon, from Amoco Carbon Corporation. Thermal stressing experiments were carried out at 450°C for 1h in stainless steel microautoclaves under 100 psi pressure of UHP grade N_2. The liquid products were analyzed quantitatively using a Hewlett-Packard 5800, series II GC,

with a FID detector. The compounds in the liquid products were identified by capillary gas chromatography-mass spectrometry (GC-MS) using a Hewlett Packard 5890, series II GC coupled with HP 5971A mass selective detector. Additionally, the liquid products from repeated experiments were separated over alumina. The hexane, toluene and tetrahydrofurane (THF)/reagent alcohol 9:1 were used for the separation of the liquid products.

Three sets of experiments were carried out on *n*-octane at 450°C for 1h in nitrogen atmosphere. One set of experiments was performed by stressing a mixture of 9.5 ml n-octane, 0.5 ml decalin and 50 mg PX-21; in the other set 150 mg PX-21 was added; and in the third set of experiments the amount of activated carbon PX-21 was 250 mg. The parallel experiments without carbon were also performed.

The other model compound, dodecane, was mixed with 200 µl decalin d_{18} and 250 mg PX-21 and was stressed at 450°C for 1h. The sample without activated carbon was stressed in parallel experiment for comparison.

1. The Effects of High Surface Area Activated Carbon PX-21 on the Thermal Stressing of *n*-Octane Mixed with 5% Decalin Our previous reports indicated that the activated carbon's surfaces appear to be effective in stabilizing the free radicals or catalyzing recombination reactions to form more paraffinic gasses and to preserve constituent alkanes in the fuel at 450°C.

Song et al. [1] reported that adding H donors, such as tetralin or decalin, to jet fuel reduced the formation of solid deposit at 450°C and decreased the extent of fuel decomposition and gas formation. The increased stability of jet fuel in the presence of H-donors is attributed to the stabilization of the reactive radicals, which contributes to inhibiting the radical decomposition, cyclization, aromatization, and condensation reactions. However, when the activated carbon is present during thermal stressing of *n*-octane+decalin one can expect that hydrogen-transferring pyrolysis mechanism to be different. Table 8 shows the percent weight of the compounds identified in the liquids after thermal stressing of *n*-octane and 5% decalin alone and with 50, 150 and 250 mg PX-21 activated carbon. Adding PX-21 considerably reduced the pressure increase during stressing of *n*-octane, and as can be seen from Table 8, the formation of lighter compounds, such as C_4, C_5 alkanes have been also reduced. The difference in the weight percent of decomposed n-octane stressed with and without carbon is between 2.5-4.5% in the behave of the sample stressed with activated carbon. The final product of H transfer reaction of the polycyclic hydrocarbon decalin which act as hydrogen donor is naphthalene. The higher amount naphthalene and the lower percent decalin identified in the liquids stressed with PX-21 is a clear indication that PX-21 catalyzes the H transfer reactions. The result of H transfer is mainly inhibiting the radical reactions and blocking solid formation. However, when the activated carbon is present the effect

of decreasing hydrocarbon degradation considerably increases, which can be seen also from the much lighter color of the liquid obtained from stressing of *n*-octane with PX-21.

Figure 26 shows the increase of naphthalene and tetralin in the stressed liquids with adding different amount of activated carbon compared to the amount of same compounds in the liquid obtained after stressing of *n*-octane and decalin alone. It seems that the amount of carbon added does not have significant effect on the catalytic reactions, although the catalytic ability increases with increasing the amount of carbon addedto 150 mg. However, this increase is not large enough to justify the necessity of adding more then 50 mg activated carbon.

The liquids from the repeated experiments of n-octane and decalin and *n*-octane+decalin+PX-21 were separated over alumina using hexane, toluene and THF. Practically, we obtained two fractions because the toluene and THF fractions were difficult to be distinguished. The compounds identified in the fractions were not calculated quantitatively because of the high risk of error possible.

In the hexane fraction of *n*-octane+decalin and *n*-octane+decalin+PX-21 wes detected the same compounds and their concentration of both liquid samples is not very different, although quantitative analysis was not performed. The toluene+THF fraction shows more interesting results. Figure 27 presents the GC of toluene+THF fraction of *n*-octane+decalin (a) and *n*-octane+decalin+150 mg PX-21 (b). There is a huge difference of the concentrations of naphthalene between two samples. The naphthalene concentration of the sample stressed with PX-21 is considerably higher than the naphthalene concentration of the sample stressed without PX-21. These results confirm again that the activated carbon added during thermal stressing of *n*-octane+decalin helps for the H transfer and conversion of decalin to naphthalene.

Figure 3 shows how the concentration of naphthalene changes with amount of PX-21 added from 50 to 250 mg. There is a considerable increase in the concentration of naphthalenes with increasing amount PX-21 added from 50 to 150 mg. It seems that further increase of PX-21 does not lead to producing higher naphthalene concentration.

The specific structure of activated carbons can explain their role as hydrogen carrier during thermal stressing of *n*-octane+decalin at 450°C. Activated carbons have a structure consisting of sheets of aromatic condensed ring systems stacked in nonpolar layers. These sheets have edges and defects, dislocations and discontinuities. The carbon atoms at these places have unpaired electrons and residual valencies and are richer in potential energy. These carbon atoms are highly reactive and constitute active sites or active centers.

A considerable amount of research was dedicated in order to understand the nature of these active sites in view of the surface and catalytic reactions of carbons. Puri and Bansal [5,6] studied the chlorination of coconut charcoals and observed that the chemisorbed hydrogen was eliminated in a number of steps depending on the temperature of the treatment. This was attributed to the fact

that hydrogen in charcoals was bonded at different types of sites associated with varying energies of activation. The activation energy of adsorption at relatively more active sites is found to be 7.4 kcal/mol.

Sherman and Eyring [7] made theoretical calculations of the energy of activation for dissociative chemisorption of hydrogen and carbon surface and found the values to vary with carbon-carbon spacing.

These data give important information in order to control the catalytic effects of activated carbons by changing their active surface. Our future work will be focusing on assignment of the surface characteristics of activated carbons used for increasing thermal stability of jet fuels.

2. The Effects of High Surface Area Activated Carbon PX-21 on the Thermal Stressing of Cis/Trans Dodecane d_{18} Mixed with 200 μL Decalin A single experiment was carried out on dodecane +200 μL decalin d_{18} because of the high price of d_{18} decalin.

The 9.8 ml dodecane mixed with 200 μL decalin d_{18} was stressed alone at 450°C for 1h and with 250 mg PX-21. The compounds identified and their percent areas are shown in Table 9. From Table 9 one can see that the percent of the short alkanes+alkenes (C_3-C_5) is higher for the sample stressed without carbon, while the long-chain alkanes, starting from C_6 are in higher concentration in the liquid that was stressed with PX-21.

Figure 29 shows the changes in n-alkane distributions after stressing at 450°C for 1h upon addition of 250 mg PX-21 The dodecane and coeluted *n*-alkanes are not present in Figure 29. In the presence of PX-21 there appeared that formation of hexane, octane, nonane, decane and undecane was suppressed significantly, especially for the first three compounds. Based on the differences of the products, it seems that the variation of product distribution with PX-21 is mainly due to distinction between different radicals. The primary radicals were more stable than the secondary. This explains also the lower concentration of light compounds C_3-C_5 in the liquid obtained from stressing of dodecane+decalin+PX-21. Table 9 shows the opposite trends for C_6-C_{10} alkene. Their concentration is higher in the liquid stressed without carbon. The results in Table 9 suggest that the active sites of PX-21 initializes the cracking process, since the concentration of dodecane in the liquid obtain after stressing of n-dodecane+decalin d_{18} is ≈3% higher than the concentration of dodecane in the liquid stressed with PX-21. However, after initializing the cracking process PX-21 stabilizes the primary pyrolysis products.

Figure 30 shows the percent area of naphthalene, cis- and trans-decalins for the liquids obtained from stressing of dodecane with and without PX-21. The data in Table 9 and Figure 30 clearly indicate that activated carbon enhanced the H-transfer. The trans- and cis-decalins are in lower concentration while the naphthalene is in higher concentration for the sample obtained from stressing dodecane with carbon. Additionally, the GC and GC/MC analysis show that the naphthalene identified in the liquids obtained from the stressing with PX-21 is d_{18} naphthalene.

Both liquid products, from stressing of dodecane+decalin d_{18} and dodecane + decalin$_{18}$ + PX-21 were separated over alumina. The method of separation is the same used for the separation of liquids products obtained from stressing of *n*-octane. There is a higher concentration of alkanes in the hexane fraction of the liquid product obtained from stressing of dodecane with PX-21, but the compounds identified are the same as in the liquid fraction obtained from stressing of dodecane without carbon. However, the differences in the concentration of alkanes can not be discuss further because the quantitative analysis of the liquid products obtained after the separation will not be reliable.

In the toluene+THF fraction no phenanthrene, pyrene and other heavier compounds than naphthalene were detected, which most probably is due to the decalin addition. As we have already mentioned, the decalin is an H donor and helps to slow down the dodecane degradation. As a matter of fact, no carbonaceous deposit was found after stressing of dodecane with PX-21 in the presence of decalin as well as negligible amount deposit was found after stressing of dodecane without PX-21 in the presence of decalin.

Figure 31 presents the GC of toluene+THF fraction of dodecane+decalin d_{18} (a) and dodecane+decalin d_{18}+ 250 mg PX-21 (b). The concentration of naphthalene in the toluene+THF fraction of the liquid obtained from stressing of dodecane+PX-21 is very big while those of the liquid product from stressing of dodecane without activated carbon is almost undetectable. The naphthalene peaks are shifted to the lower retention time which is an indication of d_{18} naphthalene.

Acknowledgments: We would like to express our thanks to Gaolin Qiao in the Fuel Science Program, who separated the liquid samples.

References

1. H. H. Schobert, S. Eser, C. Song, P. Hatcher, P. Walsh, M. Coleman, Advanced Thermally Stable Jet Fuels, Technical Progress Report, November 1992-January 1993

2. H. H. Schobert, S. Eser, C. Song, P. Hatcher, P. Walsh, M. Coleman, Advanced Thermally Stable Jet fuels, Technical Progress Report, February 1993-March 1993.

3. M. Spiro, Catalysis Today 1990, 7, 167.

4. W. Arfelli, A. Power, R. K. Solly, In proceeding of the 3rd International Conference of Stability and Handling of Liquid Fuels.

5. B. R. Puri and R. C. Bansal, Chem. Ind., London 1963, 574.

6. B. R. Puri, and R. C. Bansal, Indian Chem. Society 1972, 40, 179.

7. A. Sherman, and H. Eyring, J. Am. Chem. Society 1932, 54, 2661.

Task 4. Coal-based Fuel Stabilization Studies

In Situ Regeneration of the Thermal Stabilizer Benzyl Alcohol. (Contributed by Leena Selvaraj; John B. Stallman; Maria Sobkowiak; and Michael M. Coleman)

Introduction

We have demonstrated in earlier communications that benzyl alcohol and 1,4-benzenedimethanol function as efficient stabilizers at temperatures above 400°C and enhance the thermal stability of jet fuels and the model compound, dodecane.[1,2] In contrast, other alcohols have been found to be poor stabilizers.[1] However, the addition of ethanol to hydrocarbon/ benzyl alcohol mixtures has a significant effect on the thermal stabilization of jet fuels and related materials at temperatures above 400°C. Ethanol appears to function in a redox fashion by reducing the benzaldehyde formed during the degradation of the benzyl alcohol/ hydrocarbon mixtures. This regenerates benzyl alcohol. In other words, in the presence of ethanol less benzyl alcohol is required for thermal stabilization of the fuel.

Experimental

Thermal stressing experiments were performed on dodecane with benzyl alcohol, ethanol and mixtures of benzyl alcohol and ethanol as stabilizers. In all the experiments the molar concentration of these stabilizers was kept constant at 0.0072M, and only their molar ratio (benzyl alcohol : ethanol) was varied. A typical thermal stressing experiment was performed for six hours on 10 mL dodecane samples containing known amount of stabilizers at 425°C using 15 mL type 316 stainless steel micro reactors under 100 psi of air. The micro- reactor containing the sample was pressurized with 100 psi of air. It was then placed in a preheated sand bath at 425°C for the required reaction time, followed by quenching into cold water and depressurized.

Capillary gas chromatographic (GC) analyses were performed to analyze the liquid reaction products. A Hewlett Packard GC with a FID detector and a Rtx-50 column was used. The temperature program used was as follows: initial temperature, 40°C; initial isotime, 5min; heating rate, 4°C/min to 280°C; and the final isotime, 10 min. A split mode of injection was employed. A Hewlett Packard capillary gas chromatography GC with mass detector (GC-MS) was used for the identifying the products.

Results and Discussion

Thermal Stressing of Dodecane with Benzyl Alcohol - Ethanol Mixtures . Thermal stressing experiments were performed in the manner described above. The molar ratio of benzyl alcohol :

ethanol was varied as 3 : 0 (sample 1), 2.5 : 0.5 (sample 2), 1 : 2 (sample 3), 0.5 : 2.5 (sample 4) and 0 : 3 (sample 5). The liquid reaction products obtained after thermal stressing were quantitatively analyzed using GC. Figure 32 shows a histogram depicting the mole % of uncracked dodecane after thermal stressing. Note that in the first three samples only about 10 mole % of the dodecane has degraded. However, in samples 4 and 5, we observe that 44 and 56 mole % of the original dodecane has cracked respectively. Expressed in another way, Figure 33 shows the corresponding mole % of heptane, octane, nonane, decane and undecane formed from dodecane in the samples 1 to 5.

In an earlier communication, we indicated that degradation reactions are retarded as long as an appreciable concentration of benzyl alcohol is present in the reaction mixture[2]. The thermal stability observed in sample 1 can be attributed to the high initial concentration of benzyl alcohol. At the other extreme, the relatively poor thermal stability of sample 5 is due to the fact that ethanol is an inefficient stabilizer. The interesting results are those containing the mixtures of benzyl alcohol and ethanol, especially samples 2 and 3. Ethanol appears to be acting in a synergistic fashion.

For comparison purposes dodecane (10.00 mL) was thermally stressed with 0.0024M of benzyl alcohol alone (the same amount of benzyl alcohol initially present in sample 3) at the same temperature for the same time period. Table 10 lists the mole % of dodecane and benzyl alcohol remaining (based on the initial moles present). Note that sample 6 contains only 69 mole % of uncracked dodecane, whereas sample 3 has 88 mole% of uncracked dodecane. There is a 19 mole % increase is observed in the concentration of uncracked dodecane in sample 3 as compared to that in sample 6. In Table 10, we have also shown the amount of unreacted benzyl alcohol in these two samples. Samples 6 and 3 contain 14 and 43 mole % unreacted benzyl alcohol, respectively. There is a 29% increase in the concentration of unreacted benzyl alcohol in sample 3 as compared to sample 6.

Proposed Reaction Mechanism for the *In Situ* Regeneration of Benzyl alcohol. Malwitz and Metzger have reported that carbonyl compounds can be reduced by alcohols via a thermally initiated free radical reaction[3]. They investigated the thermal reduction of benzaldehyde in the presence of 2-propanol to provide benzyl alcohol and acetone as the only two products. The proposed mechanism for this transformation is shown in scheme I.

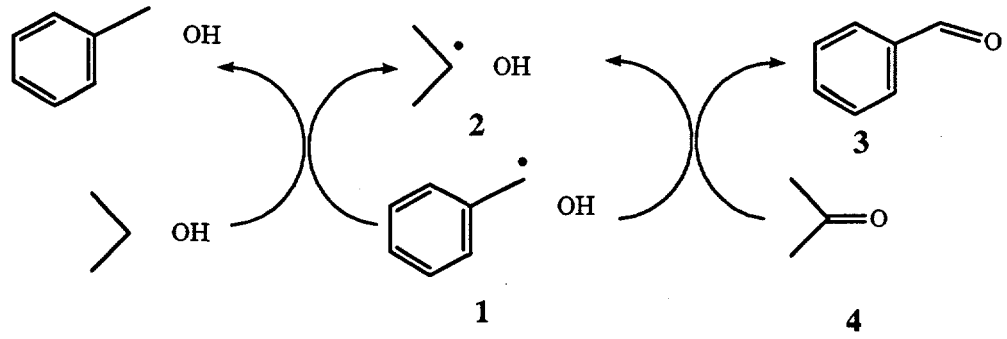

Scheme I

The chain reaction starts with the formation of the benzylic radical **1** and the isopropyl radical **2**. These radicals can then proceed either to further oxidation to give benzaldehyde **3** and acetone **4** or the benzaldehyde can receive a proton from the isopropyl radical **2** or from the 2-propanol to regenerate the benzyl alcohol.

In our reaction system we expect ethanol to react in a similar fashion with benzaldehyde and thus regenerating benzyl alcohol in the system. The proposed mechanism is shown in scheme II. After hydrogen atom abstraction of benzyl alcohol by the hydrocarbon free radicals, benzaldehyde is initially formed. In the presence of ethanol a reduction of the benzaldehyde then occurs with ethanol donating two protons to regenerate several molecules of benzyl alcohol and further yielding acetaldehyde. By this route ethanol can regenerate benzyl alcohol by an *in situ* reduction.

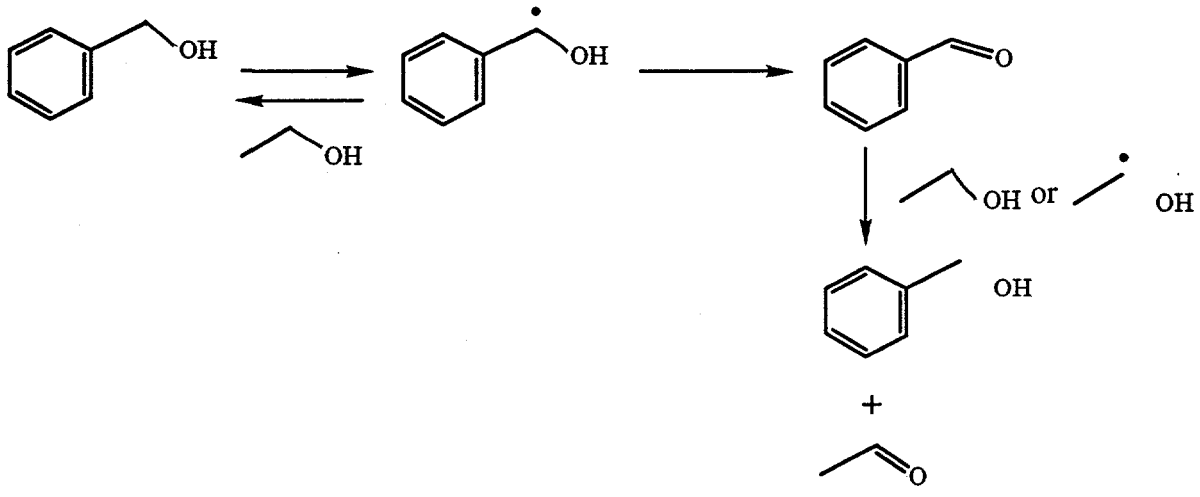

Scheme II

Thermal Stressing of an Ethanol and Benzaldehyde Mixture at 425°C. In order to further understand the reaction between ethanol and benzaldehyde, a mixture of ethanol (5.00 mL) and benzaldehyde (5.00 mL) was stressed at 425°C under 100 psi of air for 1h. The liquid products

were analyzed using GC and GC-MS. Figure 34 shows the gas chromatogram of the stressed liquid sample. In addition to ethanol and benzaldehyde, the gas chromatogram shows that benzyl alcohol is the major reaction product, while benzene and toluene are the minor products. This result indicates that ethanol indeed can generate a significant amount of benzyl alcohol in the presence of benzaldehyde.

Thermal stressing of Dodecane with Benzyl Alcohol and Labeled Ethanol.(CH_3CD_2OH)

Dodecane (10.00 mL) was thermally stressed with 0.0072M of a mixture of benzyl alcohol and CH_3CD_2OH in the ratio 1 : 2, at 425°C, under 100 psi of air for 3h. The liquid products were analyzed using GC and GC-MS. If CH_3CD_2OH reacts with the benzaldehyde formed from benzyl alcohol, then we would expect the formation of deuterated benzaldehyde and benzyl alcohol.

Figure 34(a) shows the total ion chromatogram of the liquid products between the retention time 19.80 to 21.80 min, as analyzed by the GC-MS. The twin peaks that is observed between 20.50 and 20.70 min can be attributed to benzyl alcohols as confirmed by the fragmentation patterns observed in Figures 34(b), (c), and (d). Figures 34(b), (c) and (d) show the fragmentation patterns at the retention time of 20.7 , 20.6 and 20.5 min, respectively. The peak at m/z 108, 109, 110 can be attributed to the molecular ions of $C_6H_5CH_2OH$, C_6H_5CDHOH and $C_6H_5CD_2OH$ respectively. The peaks at m/z 79, 80, and 81 can be assigned to  , 

and  , fragments respectively. Figure 35(a) shows the total ion chromatogram of the liquid products between the retention time 16.2 to 18.6 min, as analyzed by the GC-MS. The peak with a shoulder that is observed between 17.4 and 17.6 min can be attributed to benzaldehyde as confirmed by the fragmentation patterns observed in Figures 35(b) and(c). Figures 35(b) and (c) show the fragmentation patterns at the retention time of 17.53 and 17.47 min respectively. The peaks at m/z 107 and 106 can be attributed to the molecular ions of C_6H_5CDO and C_6H_5CHO respectively. The peaks at m/z 105 and 77 in Figures 35(b) and (c) can be assigned to $C_6H_5CO^+$ and $C_6H_5^+$ fragments respectively.

From the above results we conclude that ethanol donates two hydrogens to benzaldehyde and thus regenerates benzyl alcohol in the system as per scheme II. As a result, ethanol is oxidized to acetaldehyde and its degradation products. In the presence of ethanol, therefore less benzyl alcohol is required for thermal stabilization of the fuel.

References

1. Coleman, M. M., Selvaraj, L, Sobkowiak, M.,and Yoon, E., *Energy & Fuels*, **1992**, 6(5), 535.

2. Selvaraj, L, Sobkowiak, M., Song, C., Stallman J. B., and Coleman, M. M., *Energy & Fuels*, **1994**, July (in press).

3. Malwitz D., and Metzger J. O., *Chem. Ber.*, **1986**, 119, 3558.

Task 5. Exploratory Studies on the Direct Conversion of Coal to High Quality Jet Fuels.

Hydrotreatment of multicyclic compounds to produce cycloalkanes (Contributed by Richard Dutta)

Introduction

One of the most important factors controlling the high temperature thermal stability of jet fuels is their chemical composition [1]. At high temperatures, pyrolysis reactions of certain components in the fuel become significant and result in the formation of gums and insoluble solids. These materials will reduce heat transfer efficiency, degrade valve performance and deposit solids in the fuel pipeline and in fuel combustor nozzles.

With the increasing need to develop advanced jet fuel comes an increasing need to find new feedstocks that can be converted to thermally stable compounds. Jet fuels are traditionally produced from petroleum and thus they contain a large proportion of alkanes. Alkanes have been shown to be thermally unstable at elevated temperatures [2]. Previous work at Penn State has shown decalin, tetralin and cyclohexanes to be stable when stressed at high temperatures [2]. Therefore it appears that cycloalkanes are desirable components of advanced jet fuels because of their high thermal stability. With a desired product in mind, it is advantageous to select a feedstock that can be converted to the products in as few steps as possible. Therefore, if cycloalkanes are to be produced efficiently, compounds that are predominantly cycloparaffinic would make ideal feedstocks.

POTENTIAL FEEDSTOCKS

1. Resins

The higher plants contain terpenoid-based substances commonly known as resins. These resins exude from the plants if they are injured to seal up wounds. Rosin is the residue left after distilling off the volatile oil from the oleoresin obtained from *Pinus palustris* and other Pinus species. It is produced mainly in the USA for manufacture of varnishes and polishes. The constitution of rosin is about 90% resin acids (isomeric with abietic acid and dehydroabietic acid). Tall oil rosin (containing 50% resin acids) has been considered as a source of transportation fuel in the past [3] but the hydrocracking chemistry of rosin has not been addressed fully.

Dammar is the resinous exudate from a species of Dipterocarpaceae found in South East Asia. The constitution of Dammar is based on a sesquiterpenoid polymer called polycadinene, and other high molecular weight dimers, trimers and oligomers of cadinene [4,5].

Resinite occurs in various amounts in coals (0-6 wt%) and also varies in chemical structure. Coals from Utah seams contain a relatively large amount of resinite which has been

characterized as a sesquiterpenoid based resin [6]. Utah coals are considered good feedstocks for liquefaction due to the high concentration of bicyclic components in the structure and its crosslink density. Maceral composition also affects the liquefaction behavior of a coal. The high concentration of resinite in Utah coals can be considered to be a property of the coal that makes it a prime candidate for liquefaction. Therefore, the behavior of resinite under liquefaction conditions needs to be studied, if cycloalkanes are to be produced efficiently.

2. A Petroleum Fraction

The portion of petroleum that is soluble in heptane or pentane is often referred to as maltenes, and it can be further subdivided by percolation through any surface active material, *e.g.* alumina, to yield an oil fraction and a more strongly adsorbed resin fraction. Elemental constitutions of petroleum resins show that the proportions of carbon and hydrogen vary over a narrow range: 85±3% carbon and 10.5±1% hydrogen. Elemental compositions of the oils have shown that the H/C ratio is high, indicating more paraffinic or cycloparaffinic materials [7]. Both these fractions could yield desirable cycloalkanes by hydrotreatment.

3. Model compounds representing coal/resin liquids.

Model compounds have been used by fuel scientists to study the reactions of certain components of coal and its products during liquefaction. Results give a fundamental understanding of the hydrogenation and cracking behavior of these components. Data obtained by hydrotreating model compounds can provide information on the best conditions to produce a desired product from the system being modeled. Coal liquids tend to be aromatic in nature and thus need hydrotreatment to be suitable components of advanced jet fuels. Coal liquids contain multicyclic compounds varying from naphthalenes up to coronenes. The major group of compounds is naphthalenes, phenanthrenes, pyrenes and possibly chrysenes and perylenes. Resin liquids have been shown to contain some of these compounds along with bicadinanes and trimers of cadinene [8]. If cycloparaffins are to be produced from these feedstocks, it is necessary to model the hydrogenation behavior of these multicyclic compounds.

APPROACH TO THE PROBLEM

In this work, the above-mentioned starting materials will be hydrotreated and a set of time, temperature and catalyst conditions will be defined that gives high yields of desired jet fuel components, or compounds that can be easily converted to cycloparaffins. After initial studies of the chemistry involved in the reactions, the yield and composition of the liquid products will be compared for each feedstock reacted at the chosen optimum condition. The final test for each reaction system investigated will be to compare the thermal stability of surrogate liquids blended to have the same composition as the optimum feedstock products.

TECHNIQUES TO BE USED

All reactions will be carried out in 25 mL microautoclave reactors under hydrogen pressure of 7 MPa (cold). Various catalysts will be employed depending on their effectiveness in each reaction system. Products will be separated into liquid and solid (if any) fractions. Chemical composition and concentration of liquid products will be determined by GC and GC/MS. HPLC will be used on liquid products to determine if high molecular weight compounds are being produced. If necessary, heated probe mass spectrometry will be used to determine the structure of high molecular weight compounds not seen by GC/MS. The aromatic content of the liquids produced will be a major factor contributing to its thermal stability. Although GC/MS will determine any hydrogenation of specific compounds that has taken place during the reaction, it does not quantify overall changes in aromatic carbons. Liquid NMR will be used to determine the aromaticity of liquid products.

REVIEW OF RESEARCH ACCOMPLISHED TO DATE

1. Hydrogenation, dehydrogenation and cracking of Rosin.

As described in the introduction, rosin is composed primarily of isomers of abietic acid. If mono and bicyclic compounds are to be produced from rosin, the decarboxylation and cracking reactions have to be studied, along with the hydrogenation/dehydrogenation behavior of rosin and its products. The major objective of this part of the project was to ascertain how rosin product distribution varies with time of reaction, temperature and catalytic conditions. Reactions were carried out at 350, 400 and 450°C for reaction times up to 1 hour, using $NiMo/Al_2O_3$, ATTM and Ni-Y (zeolite) as catalysts. The concentrations of C_1-C_4 benzenes and C_1-C_4 naphthalenes/indenes were followed to indicate extent of cracking. Norabietatriene, tetrahydroretene and retene concentration changes were followed to indicate extent of decarboxylation and dehydrogenation (for chemical structures, see key at back of paper).

Figures 36-39 show how the product distribution varies with temperature, time and catalyst. It can be seen that in all cases, as temperature and time increase, the concentration of benzenes and naphthalenes in the liquid products increase. Benzenes are produced first in the cracking reaction. Scheme 1 shows the probable route of formation of benzenes.

Naphthalenes are produced later on in the reaction for the non-catalytic and NiMo experiments. This can be explained by cracking of the terminal ring in norabietatriene and tetrahydroretene to produce substituted naphthalenes (noncatalytic) and tetralins (catalytic). When Ni-Y is used as a catalyst, cracking reactions are predominant in the first 10 minutes. Dehydrogenation and isomerisation reactions predominate for the remainder of the reaction time.

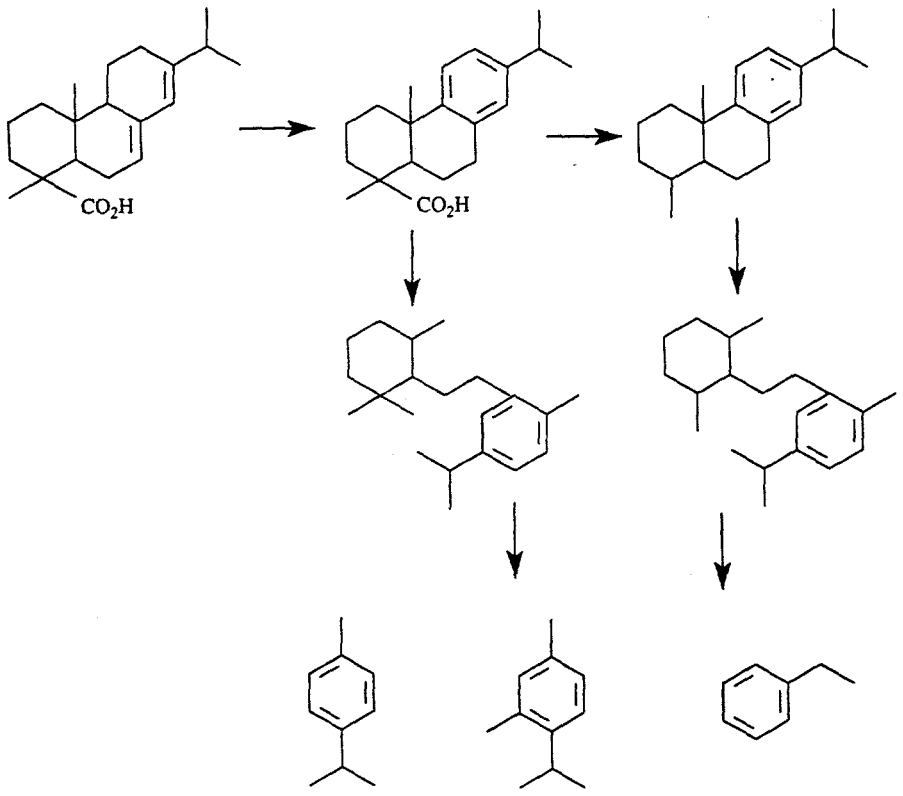

Scheme 1. Formation of benzenes from rosin

With this information, it appears that a catalytic stage is necessary to crack the three-ring structures to desirable benzenes and naphthalenes. This requires a high temperature, which favors dehydrogenation of cycloalkanes to aromatics. It is therefore necessary to stop the reaction at an optimum point, this being predicted from the product distribution graphs, lower the temperature to a point that hydrogenation will be favored over dehydrogenation, add a suitable hydrogenation catalyst and hydrogenate the products from the first stage to produce cycloalkanes. This process is termed reverse temperature staging.

Future Work

The decarboxylation of rosin needs to be studied more closely. This can be achieved by liquid NMR analysis. NMR spectra will be obtained on the liquids of the non-catalytic runs and the changes in the carboxylic acid functionality will be investigated. Liquid upgrading, *i.e.* second stage in the reverse temperature program, will be studied. Palladium on carbon catalyst is an excellent low-temperature hydrogenation catalyst. This will be used to hydrogenate the naphthalenes and phenanthrenes to tetralins and hydrophenanthrenes.

2. Hydrocracking reactions of dammar

Dammar has been shown to contain two fractions [9]. The methanol-insoluble fraction is proposed to be a polymer called polycadinene.

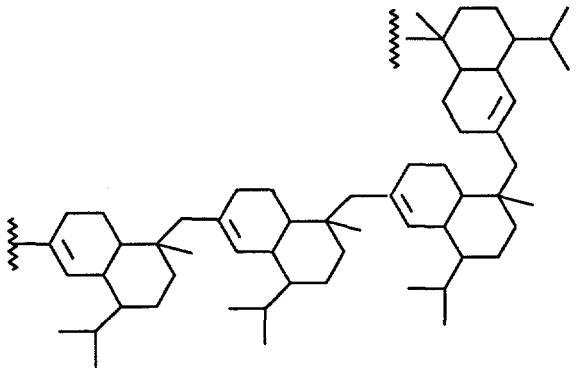

Polycadinene

The methanol-soluble fraction is composed of low molecular weight compounds shown by GC/MS to be dimers and trimers of cadinene and functionalized triterpenoids. Previous work has shown that the polymer constitutes approximately 16% of the whole resin [4]. Research into producing cycloalkanes from dammar will consist of four tasks:

1. Hydrocracking of whole dammar at various temperatures and times.

2. Separation of dammar into methanol-soluble/insoluble fractions, followed by hydrocracking of the two fractions.
3. Analysis of liquids by GC/MS and HPLC. Product distributions will be analyzed and reaction pathways proposed.
4. Utah resinite is a sesquiterpenoid polymer based on polycadinene. Dammar will be used to predict the behavior of resinite under liquefaction conditions. Results will be compared to samples of resinite obtained from coal by solvent extraction.

Figure 40 shows the product distribution for whole dammar hydrocracking for 1 hour at various reaction temperatures.

It can be seen that as reaction temperature increases, the large molecular weight compounds are being cracked to benzenes and naphthalenes. The naphthalenes are probably cracked products of polycadinene, although the extent of depolymerisation will not be known until reactions on this fraction alone are undertaken. Naphthalenes could also be produced from bicadinanes from the soluble fraction. Scheme 2 shows the possible reaction pathway.

Saturated naphthalene compounds are the likely source of benzenes in the cracking products. Figure 41 shows the product distribution for whole dammar hydrocracking at 450°C for various reaction times.

It can be seen that most of the high molecular weight compounds are cracked to dimers and trimers after only 10 minutes. These dimers and trimers then crack to produce naphthalenes. Most of this reaction occurs in the first 30 minutes. There is a steady increase in concentration of benzenes. These are produced from cracking of tetralins. From these results, it is clear that a reverse temperature stage reaction is the best way to produce cycloalkanes because most of the cracking reactions are complete after 30 minutes. If the reaction is allowed to continue, unnecessary dehydrogenation reactions will occur, making the upgrading stage more difficult. Figure 42 shows chromatograms of the naphthalenes in products before and after an upgrading step with palladium on carbon catalyst (300°C, 3 hours). It can be seen that the C_2 and C_3 naphthalenes have been almost totally converted to tetralins. The benzene fraction did not hydrogenate under these conditions.

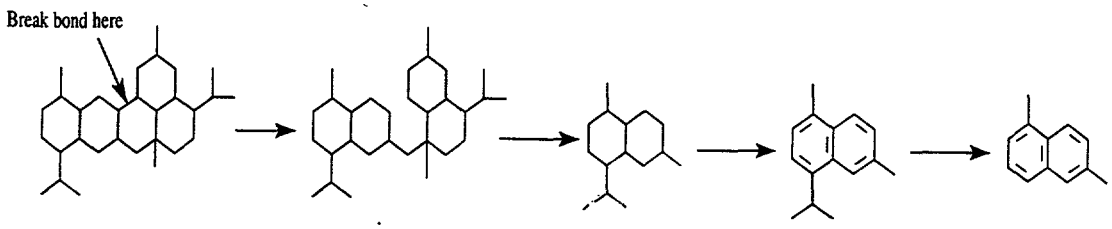

Scheme 2. Formation of naphthalenes from dammar

References

1. Song, C. and Hatcher, P.G. *Prepr. Pap.-Am. Chem. Soc., Div. Pet. Chem.* 1992, **37**(2), 529.

2. Song, C., Peng, Y., Jiang, H. and Schobert, H.H. *Prepr. Pap.-Am. Chem. Soc., Div. Pet. Chem.* 1992, **37**(2), 484.

3. Sharma, R.K. and Bakhshi, N.N. *Can. J. Chem. Eng.* 1991, **69**, 1071.

4 van Aarssen, B.G.K., Cox, H.C., Hoogendoorn, P., and de Leeuw, J.W. *Geochem. Cosmochim. Acta.* 1991, **54,** 3021.

5. Anderson, K.B., Winans, R.E., and Botto, R.E. *Org. Geochem.*. 1992, **18(6)**, 829.

6. Meuzelaar, H.L.C., Huai, H., Lo, R. and Dworzanski, J.P. *Fuel Processing Technol.* 1991, **28**, 119.

7. Speight, J.G. The Chemistry and Technology of Petroleum. (2nd ed.) 1991.

8. Mills, J.S. and Werner, A.E.A. *J. Chem. Soc.* 1955, 3132.

APPENDIX I

TABLES

Table 1. Retention Indices of Hydrocarbons Determined for Intermediately Polar (Rtx-50) and Slightly Polar (DB-5) Columns at Three Heating Rates.

Compounds	Molecular Ion	Base Peak	R.I. on Rtx-50			R.I. on DB-5		
			2°C/min	4°C/min	6°C/min	2°C/min	4°C/min	6°C/min
n-Pentane	72	43	500	500	500	500	500	500
n-Hexane	86	43	600	600	600	600	600	600
1-Hexene	84	56	606.4	607.0	607.7	588.2	587.9	587.9
n-Heptane	100	43	700	700	700	700	700	700
Cyclohexane	84	56	705.6	706.3	706.0	655.4	656.2	657.6
1-Heptene	98	56	708.3	708.4	709.5	688.0	689.0	689.4
Cyclohexene	82	67	736.1	740.0	739.3	677.1	676.7	678.8
Methylcyclohexane	98	83	748.1	749.5	752.4	718.3	720.0	720.3
Benzene	78	78	765.7	767.4	769.0	654.2	654.8	656.1
n-Octane	114	43	800	800	800	800	800	800
trans-1,4-Dimethylcyclohexane	112	97	801.8	802.3	803.5	775.6	776.7	777.3
cis-1,3-Dimethylcyclohexane	112	97	801.8	802.3	803.5	772.8	774.7	776.6
1-Octene	112	55	808.2	809.2	809.7	788.3	789.3	789.1
trans-1,2-Dimethylcyclohexane	112	97	820.9	822.4	825.0	796.7	798.0	798.4
1-Methylcyclohexene	96	81	824.1	827.0	829.2	763.9	765.3	766.4
cis-1,4-Dimethylcyclohexane	112	97	828.6	830.5	832.6	804.7	805.3	805.7
trans-1,3-Dimethylcyclohexane	112	97	830.9	832.2	835.4	804.1	805.3	806.2
cis-1,2-Dimethylcyclohexane	112	55	859.1	862.6	866.7	823.1	824.7	827.3
Ethylcyclohexane	112	83	862.3	865.5	867.4	826.9	829.1	830.9
Toluene	92	91	870.5	873.6	875.7	758.9	761.3	761.7
n-Nonane	128	43	900	900	900	900	900	900
Pyridine	79	79	908.9	910.3	913.4	735.6	736.7	739.1
1-Nonene	126	56	909.1	909.5	909.9	888.9	889.5	890.2
n-Propylcyclohexane	126	83	956.9	960.8	963.4	924.2	927.1	929.1
Ethylbenzene	106	91	968.1	971.5	975.2	853.2	856.3	857.2
1,4-Dimethylbenzene (*p*-Xylene)	106	91	972.3	975.7	979.2	861.7	864.4	866.5
1,3-Dimethylbenzene (*m*-Xylene)	106	91	974.2	977.9	981.2	861.7	864.4	866.5
n-Decane	142	43	1000	1000	1000	1000	1000	1000
1,2-Dimethylbenzene (*o*-Xylene)	106	91	1009.2	1012.5	1015.5	888.0	889.9	891.2
1-Decene	140	56	1010.3	1011.0	1011.3	989.2	989.5	990.7
trans-Octahydro-1H-indene	124	67	1011.6	1015.9	1018.8	947.7	952.0	955.3
tert-Butylcyclohexane	140	56	1015.1	1019.3	1022.6	978.1	982.2	985.2
Isopropylbenzene (cumene)	120	105	1028.2	1032.1	1034.7	919.4	922.2	923.6
cis-Octahydro-1H-indene	124	67	1053.0	1059.9	1063.2	981.0	985.8	989.5
n-Propylbenzene	120	91	1058.0	1063.0	1066.1	946.9	950.5	952.3
n-Butylcyclohexane	140	83	1059.5	1064.2	1066.5	1026.6	1030.2	1031.6
1-Ethyl-3-methylbenzene	120	105	1068.7	1073.1	1075.7	955.0	958.5	960.8
1-Ethyl-4-methylbenzene	120	105	1069.8	1074.0	1076.6	956.3	960.0	962.4
1,3,5-Trimethylbenzene (Mesitylene)	120	105	1074.4	1079.2	1081.6	961.5	964.9	967.1
tert-Butylbenzene	134	119	1097.6	1102.3	1104.5	987.1	990.5	992.0
4,5,6,7-Tetrahydroindan	122	79	1097.8	1103.7	1106.9	1008.6	1011.4	1014.8
1-Ethyl-2-methylbenzene	120	105	1098.2	1103.1	1105.3	973.3	977.2	979.7
n-Undecane	156	57	1100	1100	1100	1100	1100	1100
1,2,4-Trimethylbenzene	120	105	1106.8	1111.9	1114.6	987.5	991.1	992.8
1-Undecene	154	41	1110.6	1111.0	1111.0	1090.9	1091.4	1091.4
sec-Butylbenzene	134	105	1112.9	1117.6	1120.3	1006.4	1008.9	1011.7
trans-Decalin	138	138	1114.7	1122.4	1127.2	1045.7	1051.8	1055.9
1,1'-Bicyclopentyl	138	68	1138.6	1145.9	1151.2	1071.8	1077.6	1080.9
1,2,3-Trimethylbenzene	120	105	1147.6	1155.0	1158.9	1016.0	1019.9	1022.7
Phenylethylether	122	94	1150.0	1154.1	1156.9	988.8	991.1	992.4
n-Butylbenzene	134	91	1163.2	1168.6	1171.1	1050.1	1053.7	1055.9
n-Pentylcyclohexane	154	83	1163.7	1169.4	1172.0	1130.2	1134.7	1136.0
cis-Decalin	138	67	1174.6	1184.4	1190.2	1089.5	1096.1	1100.4
Indan	118	117	1180.4	1188.7	1193.5	1027.4	1032.4	1035.5
n-Dodecane	170	57	1200	1200	1200	1200	1200	1200
1-Dodecene	168	55	1211.6	1212.4	1211.9	1191.3	1191.3	1191.3
2-Methylindan	132	117	1212.8	1220.8	1225.8	1074.3	1079.5	1082.0
1-Methylindan	132	117	1222.7	1231.2	1236.5	1079.3	1084.8	1087.1
1,2,4,5-Tetramethylbenzene	134	119	1235.1	1242.4	1247.5	1109.7	1114.1	1115.8
n-Hexylcyclohexane	168	83	1269.0	1274.4	1276.6	1233.9	1237.7	1239.5
1,4-Diisopropylbenzene	162	147	1279.9	1285.1	1288.1	1170.1	1173.4	1174.7
5-Methylindan	132	117	1282.5	1292.7	1298.4	1131.1	1137.1	1139.9
1,2,3,4-Tetramethylbenzene	134	119	1286.4	1296.3	1302.6	1144.2	1149.9	1153.8
2,6-Dimethylphenol	122	107	1297.6	1305.3	1310.7	1102.3	1104.6	1105.5
n-Tridecane	184	57	1300	1300	1300	1300	1300	1300
4-Methylindan	132	117	1301.2	1312.0	1318.8	1141.6	1147.7	1151.4
1-Tridecene	182	55	1311.8	1312.0	1312.4	1291.5	1291.3	1292.2
Tetralin	132	104	1324.1	1336.0	1343.6	1151.7	1158.5	1162.5
1,3,5-Triethylbenzene	162	147	1338.5	1343.6	1346.2	1219.6	1222.3	1224.3
1,2-Dihydronaphthalene	130	130	1345.7	1358.8	1366.2			
n-Hexylbenzene	162	91	1370.1	1376.3	1379.9	1254.6	1258.4	1260.9
Bicyclohexyl	166	82	1377.5	1390.4	1397.4	1293.1	1301.5	1307.8
Naphthalene	128	128	1386.8	1401.2	1410.9	1171.5	1179.7	1183.4
2,4,6-Trimethylphenol	136	121	1397.4	1406.7	1412.2	1199.1	1202.5	1204.1
n-Tetradecane	198	57	1400	1400	1400	1400	1400	1400
1-Tetradecene	196	55	1412.5	1412.8	1412.7	1391.7	1391.4	1392.2
Benzothiophene	134	134	1415.7	1432.0	1442.5	1180.5	1188.3	1192.9
2,3-Dihydroindole	119	118	1455.5	1469.2	1479.2	1195.8	1202.2	1206.6
Cyclohexylbenzene	160	104	1475.5	1489.0	1497.7	1308.9	1317.7	1322.9

Table 1 (continued)

Compounds	Molecular Ion	Base Peak	R.I. on Rtx-50			R.I. on DB-5		
			2°C/min	4°C/min	6°C/min	2°C/min	4°C/min	6°C/min
1-Indanol	134	133	1476.6	1489.0	1496.8	1224.7	1229.9	1232.9
n-Octylcyclohexane	196	83	1480.1	1485.7	1489.6	1442.4	1447.5	1449.1
Quinoline	129	129	1493.6	1510.6	1521.6	1224.7	1233.0	1237.4
n-Pentadecane	212	57	1500	1500	1500	1500	1500	1500
2-Methylnaphthalene	142	142	1501.0	1517.3	1528.6	1281.5	1290.5	1296.3
1-Pentadecene	210	55	1512.7	1513.1	1513.1	1492.4	1492.5	1492.3
1-Methylnaphthalene	142	142	1530.2	1548.7	1559.6	1297.1	1306.8	1313.4
Dodecahydrofluorene	178	97	1556.9	1576.9	1588.7			
8-Methylquinoline	143	143	1562.7	1580.1	1591.1	1304.5	1313.9	1319.5
1,2-Dicyclohexylethane	194	83	1568.2	1582.1	1589.2	1486.9	1496.3	1501.0
5,6,7,8-Tetrahydro-3-methylquinoline	147	146	1571.5	1586.5	1595.8	1330.2	1338.6	1343.7
n-Octylbenzene	190	92	1580.2	1587.2	1590.6	1461.6	1466.5	1468.2
n-Hexadecane	226	57	1600	1600	1600	1600	1600	1600
1,2,3,4-Tetrahydroquinoline	133	132	1600.0	1617.6	1627.8	1318.5	1326.8	1332.5
2,6-Di-tert-butylphenol	206	191	1603.1	1613.2	1619.7	1433.6	1440.1	1443.2
2-Ethylnaphthalene	156	141	1604.3	1621.6	1632.3	1380.6	1390.6	1396.1
1-Hexadecene	224	55	1613.1	1613.2	1613.1	1591.7	1591.6	1592.7
2,7-Dimethylnaphthalene	156	156	1613.3	1631.8	1641.9	1392.1	1402.2	1409.5
2,6-Dimethylnaphthalene	156	156	1615.5	1633.1	1643.9	1390.6	1400.9	1407.3
1,1'-Biphenyl (Diphenyl)	154	154	1615.7	1631.8	1641.9	1368.5	1377.3	1381.8
2-Methylbiphenyl	168	168	1620.2	1634.5	1644.4	1390.0	1397.6	1402.3
1-Ethylnaphthalene	156	141	1621.0	1639.2	1650.0	1383.6	1393.8	1400.0
1,3-Dimethylnaphthalene	156	156	1642.2	1661.8	1673.2	1405.3	1416.5	1422.3
1,6-Dimethylnaphthalene	156	156	1643.3	1662.5	1675.3	1408.4	1419.6	1427.3
2-Isopropylnaphthalene	170	155	1660.5	1677.4	1687.9	1443.9	1454.0	1459.1
1,4-Dimethylnaphthalene	156	156	1672.6	1692.9	1707.4	1424.2	1436.3	1443.2
1,5-Dimethylnaphthalene	156	156	1678.1	1699.0	1714.2	1428.3	1439.8	1446.4
1-Isopropylnaphthalene	170	155	1684.5	1701.8	1713.7	1451.1	1460.9	1465.9
n-Decylcyclohexane	224	83	1692.2	1698.0	1702.1	1650.7	1656.2	1658.4
1,2-Dimethylnaphthalene	156	156	1692.4	1713.6	1728.6	1439.6	1452.2	1459.1
n-Heptadecane	240	57	1700	1700	1700	1700	1700	1700
5,6,7,8-Tetrahydro-1-naphthol	148	120	1725.3	1743.8	1756.3	1440.8	1447.2	1450.9
3-Methylbiphenyl	168	168	1725.5	1742.3	1753.7	1474.5	1483.5	1487.7
1,8-Dimethylnaphthalene	156	156	1730.1	1752.7	1765.3	1459.7	1472.7	1480.0
4-Methylbiphenyl	168	168	1735.7	1753.4	1766.3	1482.8	1492.2	1497.3
Acenaphthene	154	154	1752.8	1777.6	1794.2	1468.0	1481.4	1488.6
1,2-Diphenylethane (Bibenzyl)	182	91	1758.7	1776.5	1787.9	1508.8	1519.2	1524.3
Dibenzofuran	168	168	1783.4	1808.2	1825.4	1499.4	1513.0	1520.9
n-Decylbenzene	218	92	1791.1	1799.6	1805.5	1669.5	1674.8	1677.7
n-Octadecane	254	57	1800	1800	1800	1800	1800	1800
1-Octadecene	252	55	1814.4	1814.5	1814.9	1792.6	1792.1	1793.5
3,3'-Dimethylbiphenyl	182	182	1837.3	1853.9	1865.7	1580.2	1589.0	1594.2
2-Naphthol	144	144	1849.4	1871.7	1885.6	1514.5	1520.5	1523.8
4,4'-Dimethylbiphenyl	182	182	1856.6	1875.1	1887.8	1596.8	1607.6	1614.2
Fluorene	166	166	1869.3	1895.2	1913.9	1565.2	1579.5	1587.9
n-Nonadecane	268	57	1900	1900	1900	1900	1900	1900
2,6-Diisopropylnaphthalene	212	197	1925.5	1943.7	1956.1	1716.8	1728.0	1735.5
Dibenzylether	198	92	1943.4	1961.4	1974.0	1641.4	1650.3	1656.9
9,10-Dihydroanthracene	180	179	1983.3	2011.1	2028.7	1662.1	1676.6	1685.3
n-Eicosane	282	57	2000	2000	2000	2000	2000	2000
n-Dodecylbenzene	246	92	2005.0	2014.4	2019.5			
9,10-Dihydrophenanthrene	180	180	2010.2	2040.3	2059.1	1673.5	1689.8	1699.5
1,2,3,4,5,6,7,8-Octahydroanthracene	186	186				1680.2	1694.1	1703.2
1,2,3,4,5,6,7,8-Octahydrophenanthrene	186	186				1705.5	1721.1	1730.6
1,2,3,4,5,6,7,8-Octahydroacridine	187	186	2037.8	2067.9	2086.0	1712.2	1726.5	1736.6
1,2,3,4-Tetrahydroanthracene	182	182				1731.3	1748.7	1760.2
1,2,3,4-Tetrahydrophenanthrene	182	182				1737.6	1755.2	1767.7
n-Henicosane	296	57	2100	2100	2100	2100	2100	2100
Phenanthrene	178	178	2136.9	2174.0	2196.8	1756.9	1776.3	1789.2
Anthracene	178	178	2146.5	2183.0	2207.3	1767.0	1786.4	1800.0
1,2,3,4-Tetrahydrocarbazole	171	143	2190.6	2229.6	2250.0	1786.6	1800.4	1811.8
n-Docosane	310	57	2200	2200	2200	2200	2200	2200
1-Phenylnaphthalene	204	204	2224.1	2256.1	2276.0	1841.7	1858.2	1868.0
n-Tricosane	324	57	2300	2300	2300	2300	2300	2300
1-Methylanthracene	192	192				1934.8	1959.3	1976.3
n-Tetracosane	338	57	2400	2400	2400	2400	2400	2400
Fluoranthene	202	202	2494.8	2544.9	2578.2	2032.6	2060.1	2076.5
n-Pentacosane	352	57	2500	2500	2500	2500	2500	2500
Pyrene	202	202	2580.4	2636.3	2673.1	2082.6	2113.4	2132.5
9,10-Dimethylanthracene	206	206	2582.5	2632.1	2664.6	2107.6	2135.5	2152.6
n-Hexacosane	366	57	2600	2600	2600	2600	2600	2600
p-Terphenyl	230	230	2627.1	2665.3	2690.0	2171.1	2190.9	2204.0
n-Triacontane	422	57	3000	3000	3000	3000	3000	3000
Chrysene	228	228	3036.9	3107.4	3153.2	2434.2	2472.3	2494.9
n-Hentriacontane	436	57	3100	3100	3100	3100	3100	3100

Table 2. Final Elution Temperatures and Retention Indices of 1-Alkenes on Rtx-50 Column at Three Heating Rates.

	Heating rates					
	2°C/min		4°C/min		6°C/min	
Compounds	T (°C)	R.I.	T (°C)	R.I.	T (°C)	R.I.
1-Hexene	43.7	606.4	47.4	607.0	51.1	607.7
1-Heptene	44.8	708.3	49.3	708.4	53.7	709.5
1-Octene	47.1	808.2	53.4	809.2	59.1	809.7
1-Nonene	51.8	909.1	60.8	909.5	68.1	909.9
1-Decene	59.9	1010.3	71.7	1011.0	80.7	1011.3
1-Undecene	71.0	1110.6	84.9	1111.0	95.0	1111.0
1-Dodecene	83.9	1211.6	99.2	1212.4	109.9	1211.9
1-Tridecene	97.3	1311.8	113.4	1312.0	124.5	1312.4
1-Tetradecene	110.5	1412.5	127.1	1412.8	138.5	1412.7
1-Pentadecene	123.2	1512.7	140.2	1513.1	151.8	1513.1
1-Hexadecene	135.3	1613.1	152.6	1613.2	164.4	1613.1
1-Octadecene	157.9	1814.4	175.6	1814.5	187.8	1814.9

Table 3. Temperature Dependence of Retention Indices for Cycloalkanes and Benzenes.

Compounds	Rtx-50			DB-5		
	Temp. Range (°C)	R.I. Range	ΔR.I./ΔT	Temp. Range (°C)	R.I. Range	ΔR.I./ΔT
Cyclohexane	44.7-53.6	705.6-706.0	0.04	44.6-53.1	655.4-657.6	0.25
Cyclohexene	45.4-55.2	736.1-739.3	0.32	44.9-53.9	677.1-678.8	0.19
Methylcyclohexane	45.6-55.9	748.1-752.4	0.41	46.0-56.3	718.3-720.3	0.19
Benzene	46.0-56.7	765.7-769.0	0.31	44.5-53.0	654.2-656.1	0.22
trans-1,4-Dimethylcyclohexane	46.8-58.6	801.8-803.5	0.14	48.0-60.7	775.6-777.3	0.14
cis-1,3-Dimethylcyclohexane	46.8-58.6	801.8-803.5	0.14	47.9-60.6	772.8-776.6	0.30
trans-1,2-Dimethylcyclohexane	47.7-60.5	820.9-825.0	0.32	48.8-62.3	796.7-798.4	0.13
1-Methylcyclohexene,	47.8-60.8	824.1-829.2	0.39	47.6-59.9	763.9-766.4	0.20
cis-1,4-Dimethylcyclohexane	48.0-61.1	828.6-832.6	0.31	49.2-63.1	804.7-805.7	0.07
trans-1,3-Dimethylcyclohexane	48.1-61.4	830.9-835.4	0.34	49.2-63.2	804.1-806.2	0.15
cis-1,2-Dimethylcyclohexane	49.3-64.1	859.1-866.7	0.51	50.5-65.6	823.1-827.3	0.28
Ethylcyclohexane	49.5-64.1	862.3-867.4	0.35	50.7-66.0	826.9-830.9	0.26
Toluene	49.8-64.8	870.5-875.7	0.35	47.4-59.5	758.9-761.7	0.23
n-Propylcyclohexane	55.5-74.6	956.9-963.4	0.34	58.3-78.2	924.2-929.1	0.24
Ethylbenzene	56.4-76.1	968.1-975.2	0.36	52.5-69.1	853.2-857.2	0.24
1,4-Dimethylbenzene	56.7-76.5	972.3-979.2	0.35	53.1-70.2	861.7-866.5	0.28
1,3-Dimethylbenzene	56.8-76.8	974.2-981.2	0.35	53.1-70.2	861.7-866.5	0.28
1,2-Dimethylbenzene	59.8-81.3	1009.2-1015.5	0.29	54.9-73.1	888.0-891.2	0.18
trans-Octahydro-1H-Indene	60.1-81.8	1011.6-1018.8	0.33	60.7-81.9	947.7-955.3	0.36
tert-Butylcyclohexane	60.4-82.3	1015.1-1022.6	0.34	63.9-86.2	978.1-985.2	0.32
Isopropylbenzene	61.9-84.0	1028.2-1034.7	0.30	57.8-77.4	919.4-923.6	0.21
cis-Octahydro-1H-Indene	64.6-88.1	1053.0-1063.2	0.43	64.2-86.8	981.0-989.5	0.38
n-Propylbenzene	65.1-88.5	1058.0-1066.1	0.35	60.6-81.5	946.9-952.3	0.26
n-Butylcyclohexane	65.3-88.6	1059.5-1066.5	0.30	69.5-93.2	1026.6-1031.6	0.21
1-Ethyl-3-methylbenzene	66.2-89.9	1068.7-1075.7	0.29	61.5-82.7	955.0-960.8	0.27
1-Ethyl-4-methylbenzene	66.4-90.0	1069.8-1076.6	0.29	61.6-83.0	956.3-962.4	0.29
1,3,5-Trimethylbenzene	66.9-90.8	1074.4-1081.6	0.30	62.1-83.6	961.5-967.1	0.26
tert-Butylbenzene	69.4-94.1	1097.6-1104.5	0.28	64.8-87.2	987.1-992.0	0.21
4,5,6,7-Tetrahydroindan	69.4-94.4	1097.8-1106.9	0.36	67.2-90.6	1008.6-1014.8	0.27
1-Ethyl-2-methylbenzene	69.5-94.2	1098.2-1105.3	0.29	63.4-85.4	973.3-979.7	0.29
1,2,4-Trimethylbenzene	70.5-95.6	1106.8-1114.6	0.31	64.8-87.3	987.5-992.8	0.24
sec-Butylbenzene	71.3-96.4	1112.9-1120.3	0.29	67.0-90.1	1006.4-1011.7	0.23
trans-Decalin	71.5-97.4	1114.7-1127.2	0.49	72.0-96.9	1045.7-1055.9	0.41
1,1'-Bicyclopentyl	74.6-101.0	1138.6-1151.2	0.48	75.3-100.7	1071.8-1080.9	0.35
1,2,3-Trimethylbenzene	75.7-102.1	1147.6-1158.9	0.43	68.2-91.8	1016.0-1022.7	0.28
Phenylethylether	76.0-101.8	1150.0-1156.9	0.27	65.0-87.2	988.8-992.4	0.16
n-Butylbenzene	77.7-103.9	1163.2-1171.1	0.30	72.5-96.9	1050.1-1055.9	0.24
n-Pentylcyclohexane	77.7-104.0	1163.7-1172.0	0.31	83.1-109.1	1130.2-1136.0	0.22
cis-Decalin	79.1-106.7	1174.6-1190.2	0.57	77.6-103.7	1089.5-1100.4	0.42
Indan	79.9-107.2	1180.4-1193.5	0.48	69.6-93.8	1027.4-1035.5	0.34
2-Methylindan	84.1-111.9	1212.8-1225.8	0.47	75.6-100.9	1074.3-1082.0	0.30
1-Methylindan	85.4-113.5	1222.7-1236.5	0.49	76.3-101.7	1079.3-1087.1	0.31
1,2,4,5-Tetramethylbenzene	87.0-115.1	1235.1-1247.5	0.44	80.3-106.1	1109.7-1115.8	0.24
n-Hexylcyclohexane	91.6-119.4	1269.0-1276.6	0.28	97.3-124.6	1233.9-1239.5	0.21
1,4-Diisopropylbenzene	93.0-121.1	1279.9-1288.1	0.29	88.6-115.0	1170.1-1174.7	0.18
5-Methylindan	93.4-122.6	1282.5-1298.4	0.54	83.2-109.7	1131.1-1139.9	0.33
1,2,3,4-Tetramethylbenzene	93.9-123.2	1286.4-1302.6	0.55	85.0-111.8	1144.2-1153.8	0.36
4-Methylindan	95.9-125.4	1301.2-1318.8	0.60	84.6-111.5	1141.6-1151.4	0.37
1,3,5-Triethylbenzene	100.8-129.3	1338.5-1346.2	0.27	95.4-122.4	1219.6-1224.3	0.17
n-Hexylbenzene	105.0-134.0	1370.1-1379.9	0.34	100.2-127.7	1254.6-1260.9	0.23
Bicyclohexyl	106.0-136.5	1377.5-1397.4	0.65	105.4-134.5	1293.1-1307.8	0.50
n-Octylcyclohexane	119.1-148.7	1480.1-1489.6	0.32	124.9-153.8	1442.4-1449.1	0.23
1,2-Dicyclohexylethane	129.9-161.5	1568.2-1589.2	0.67	130.5-160.6	1486.9-1501.0	0.47
n-Octylbenzene	131.4-161.7	1580.2-1590.6	0.34	127.3-156.3	1461.6-1468.2	0.23
n-Decylcyclohexane	144.5-175.0	1692.2-1702.1	0.32	149.9-179.7	1650.7-1658.4	0.26
n-Decylbenzene	155.4-186.8	1791.1-1805.5	0.46	152.1-182.0	1669.5-1677.7	0.27
n-Dodecylbenzene	177.4-209.3	2005.0-2019.5	0.45			

Table 4. Temperature Dependence of Retention Indices for Aromatics, and N-, S-, and O-Containing Compounds.

Compounds	Rtx-50			DB-5		
	Temp. Range (°C)	R.I. Range	ΔR.I./ΔT	Temp. Range (°C)	R.I. Range	ΔR.I./ΔT
Tetralin	98.9-128.9	1324.1-1343.6	0.65	86.0-113.1	1151.7-1162.5	0.40
1,2-Dihydronaphthalene	101.8-132.1	1345.7-1366.2	0.68			
Naphthalene	107.2-138.3	1386.8-1410.9	0.77	88.8-116.3	1171.5-1183.4	0.43
2-Methylnaphthalene	121.8-153.8	1501.0-1528.6	0.87	103.8-132.9	1281.5-1296.3	0.51
1-Methylnaphthalene	125.3-157.7	1530.2-1559.6	0.91	106.0-135.3	1297.1-1313.4	0.56
Dodecahydrofluorene	128.6-161.4	1556.9-1588.7	0.97			
2-Ethylnaphthalene	134.3-166.7	1604.3-1632.3	0.86	117.0-146.7	1380.6-1396.1	0.52
2,7-Dimethylnaphthalene	135.3-167.9	1613.3-1641.9	0.88	118.5-148.5	1392.1-1409.5	0.58
2,6-Dimethylnaphthalene	135.6-168.1	1615.5-1643.9	0.87	118.3-148.2	1390.6-1407.3	0.56
1,1'-Biphenyl	135.6-167.9	1615.7-1641.9	0.81	115.4-144.8	1368.5-1381.8	0.45
2-Methylbiphenyl	136.1-168.2	1620.2-1644.4	0.76	118.3-147.6	1390.0-1402.3	0.42
1-Ethylnaphthalene	136.2-168.8	1621.0-1650.0	0.89	117.4-147.3	1383.6-1400.0	0.55
1,7-Dimethylnaphthalene	138.3-171.2	1638.6-1670.2	0.96			
1,3-Dimethylnaphthalene	138.7-171.6	1642.2-1673.2	0.94	120.2-150.2	1405.3-1422.3	0.57
1,6-Dimethylnaphthalene	138.8-171.8	1643.3-1675.3	0.97	120.6-150.9	1408.4-1427.3	0.62
2-Isopropylnaphthalene	140.8-173.3	1660.5-1687.9	0.84	125.1-155.1	1443.9-1459.1	0.51
2,3-Dimethylnaphthalene	141.4-174.6	1665.9-1698.5	0.98			
1,4-Dimethylnaphthalene	142.2-175.6	1672.6-1707.4	1.04	122.6-153.0	1424.2-1443.2	0.63
1,5-Dimethylnaphthalene	142.9-176.4	1678.1-1714.2	1.08	123.1-153.4	1428.3-1446.4	0.60
1-Isopropylnaphthalene	143.6-176.3	1684.5-1713.7	0.89	126.0-156.0	1451.1-1465.9	0.49
1,2-Dimethylnaphthalene	144.5-178.1	1692.4-1728.6	1.08	124.6-155.1	1439.6-1459.1	0.64
3-Methylbiphenyl	148.2-180.9	1725.5-1753.7	0.86	128.9-158.9	1474.5-1487.7	0.44
1,8-Dimethylnaphthalene	148.7-182.2	1730.1-1765.3	1.05	127.1-157.8	1459.7-1480.0	0.66
4-Methylbiphenyl	149.3-182.3	1735.7-1766.3	0.93	130.0-160.1	1482.8-1497.3	0.48
Acenaphthene	151.2-185.5	1752.8-1794.2	1.21	128.1-159.0	1468.0-1488.6	0.67
1,2-Diphenylethane (Bibenzyl)	151.8-184.8	1758.7-1787.9	0.89	133.2-163.5	1508.8-1524.3	0.51
3,3'-Dimethylbiphenyl	160.3-193.3	1837.3-1865.7	0.86	141.8-172.1	1580.2-1594.2	0.46
4,4'-Dimethylbiphenyl	162.4-195.7	1856.6-1887.8	0.94	143.8-174.5	1596.8-1614.2	0.57
Fluorene	163.7-198.5	1869.3-1913.9	1.28	140.0-171.3	1565.2-1587.9	0.72
2,6-Diisopropylnaphthalene	169.5-202.8	1925.5-1956.1	0.92	157.4-188.6	1716.8-1735.5	0.60
9,10-Dihydroanthracene	175.2-210.2	1983.3-2028.7	1.30	151.2-182.9	1662.1-1685.3	0.73
9,10-Dihydrophenanthrene	177.9-213.2	2010.2-2059.1	1.39	152.5-184.6	1673.5-1699.5	0.81
1,2,3,4,5,6,7,8-Octahydroanthracene				153.3-185.0	1680.2-1703.2	0.73
1,2,3,4,5,6,7,8-Octahydrophenanthrene				156.1-188.1	1705.5-1730.6	0.79
1,2,3,4-Tetrahydroanthracene				158.9-191.4	1731.3-1760.2	0.89
1,2,3,4-Tetrahydrophenanthrene				159.6-192.2	1737.6-1767.7	0.93
Phenanthrene	189.9-226.4	2136.9-2196.8	1.64	161.7-194.6	1756.9-1789.2	0.98
Anthracene	190.8-227.4	2146.5-2207.3	1.66	162.8-195.8	1767.0-1800.0	1.00
1-Phenylnaphthalene	197.8-233.6	2224.1-2276.0	1.45	170.7-203.1	1841.7-1868.0	0.81
1-Methylanthracene				180.2-214.2	1934.8-1976.3	1.22
Fluoranthene	220.6-259.0	2494.8-2578.2	2.17	189.7-224.1	2032.6-2076.5	1.28
Pyrene	227.3-266.4	2580.4-2673.1	2.37	194.4-229.4	2082.6-2132.5	1.43
9,10-Dimethylanthracene	227.5-265.8	2582.5-2664.6	2.14	196.7-231.2	2107.6-2152.6	1.30
p-Terphenyl	230.9-267.8	2627.1-2690.0	1.71	202.4-236.0	2171.1-2204.0	0.98
Chrysene	259.9-300.2	3036.9-3153.2	2.88	224.6-260.9	2434.2-2494.9	1.67
2,6-Dimethylphenol	95.4-124.3	1297.6-1310.7	0.45	79.2-104.5	1102.3-1105.5	0.13
2,4,6-Trimethylphenol	108.6-138.5	1397.4-1412.2	0.50	92.6-119.4	1199.1-1204.1	0.19
Benzothiophene	110.9-142.5	1415.7-1442.5	0.85	90.0-117.8	1180.5-1192.9	0.45
2,3-Dihydroindole	116.0-147.3	1455.5-1479.2	0.76	92.1-119.8	1195.8-1206.6	0.39
1-Indanol	118.7-149.7	1476.6-1496.8	0.65	96.1-123.6	1224.7-1232.9	0.30
Quinoline	120.9-152.9	1493.6-1521.6	0.88	96.1-124.3	1224.7-1237.4	0.45
8-Methylquinoline	129.3-161.7	1562.7-1591.1	0.87	107.0-136.1	1304.5-1319.5	0.51
5,6,7,8-Tetrahydro-3-methylquinoline	130.3-162.3	1571.5-1595.8	0.76	110.4-139.5	1330.2-1343.7	0.47
1,2,3,4-Tetrahydroquinoline	133.8-166.2	1600.0-1627.8	0.86	108.8-137.9	1318.5-1332.5	0.48
2,6-Di-*tert*-butylphenol	134.2-165.2	1603.1-1619.7	0.53	123.8-153.0	1433.6-1443.2	0.33
5,6,7,8-Tetrahydro-1-naphthol	148.2-181.2	1725.3-1756.3	0.94	124.7-154.0	1440.8-1450.9	0.35
Dibenzofuran	154.6-188.9	1783.4-1825.4	1.22	132.1-163.1	1499.4-1520.9	0.69
2-Naphthol	161.6-195.5	1849.4-1885.6	1.07	133.9-163.4	1514.5-1523.8	0.31
Dibenzylether	171.3-204.7	1943.4-1974.0	0.92	148.9-179.6	1641.4-1656.9	0.50
1,2,3,4,5,6,7,8-Octahydroacridine	180.5-215.9	2037.8-2086.0	1.36	156.9-188.7	1712.2-1736.6	0.77
1,2,3,4-Tetrahydrocarbazole	194.8-231.2	2190.6-2250.0	1.63	164.9-197.1	1786.6-1811.8	0.79

Table 5. Retention Times and Retention Indices on DB-5 Column Measured at the Heating Rate of 4 °C/min with and without Isothermal Initial Holding Period.

Compounds	Retention time (min)			Retention index		
	IH[a]=0	IH=5	difference	IH=0	IH=5	difference
Benzene	2.21	2.34	0.13	654.8	653.8	-0.9
Cyclohexane	2.22	2.35	0.13	656.2	654.9	-1.2
1-Octene	3.88	4.82	0.94	789.3	788.4	-0.9
cis-1,2-Dimethylcyclohexane	4.65	6.09	1.44	824.7	824.4	-0.2
Ethylcyclohexane	4.76	6.25	1.49	829.1	828.4	-0.8
Ethylbenzene	5.43	7.36	1.93	856.3	855.5	-0.8
n-Propylcyclohexane	7.39	10.36	2.97	927.1	926.4	-0.7
1-Ethyl-3-methylbenzene	8.41	11.80	3.39	958.5	958.6	0.2
4,5,6,7-Tetrahydroindan	10.17	14.07	3.90	1011.4	1009.9	-1.5
n-Butylcyclohexane	10.85	14.88	4.03	1030.2	1028.9	-1.3
trans-Decalin	11.63	15.77	4.14	1051.8	1049.8	-2.0
n-Butylbenzene	11.70	15.92	4.22	1053.7	1053.3	-0.5
5-Methylindan	14.74	19.30	4.56	1137.1	1135.1	-2.0
1,2,3,4-Tetramethylbenzene	15.21	19.82	4.61	1149.9	1148.2	-1.6
2,3-Dihydroindole	17.14	21.89	4.75	1202.2	1200.5	-1.7
2,4,6-Trimethylphenol	17.15	21.93	4.78	1202.5	1201.6	-0.9
1,3,5-Triethylbenzene	17.86	22.68	4.82	1222.3	1222.0	-0.4
1-Indanol	18.13	22.92	4.79	1229.9	1228.5	-1.4
n-Hexylcyclohexane	18.41	23.24	4.83	1237.7	1237.1	-0.6
1-Tridecene	20.33	25.26	4.93	1291.3	1291.9	0.5
Bicyclohexyl	20.69	25.60	4.91	1301.5	1301.2	-0.3
1-Methylnaphthalene	20.87	25.75	4.88	1306.8	1305.5	-1.3
1,2,3,4-Tetrahydroquinoline	21.55	26.43	4.88	1326.8	1325.1	-1.7
1,1'-Biphenyl	23.26	28.17	4.91	1377.3	1375.4	-1.9
2-Ethylnaphthalene	23.71	28.66	4.95	1390.6	1389.6	-1.0
1-Ethylnaphthalene	23.82	28.78	4.96	1393.8	1393.1	-0.7
2,6-Dimethylnaphthalene	24.06	29.02	4.96	1400.9	1400.0	-0.9
5,6,7,8-Tetrahydronaphthalenol	25.55	30.51	4.96	1447.2	1446.1	-1.1
n-Octylcyclohexane	25.56	30.54	4.98	1447.5	1447.1	-0.5
1,2-Dimethylnaphthalene	25.71	30.67	4.96	1452.2	1451.1	-1.1
2-Isopropylnaphthalene	25.77	30.75	4.98	1454.0	1453.6	-0.5
n-Octylbenzene	26.17	31.16	4.99	1466.5	1466.3	-0.2
1,8-Dimethylnaphthalene	26.37	31.35	4.98	1472.7	1472.1	-0.5
Acenaphthene	26.65	31.62	4.97	1481.4	1480.5	-0.9
4-Methylbiphenyl	27.00	32.00	5.00	1492.2	1492.3	0.0
1,2-Dicyclohexylethane	27.13	32.09	4.96	1496.3	1495.0	-1.2
Dibenzofuran	27.65	32.62	4.97	1513.0	1512.0	-1.0
2-Naphthol	27.88	32.87	4.99	1520.5	1520.1	-0.3
Fluorene	29.70	34.68	4.98	1579.5	1578.9	-0.6
3,3'-Dimethylbiphenyl	29.99	34.98	4.99	1589.0	1588.6	-0.3
1-Hexadecene	30.07	35.08	5.01	1591.6	1591.9	0.3
Dibenzylether	31.79	36.77	4.98	1650.3	1649.7	-0.7
n-Decylcyclohexane	31.96	36.95	4.99	1656.2	1655.9	-0.3
n-Decylbenzene	32.50	37.49	4.99	1674.8	1674.5	-0.3
9,10-Dihydroanthracene	32.55	37.54	4.99	1676.6	1676.2	-0.3
9,10-Dihydrophenanthrene	32.92	37.90	4.98	1689.3	1688.6	-0.7
1,2,3,4,5,6,7,8-Octahydroanthracene	33.06	38.06	5.00	1694.1	1694.1	0.0
1,2,3,4,5,6,7,8-Octahydroacridine	33.97	38.96	4.99	1726.5	1726.2	-0.4
2,6-Diisopropylnaphthalene	34.01	39.01	5.00	1728.0	1728.0	0.0
1,2,3,4-Tetrahydroanthracene	34.59	39.59	5.00	1748.7	1748.7	0.0
Phenanthrene	35.36	40.36	5.00	1776.3	1776.3	0.0
1-Octadecene	35.80	40.80	5.00	1792.1	1792.1	0.0
1,2,3,4-Tetrahydrocarbazole	36.03	41.02	4.99	1800.4	1800.0	-0.4
1-Phenylnaphthalene	37.54	42.54	5.00	1858.2	1858.2	0.0
Fluoranthene	42.59	47.59	5.00	2060.1	2060.1	0.0
Pyrene	43.85	48.85	5.00	2113.4	2113.4	0.0
9,10-Dimethylanthracene	44.36	49.35	4.99	2135.5	2135.1	-0.4
Dibenzylsulfid	44.62	49.60	4.98	2146.8	2145.9	-0.9
p-Terphenyl	45.64	50.64	5.00	2190.9	2190.9	0.0
Chrysene	51.64	56.63	4.99	2472.3	2471.8	-0.5

a) IH=isothermal initial holding period (minutes)

Table 6. Hydrocarbons in Coal-Derived JP-8C Jet Fuel Identified by Matching Retention Index on Rtx-50 Column at Two Heating Rates.

	R.I. at 4°C/min		R.I. at 6°C/min	
Compounds[a]	Std	JP-8C	Std	JP-8C
Cyclohexane	706.3	705.4	706.0	706.0
Methylcyclohexane	749.5	750.0	752.4	751.8
Benzene	767.4	767.4	769.0	768.7
trans-1,4-Dimethylcyclohexane	802.3	802.4	803.5	803.5
cis-1,3-Dimethylcyclohexane	802.3	802.4	803.5	803.5
trans-1,2-Dimethylcyclohexane	822.4	822.9	825.0	824.6
cis-1,4-Dimethylcyclohexane	830.5	831.2	832.6	832.4
trans-1,3-Dimethylcyclohexane	832.2	832.9	835.4	835.2
Ethylcyclohexane	865.5	865.3	867.4	866.9
Toluene	873.6	873.5	875.7	875.4
n-Propylcyclohexane	960.8	960.9	963.4	963.5
Ethylbenzene	971.5	971.6	975.2	975.5
1,4-Dimethylbenzene	975.7	975.5	979.2	978.5
1,3-Dimethylbenzene	977.9	977.4	981.2	980.5
1,2-Dimethylbenzene	1012.5	1012.3	1015.5	1015.6
trans-Octahydro-1H-indene	1015.9	1016.0	1018.8	1019.4
Isopropylbenzene	1032.1	1032.4	1034.7	1035.0
cis-Octahydro-1H-indene	1059.9	1060.2	1063.2	1063.7
n-Propylbenzene	1063.0	1063.3	1066.1	1066.2
n-Butylcyclohexane	1064.2	1064.5	1066.5	1067.1
1-Ethyl-4-methylbenzene	1074.0	1074.4	1076.6	1076.8
1,3,5-Trimethylbenzene	1079.2	1079.3	1081.6	1082.3
1-Ethyl-2-methylbenzene	1103.1	1103.1	1105.3	1105.7
1,2,4-Trimethylbenzene	1111.9	1112.2	1114.6	1115.1
trans-Decalin	1122.4	1122.4	1127.2	1127.8
1,2,3-Trimethylbenzene	1155.0	1155.0	1158.9	1159.2
n-Butylbenzene	1168.6	1168.3	1171.1	1171.8
n-Pentylcyclohexane	1169.4	1168.8	1172.0	1172.2
cis-Decalin	1184.4	1183.9	1190.2	1190.6
Indan	1188.7	1188.4	1193.5	1193.9
2-Methylindan	1220.8	1219.8	1225.8	1225.5
1-Methylindan	1231.2	1230.9	1236.5	1236.2
1,2,4,5-Tetramethylbenzene	1242.4	1242.5	1247.5	1247.3
n-Hexylcyclohexane	1274.4	1274.2	1276.6	1277.4
5-Methylindan	1292.7	1292.4	1298.4	1298.4
1,2,3,4-Tetramethylbenzene	1296.3	1296.3	1302.6	1302.6
4-Methylindan	1312.0	1312.0	1318.8	1318.9
Tetralin	1336.0	1335.9	1343.6	1343.3
n-Hexylbenzene	1376.3	1376.1	1379.9	1380.3
Bicyclohexyl	1390.4	1389.5	1397.4	1397.9
Naphthalene	1401.2	1401.2	1410.9	1410.8
n-Octylcyclohexane	1485.7	1485.9	1489.6	1489.6
Cyclohexylbenzene	1489.0	1489.0	1497.7	1497.3
2-Methylnaphthalene	1517.3	1517.4	1528.6	1528.0
1-Methylnaphthalene	1548.7	1548.6	1559.6	1559.7
1,2-Dicyclohexylethane	1582.1	1582.0	1589.2	1589.6
n-Octylbenzene	1587.2	1587.5	1590.6	1591.0
2,7-Dimethylnaphthalene	1631.8	1631.2	1641.9	1642.2
1,1'-Biphenyl	1631.8	1631.2	1641.9	1642.2
2,6-Dimethylnaphthalene	1633.1	1632.5	1643.9	1644.2
1,3-Dimethylnaphthalene	1661.8	1662.0	1673.2	1673.4
1,6-Dimethylnaphthalene	1662.5	1662.7	1675.3	1674.9
n-Decylcyclohexane	1698.0	1698.0	1702.1	1702.1
3-Methylbiphenyl	1742.3	1742.9	1753.7	1753.7

a) Excluding the n-alkanes that are also present in JP-8C jet fuel.

Table 7. Compositions and LC and Distillate Fractions of JP-8P and JP-8C Jet Fuels.

Compositions, Wt %		
Compound Classes	JP-8P	JP-8C
Paraffins	61	10
Cyclohexanes	14	40
Benzenes	15	11
Decalins	1	15
Tetralins	<1	8
Indans	1	6
Others[a]	7	10

LC fraction, Wt %[b]			
Fraction No.	Elution System solvent	JP-8P	JP-8C
1	n-Pentane	85.2	77.9
2	5% Benzene-Pentane	6.9	9.1
3	Benzene	4.9	11.1
4	1% EtOH-Chloroform	0.7	0.5
5	10% EtOH-THF	1.0	1.0

Distillate fraction, Vol %[c]		
Temperature	JP-8P	JP-8C
IBP-165°C	8.3	27.0
165-185°C	22.2	14.9
185-215°C	32.8	22.2
215-240°C	22.9	17.1
240+°C	13.8	18.8

a) Including polycyclic alkanes, aromatics, and hydroaromatics as well as polar compounds including antioxidants, and trace amounts of unidentified compounds.

b) From separation on neutral alumina column, as described in reference 15.

c) From reference 14.

Table 8. Percent Weight of the Compounds Identified in the Liquids after Thermal Stressing of n-Octane+Decalin Alone and with 50, 150 and 250 mg PX-21.

Compounds identified	n octane+ decalin	n octane+ decalin+ 50 mg PX21	n octane+ decalin+ 150 mg PX-21	n octane+ decalin+ 250 mg PX-21
n propane+propene	0.70	0.03	0.46	0.63
n butane+butene	3.18	1.15	2.51	2.76
2 methyl butene	0.24	0.12	0.19	0.13
n pentane+pentene	5.92	5.44	4.74	4.86
pentene	0.46	0.06	0.19	0.06
2 methyl pentane	0.15	0.09	0.09	0.10
3.methyl pentane	0.17	0.06	0.07	0.10
n hexane	1.98	2.29	2.64	2.29
hexene	1.00	0.58	0.42	0.69
hexene	0.59	0.34	0.27	0.27
hexene	0.22	0.11	0.08	0.09
methyl cyclopentane	0.44	0.33	0.24	0.18
3 methyl hexane	0.44	0.26	0.18	0.21
n heptane	1.28	1.19	1.06	0.97
dimethyl cyclopentane	0.60	0.47	0.34	0.30
heptane	0.10	0.06	0.04	0.04
heptene	0.25	0.16	0.10	0.10
dimethyl cyclopentene	0.15	0.10	0.05	0.03
methyl cyclohexane+methyl cyclohexene	0.04	0.02	0.01	0.01
4 methyl heptane	0.40	0.29	0.25	0.19
3 methyl heptane	1.28	1.28	1.21	1.17
n octane	65.55	71.03	73.01	73.28
octene	0.24	0.10	0.09	0.05
octene	0.21	0.19	0.22	0.24
octene+dimethyl cyclohexane	0.28	0.37	0.40	0.41
octene	0.23	0.22	0.24	0.26
octene	0.11	0.10	0.11	0.13
4 methyl octane	0.42	0.35	0.30	0.26
ethyl cyclohexane+br. alkane	0.31	0.28	0.23	0.20
toluene	0.18	0.20	0.13	0.09
n nonane	0.75	0.60	0.41	0.37
nonene	0.14	0.13	0.07	0.07
c3 cyclohexane+nonene	0.10	0.08	0.08	0.04
nonene	0.02	0.06	0.01	0.01
5 methyl nonane	0.13	0.11	0.07	0.07
4 methyl nonane	0.19	0.16	0.11	0.10
3 methyl nonane+ethyl benzene	0.38	0.31	0.23	0.21
xylenes	0.14	0.20	0.15	0.09
n decane	0.52	0.43	0.29	0.29
decene	0.13	0.09	0.05	0.03
o xylene	0.06	0.13	0.11	0.08

Compounds identified	n octane+ decalin	n octane+ decalin+ 50 mg PX21	n octane+ decalin+ 150 mg PX-21	n octane+ decalin+ 250 mg PX-21
decene	0.08	0.04	0.02	0.02
c3 cyclohexane	0.03	0.05	0.03	0.01
br. alkane	0.18	0.14	0.11	0.08
dimethyl nonane	0.29	0.20	0.11	0.12
5 methyl decane	0.13	0.10	0.06	0.06
4 methyl decane	0.66	0.41	0.27	0.29
br alkane	0.07	0.10	0.05	0.06
c3 benzene	0.05	0.08	0.05	0.03
n butyl cyclohexene	0.02	0.03	0.01	0.01
c3 benzene	0.07	0.02	0.03	0.03
n undecane	0.56	0.42	0.30	0.27
trans decalin	3.35	3.41	2.82	2.93
br alkane	0.22	0.15	0.08	0.12
br alkane	0.14	0.09	0.06	0.07
dimethyl decane	0.35	0.22	0.16	0.16
n butyl benzene	0.10	0.11	0.07	0.07
cis decalin	1.76	1.94	1.62	1.44
n dodecane	0.31	0.25	0.16	0.16
br alkane	0.09	0.06	0.04	0.04
br alkane	0.18	0.11	0.06	0.08
6 methyl dodecane	0.24	0.16	0.09	0.14
n tridecane	0.17	0.13	0.08	0.07
br alkane	0.10	0.06	0.05	0.05
6 methyl tridecane	0.12	0.08	0.03	0.05
tetralin	0.10	0.18	0.12	0.15
dimethyl dodecane	0.27	0.17	0.09	0.11
c3 decalin	0.10	0.07	0.03	0.03
c3 decalin	0.04	0.04	0.02	0.02
naphthalene	0.17	1.23	1.71	1.66
n tetradecane	0.04	0.04	0.01	0.01
br alkane	0.03	0.03	0.02	0.01
c3 decalin	0.04	0.03	0.01	0.01
br alkane	0.10	0.08	0.04	0.04
c3 decalin	0.02	0.04	0.01	0.02
n pentadecane	0.05	0.03	0.02	0.02
2 methyl naphthalene	0.01	0.06	0.06	0.03
1 methyl naphthalene	0.02	0.07	0.06	0.04
br alkane	0.03	0.03	0.01	0.01
	100.00	100.00	100.00	100.00

Table 9. Percent Weight of the Compounds Identified in the Liquids after Thermal Stressing of n-Dodecane+ d18-Decalin Alone and with 250 mg PX-21

compounds identified	n-dodecane+ 200 µl d_{18}-decalin	n-dodecane+ 200 µl d_{18}-decalin+ 250 mg PX-21
n-propane+propene	0.36	0.16
n-butane+butene	1.73	1.27
2-methyl butane	0.19	0.08
n-pentane+pentene	3.29	3.05
pentene	0.28	0.19
pentene	0.16	0.13
2-methyl pentane	0.16	0.13
3-methyl pentane	0.10	0.07
n-hexane	3.20	4.02
hexene	1.08	0.41
hexene	0.32	0.34
hexene	0.15	0.12
methyl cyclopentane	0.37	0.32
3-methyl hexane	0.17	0.16
n-heptane+methyl cyclopentene	3.21	4.11
heptene	1.26	0.84
heptene	0.08	0.09
heptene	0.27	0.25
methyl cyclopentene	0.13	0.12
methyl cyclohexane+branched alkane	0.38	0.36
ethyl cyclopentane	0.17	0.17
3-methyl heptane	0.21	0.23
n-octane	3.00	4.12
octene	1.14	0.79
octene+dimethyl cyclohexane	0.23	0.23
octene	0.26	0.24
octene	0.10	0.12
4-methyl octane+octene	0.32	0.38
ethyl cyclohexane+branched alkane	0.31	0.31
toluene	0.19	0.23
n-nonane	3.03	4.03
nonene	0.95	0.61
nonene	0.06	0.05
nonene	0.13	0.13
c3-cyclohexane	0.21	0.20
branched alkane	0.08	0.09
branched alkane+n-propyl cyclo hexane	0.17	0.22
c3-cyclohexane	0.08	0.11
ethyl benzene	0.10	0.17
p-and m-xylenes	0.14	0.18
n-decane	1.10	1.89
o-xylene	0.23	0.19

compounds identified	n-dodecane+ 200 µl d_{18}-decalin	n-dodecane+ 200 µl d_{18}-decalin+ 250 mg PX-21
decene	0.91	0.75
c3-cyclohexane	0.06	0.06
decene	0.13	0.12
decene	0.12	0.10
n-propyl benzene	0.09	0.07
c3-benzene	0.12	0.11
n-undecane	0.64	0.95
trans-decalin	4.76	4.49
undecene	0.06	0.09
cis-decalin	0.49	0.41
c4-benzene	0.03	0.06
n-dodecane	57.89	54.33
dimethyl undecane	0.09	0.16
dodecene	0.25	0.67
dodecene	0.09	0.29
branched alkane	0.09	0.15
branched alkane	0.07	0.09
branched alkane	0.09	0.11
branched alkane	0.04	0.06
branched alkane	0.05	0.10
branched alkane	0.06	0.09
c4-benzene	0.04	0.02
n-tridecane	0.40	0.41
tridecene	0.11	0.08
tridecene	0.06	0.04
tridecene	0.04	0.04
branched alkane	0.10	0.09
c5-benzene	0.06	0.13
branched alkane	0.05	0.12
branched alkane	0.06	0.06
branched alkane	0.05	0.05
branched alkane	0.05	0.06
dimethyl dodecane	0.11	0.19
n-hexyl benzene	0.00	0.01
c6-benzene	0.02	0.15
naphthalene+deuterated naphthalenes	0.09	0.47
n-tetradecane	0.30	0.32
branched alkane	0.09	0.09
dimethyl tridecane	0.11	0.09
branched alkane	0.17	0.19
branched alkane	0.24	0.26
branched alkane	0.07	0.08
branched alkane	0.06	0.08
n-pentadecane	0.28	0.29
branched alkane	0.06	0.06
branched alkane	0.06	0.06

compounds identified	n-dodecane+ 200 µl d_{18}-decalin	n-dodecane+ 200 µl d_{18}-decalin+ 250 mg PX-21
branched alkane	0.06	0.06
branched alkane	0.14	0.14
branched alkane	0.06	0.06
branched alkane	0.04	0.04
branched alkane	0.04	0.05
n-hexadecane	0.17	0.18
branched alkane	0.05	0.07
branched alkane	0.11	0.14
branched alkane	0.04	0.05
branched alkane	0.04	0.04
branched alkane	0.04	0.04
n-heptadecane	0.11	0.14
branched alkane	0.07	0.08
branched alkane	0.14	0.14
branched alkane	0.03	0.04
branched alkane	0.04	0.04
branched alkane	0.04	0.05
n-octadecane	0.09	0.10
branched alkane	0.07	0.06
branched alkane	0.09	0.12
branched alkane	0.03	0.03
branched alkane	0.03	0.03
branched alkane	0.03	0.04
n-nonadecane	0.05	0.07
branched alkane	0.04	0.05
branched alkane	0.07	0.09
branched alkane	0.02	0.02
branched alkane	0.02	0.03
branched alkane	0.02	0.03
n-eicosane	0.04	0.04
branched alkane	0.03	0.04
branched alkane	0.05	0.09
branched alkane	0.01	0.03
branched alkane	0.03	0.03
branched alkane	0.02	0.03
n-heneicosane	0.03	0.03
branched alkane	0.03	0.03
branched alkane	0.05	0.06
	100.00	100.00

Table 10

Sample Description	Mole % remaining after thermal stressing at 425°C, for 6h, under 100 psi air.	
	Dodecane	Benzyl alcohol
Sample # 6 Dodecane (10.00ml) Benzyl alcohol (0.0024M)	69	14
Sample # 3 Dodecane (10.00ml) Benzyl alcohol (0.0024M) Ethanol (0.0048M)	88	43

APPENDIX II

FIGURES

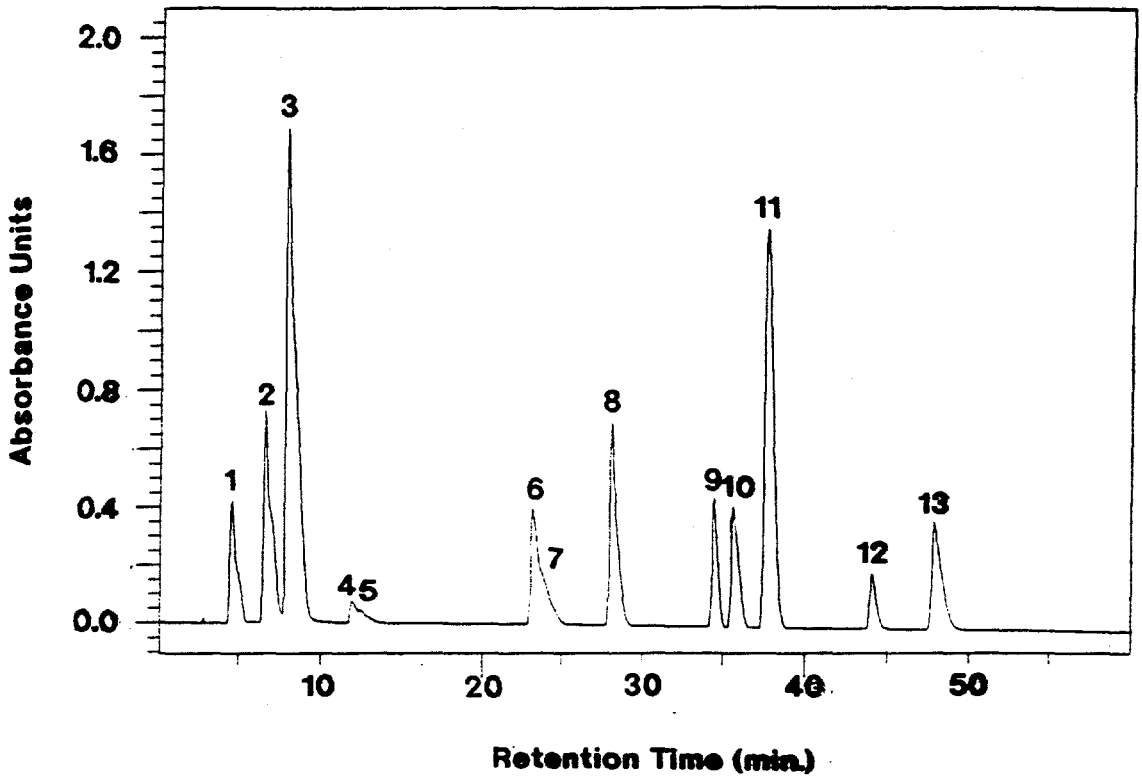

1. Naphthalene
2. Acenaphthalene and Fluorene
3. Acenaphthylene
4. Anthracene
5. Phenanthrene
6. Fluoranthene
7. Pyrene
8. Chrysene and Benzo [a] anthracene
9. Benzo [b] fluoranthene
10. Benzo [k] fluoranthene
11. Dibenzo [a, h] anthracene and Benzo [a] pyrene
12. Indeno [1, 2, 3-cd] pyrene
13. Benzo [g, h, i] perylene

Figure 1. Chromatogram at maximum UV absorbance for a standard mixture of PAH's.

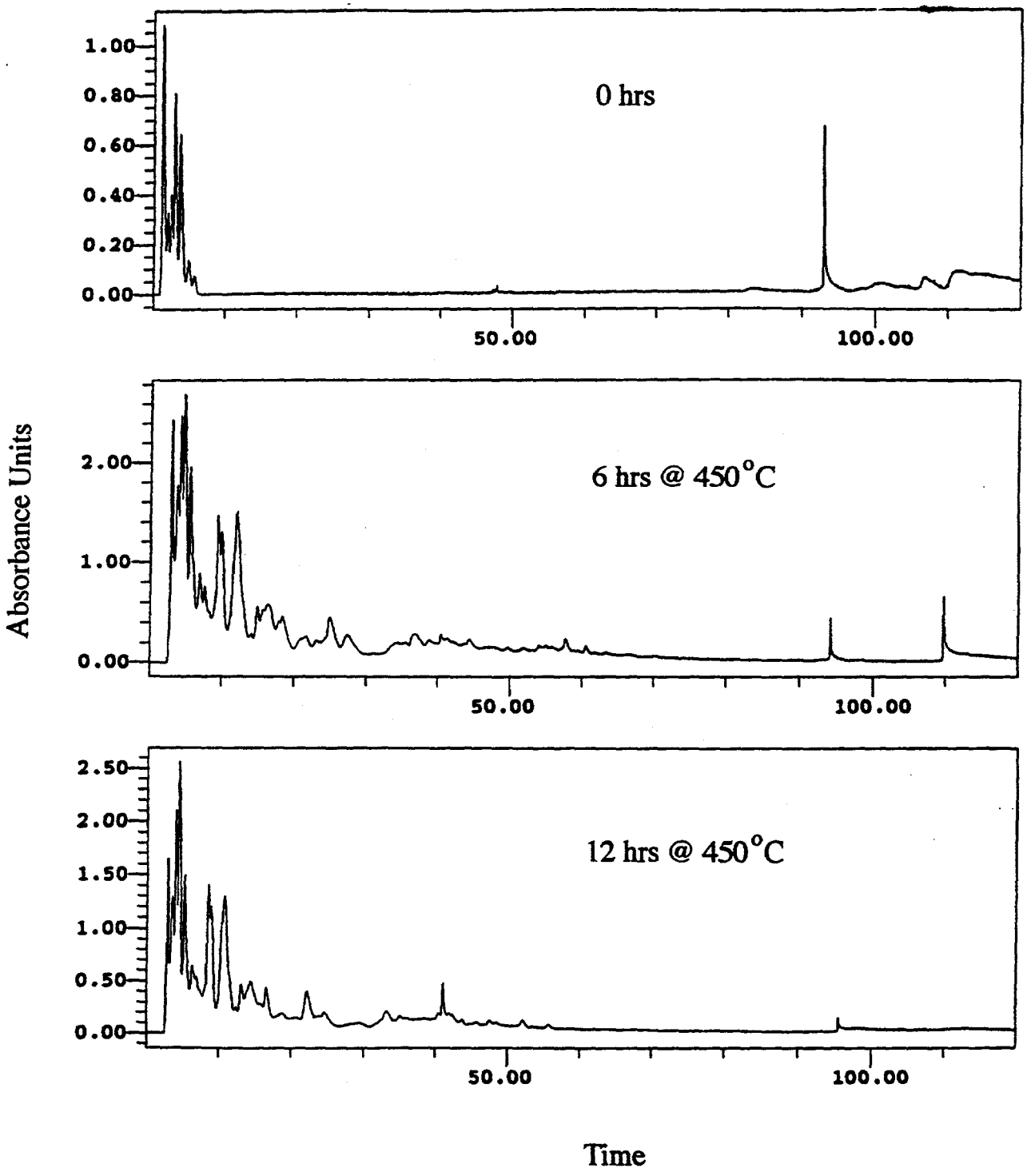

Figure 2. Max-plots from 2-D HPLC on Jet A stressed at 450° C for alotted times.

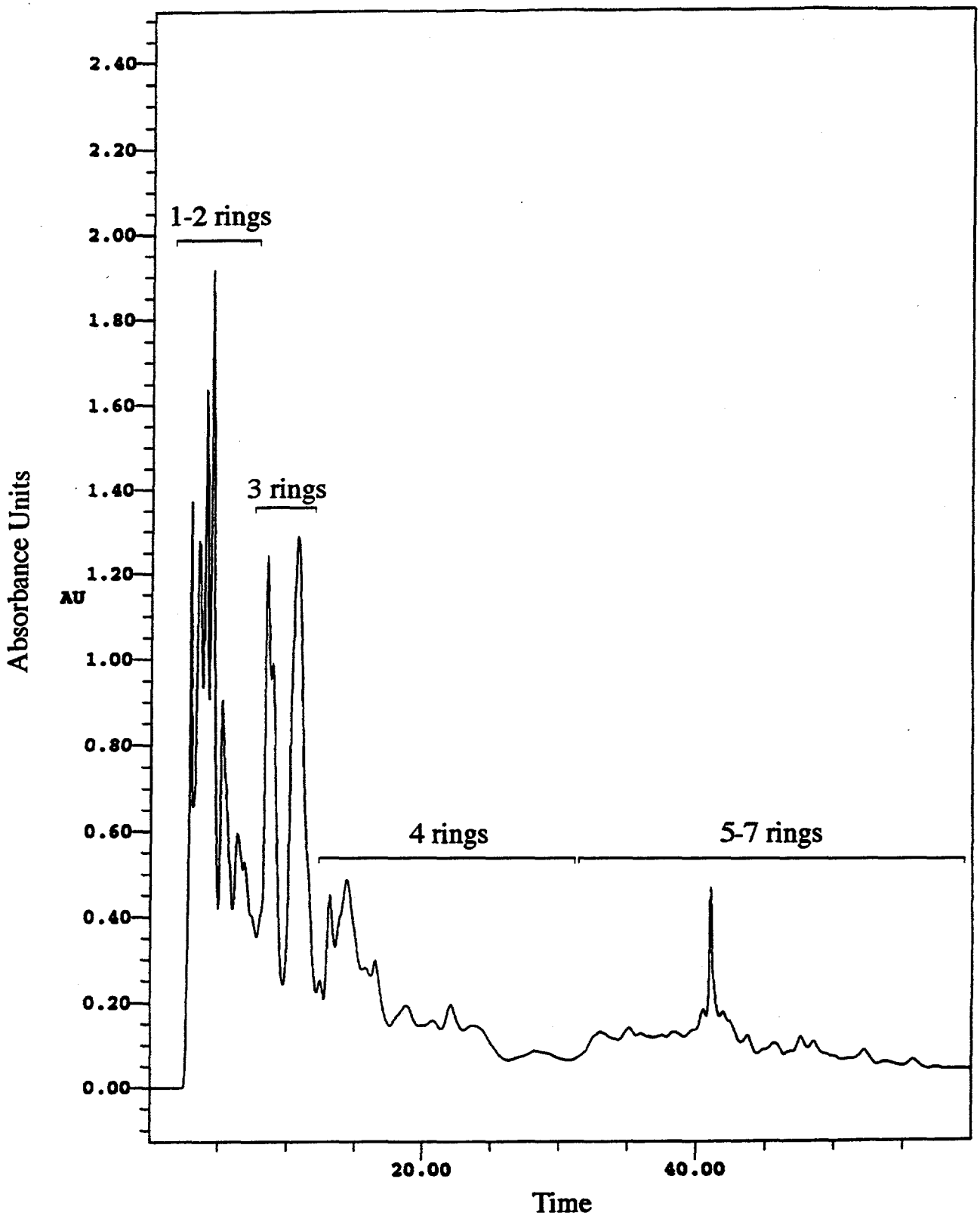

Figure 3. 254 nm cut from 2-D HPLC on Jet A stressed at 450° C for 12 hours. (Labels show number of fused rings).

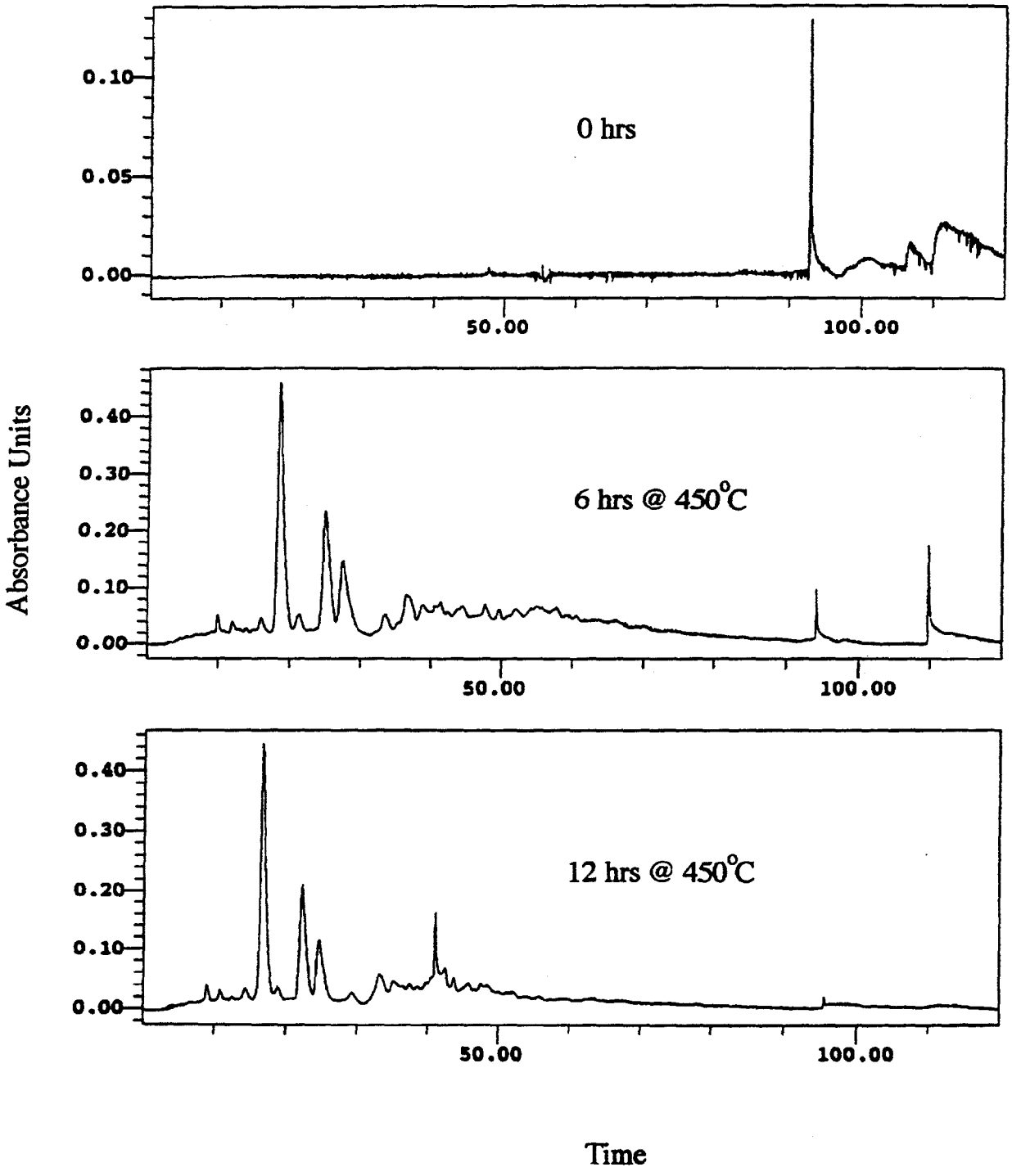

Figure 4. 335 nm cut from 2-D HPLC on Jet A stressed at 450° C for alotted times. (Pyrene family enhanced).

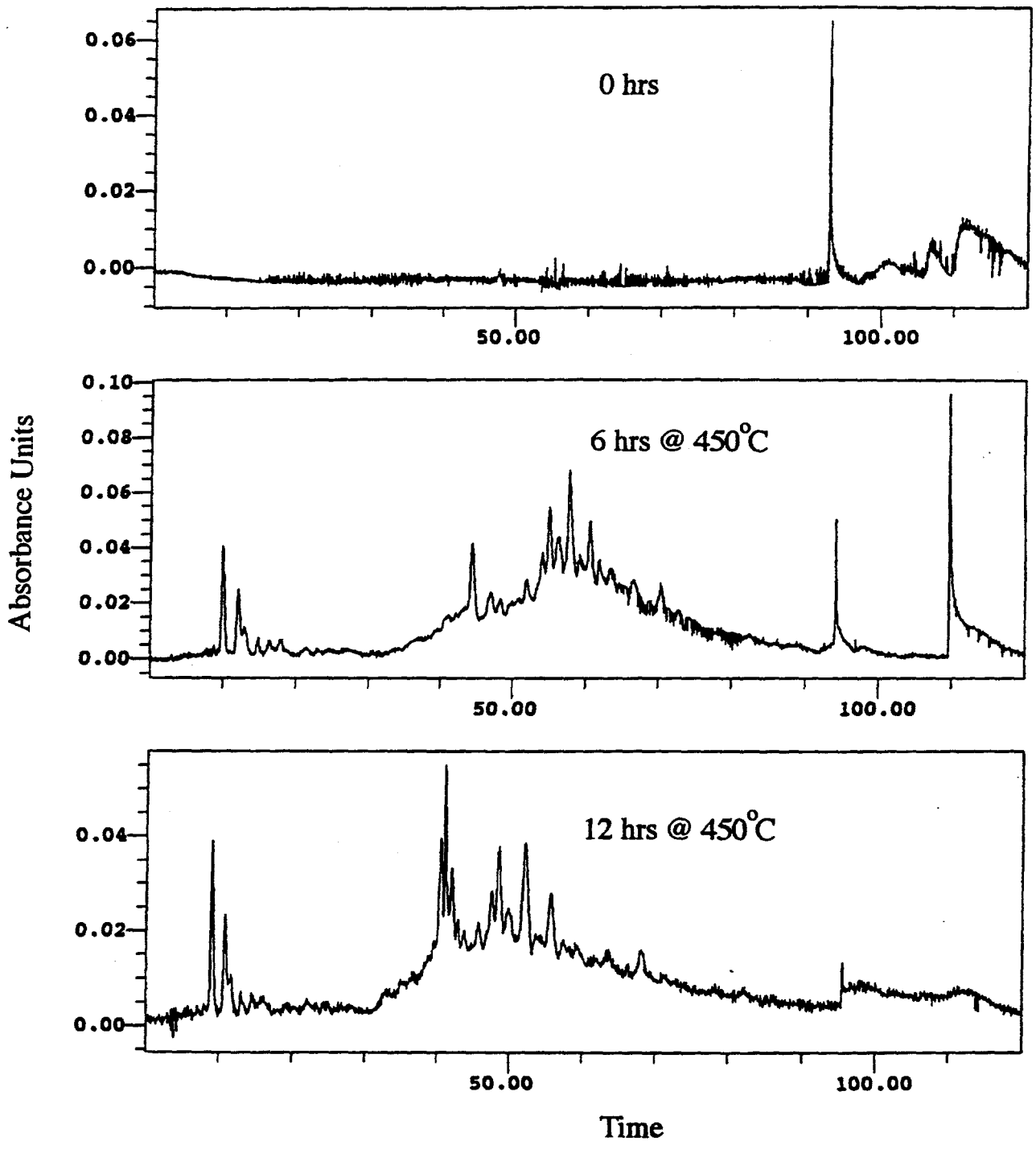

Figure 5. 375 nm cut from 2-D HPLC on Jet A stressed at 450° C for alotted times. (Greater than 4 rings enhanced).

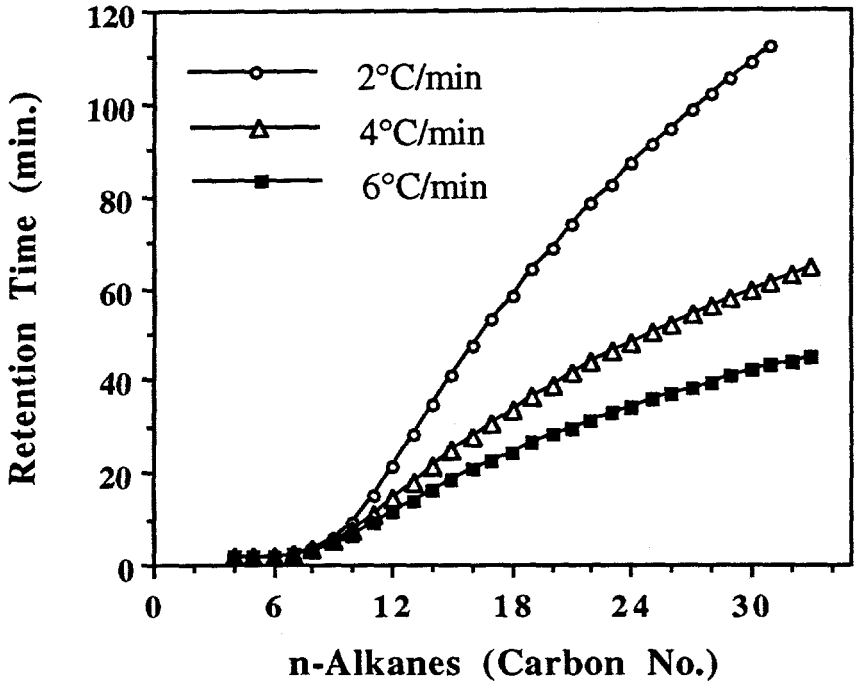

Figure 6. Retention Times of *n*-Alkanes at Three Different Heating Rates (Rtx-50 Column, 40°C to 310°C).

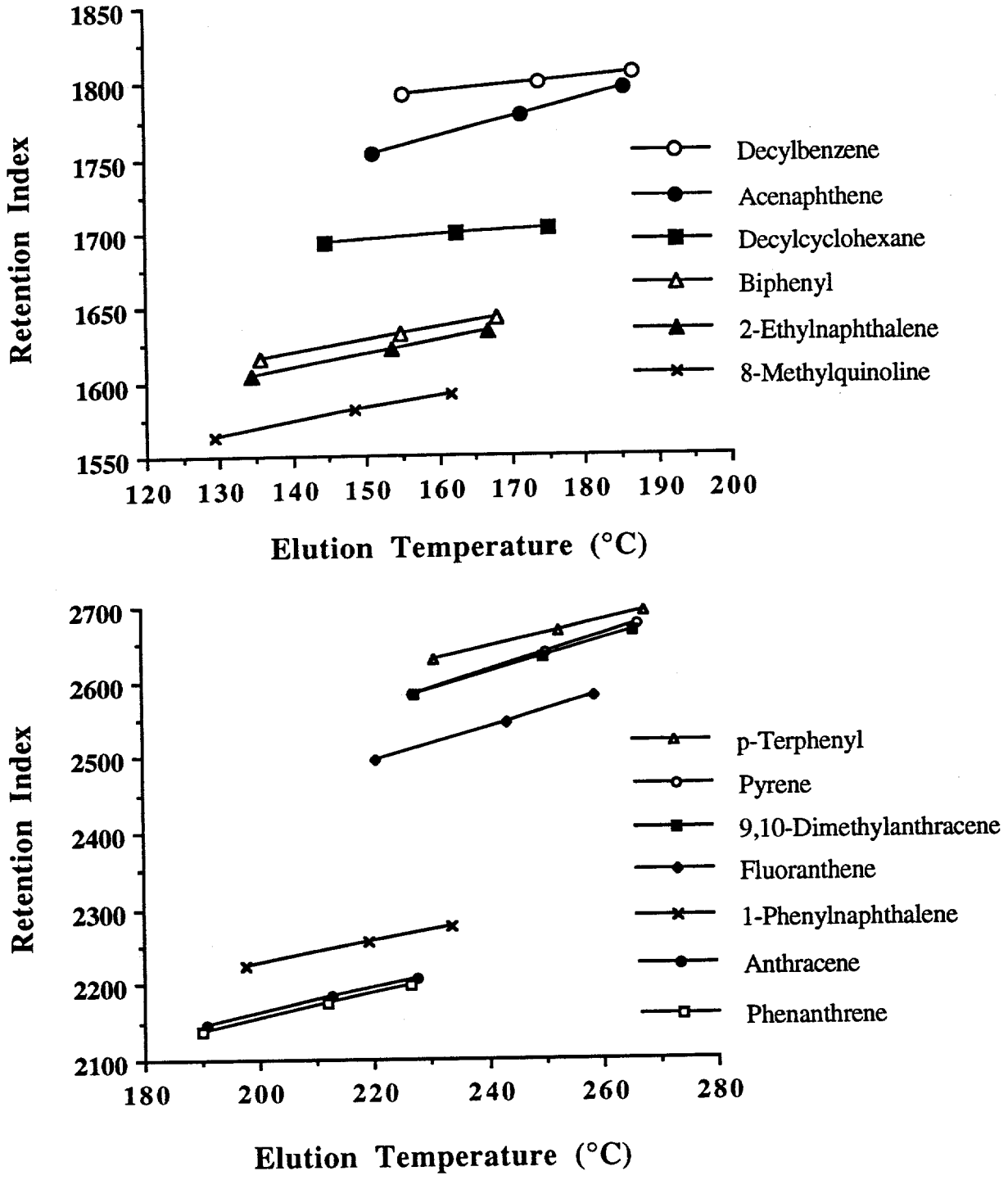

Figure 7. Retention Index versus Final Elution Temperature (Rtx-50 Column, 40°C to 310°C).

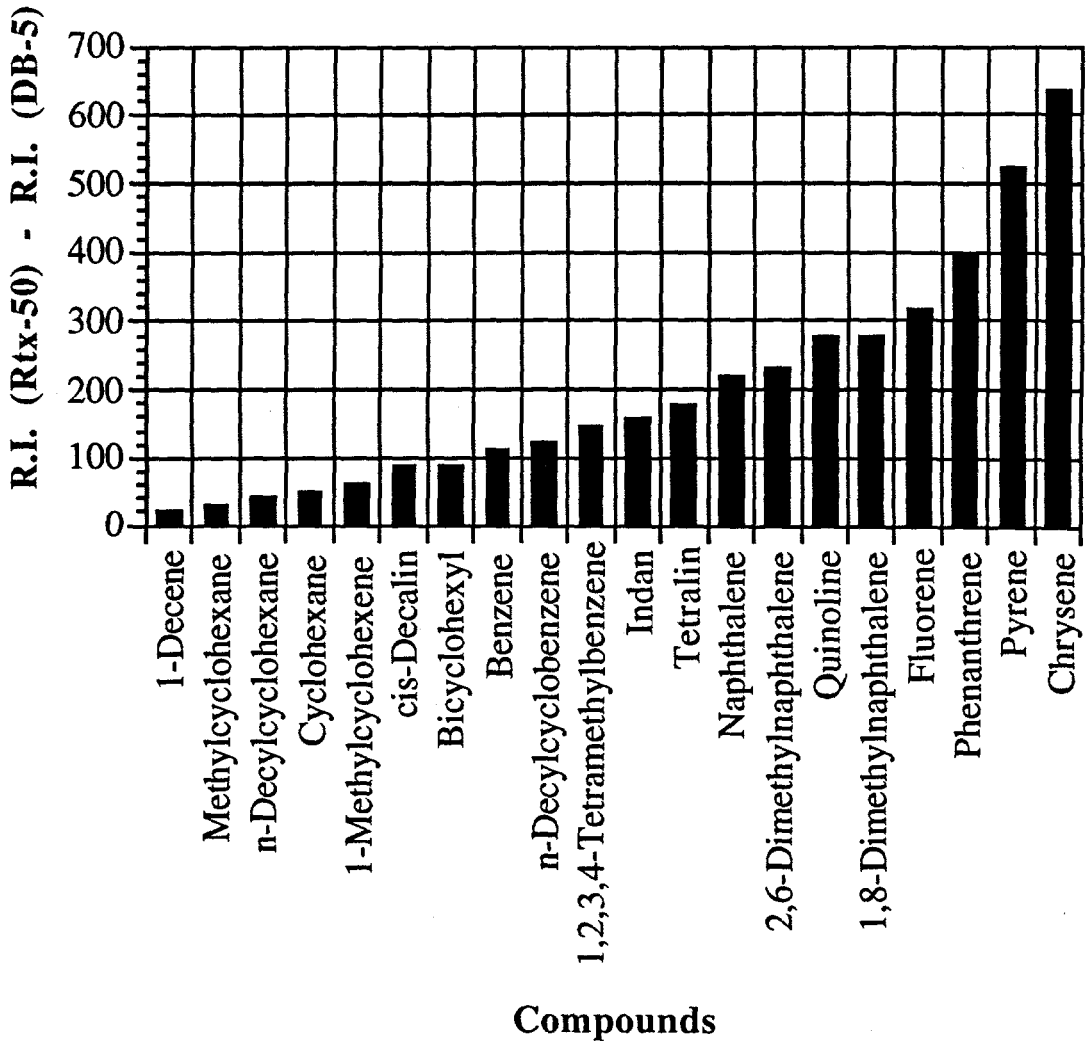

Figure 8. Retention Index Difference between Rtx-50 Column and DB-5 Column (Δ_{pol}R.I.) for 20 Representative Compounds.

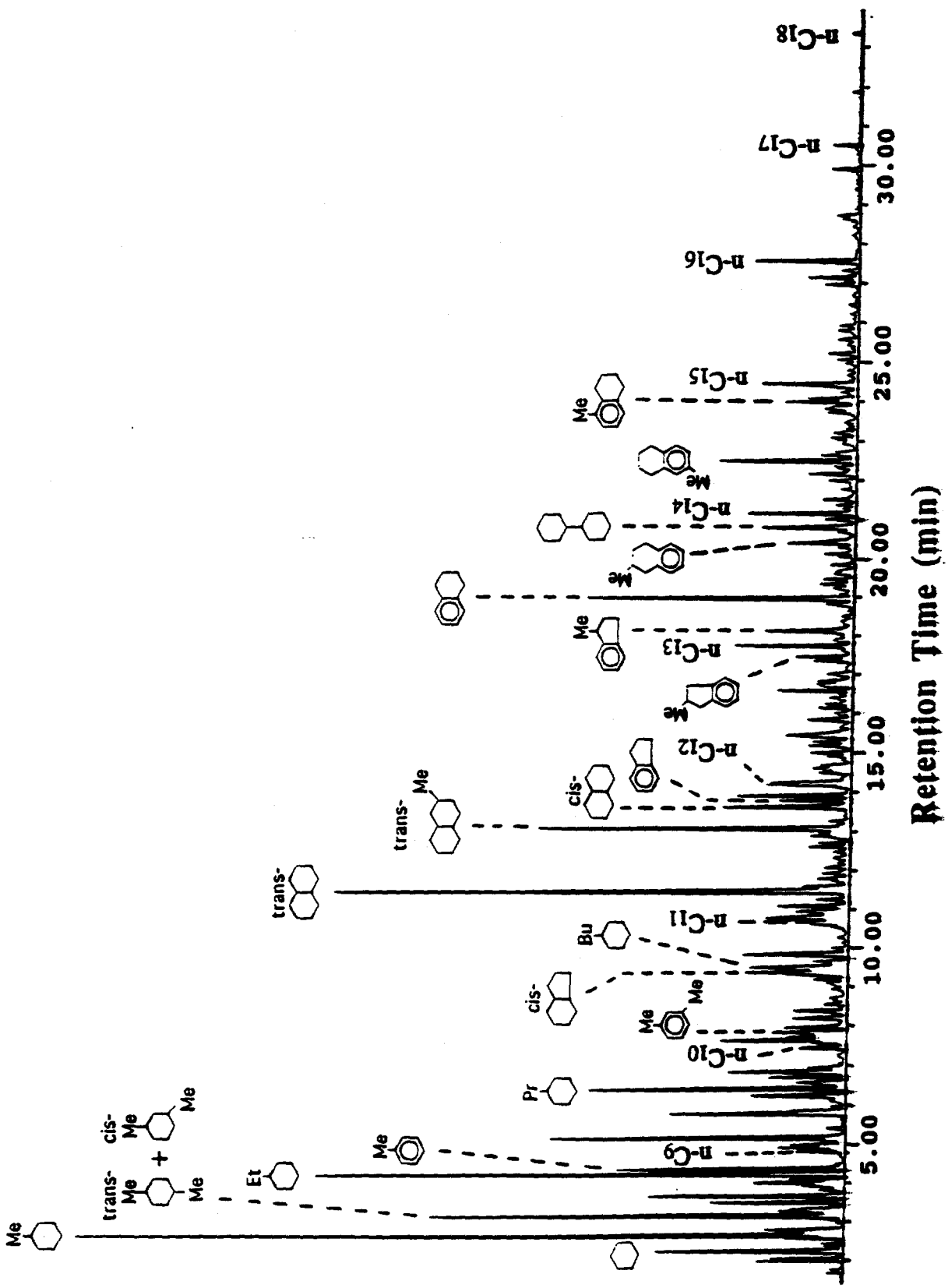

Figure 9. GC-MS Total Ion Chromatogram of Unfractionated JP-8C Jet Fuel (Rtx-50 Column, 40°C to 310°C at 4°C/min, Split).

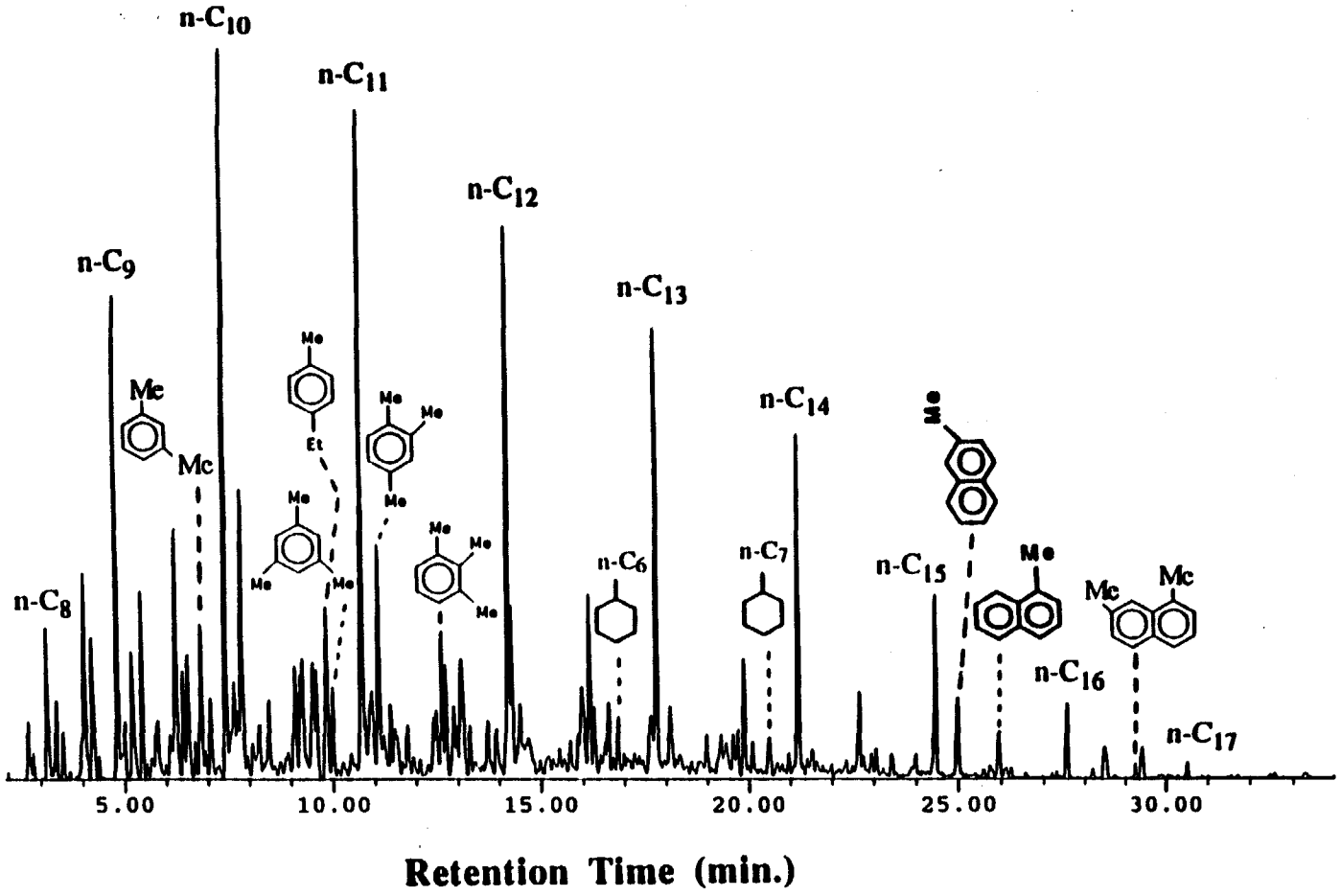

Figure 10. GC-MS Total Ion Chromatogram of Unfractionated JP-8P Jet Fuel (Rtx-50 Column, 40°C to 310°C at 4°C/min, Split).

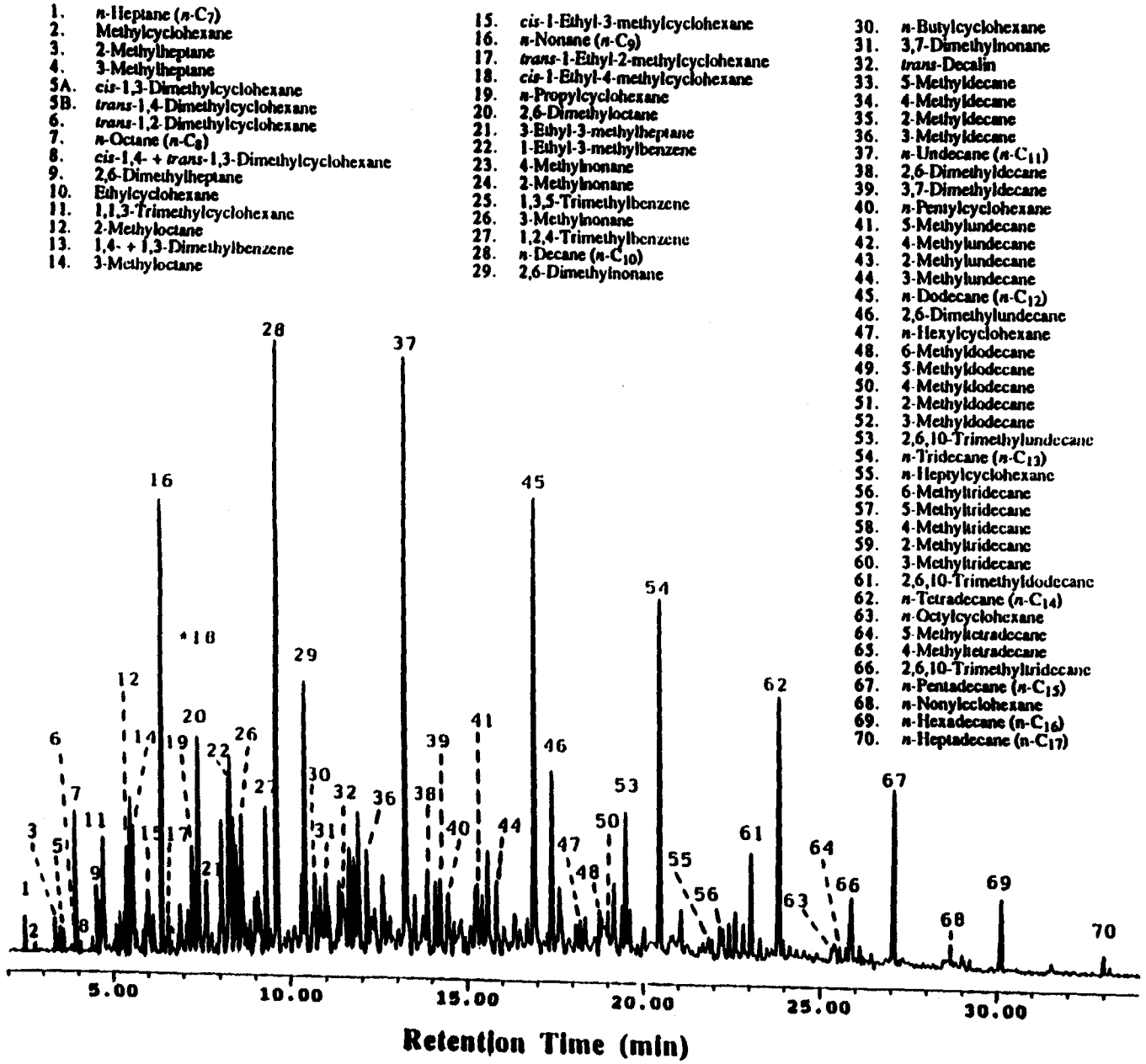

Figure 11. GC-MS Total Ion Chromatogram of Fraction 1 (Saturate Fraction, *n*-Pentane Elute) of JP-8P Jet Fuel (DB-5 Column, 40°C to 310°C at 4°C/min, Split).

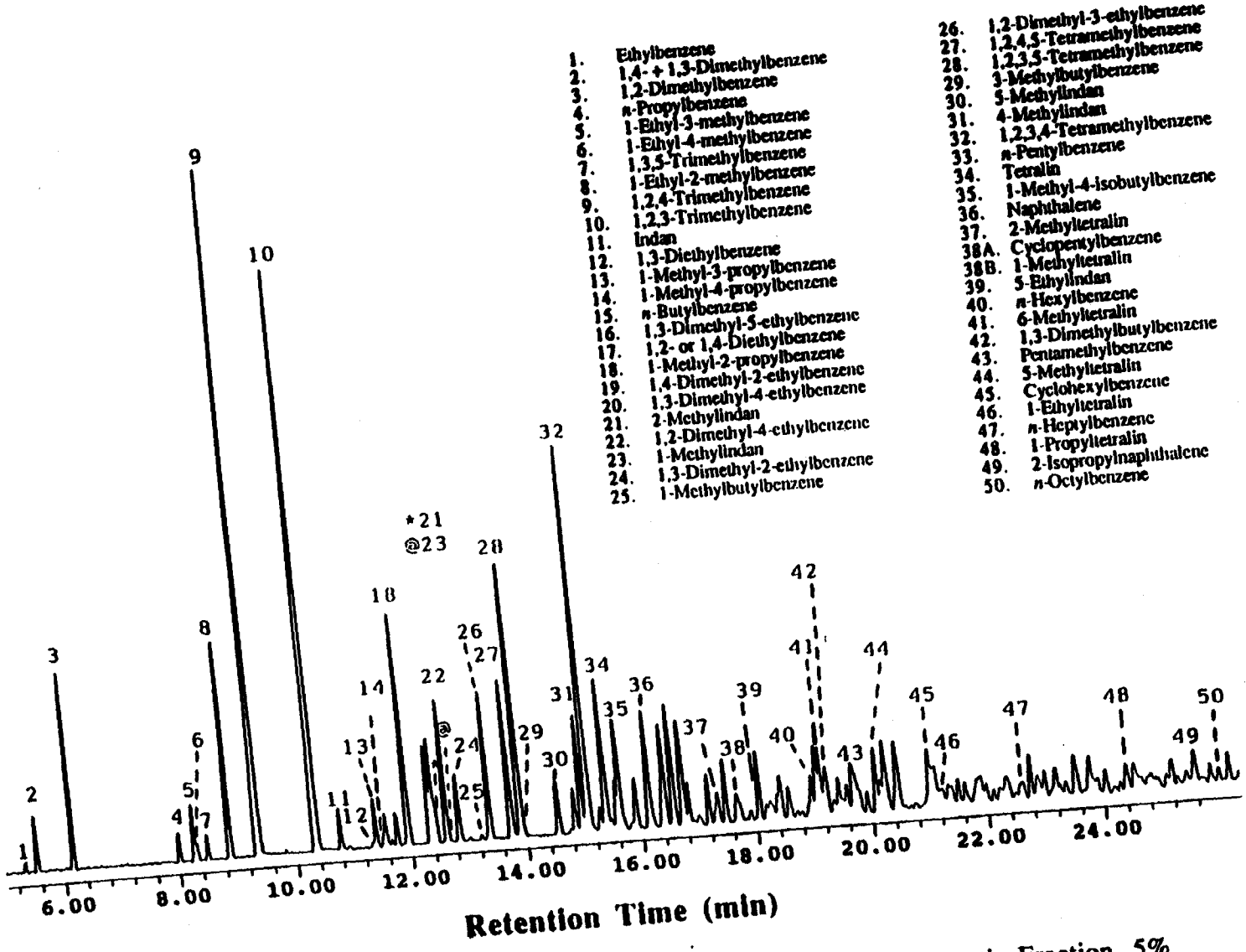

Figure 12. GC-MS Total Ion Chromatogram of Fraction 2 (Monoaromatic Fraction, 5% Benzene-Pentane Elute) of JP-8P Jet Fuel (DB-5 Column, 40°C to 310°C at 4°C/min, Split).

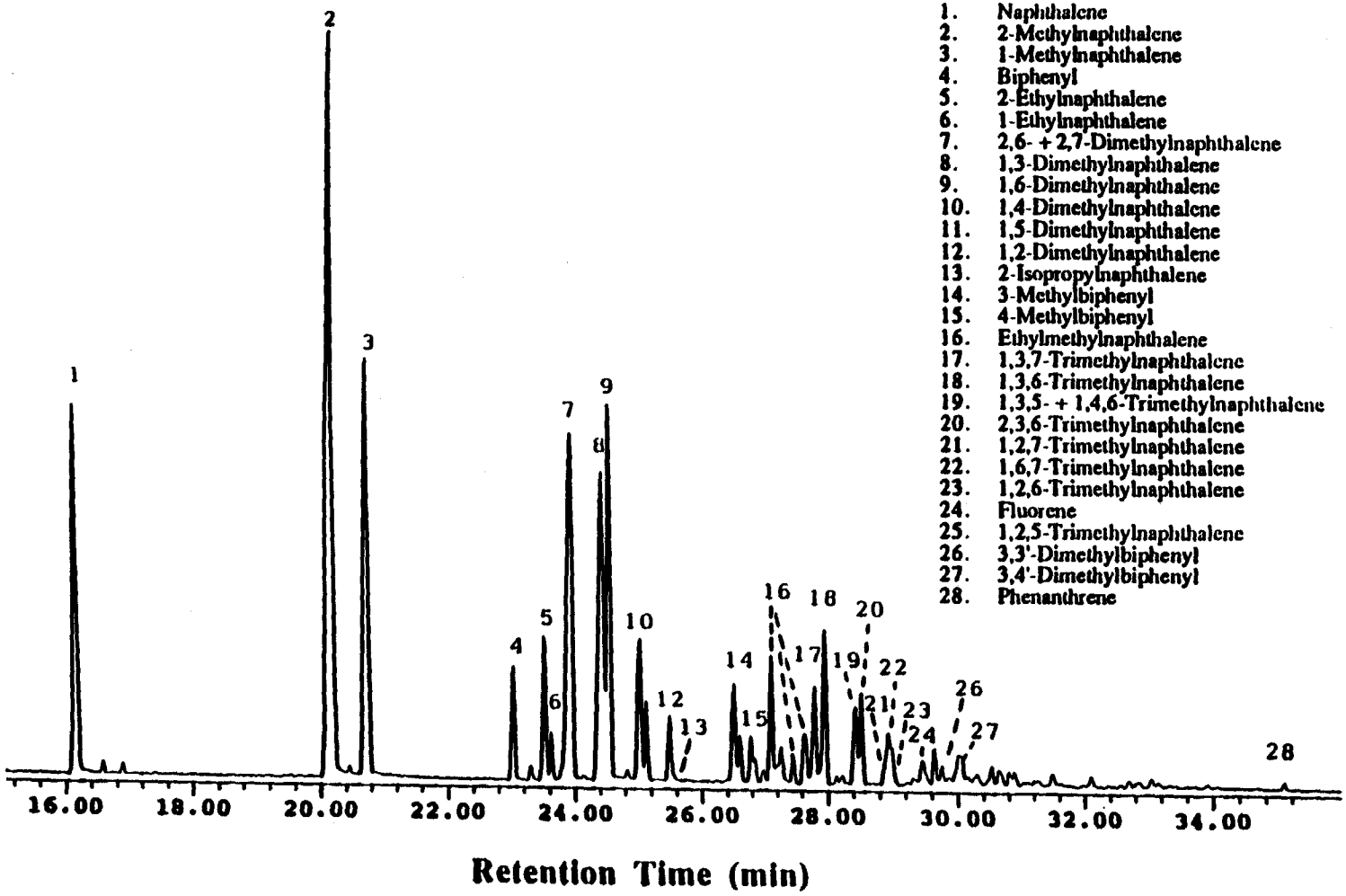

Figure 13. GC-MS Total Ion Chromatogram of Fraction 3 (Aromatic Fraction, Benzene Elute) of JP-8P Jet Fuel (DB-5 Column, 40°C to 310°C at 4°C/min, Split).

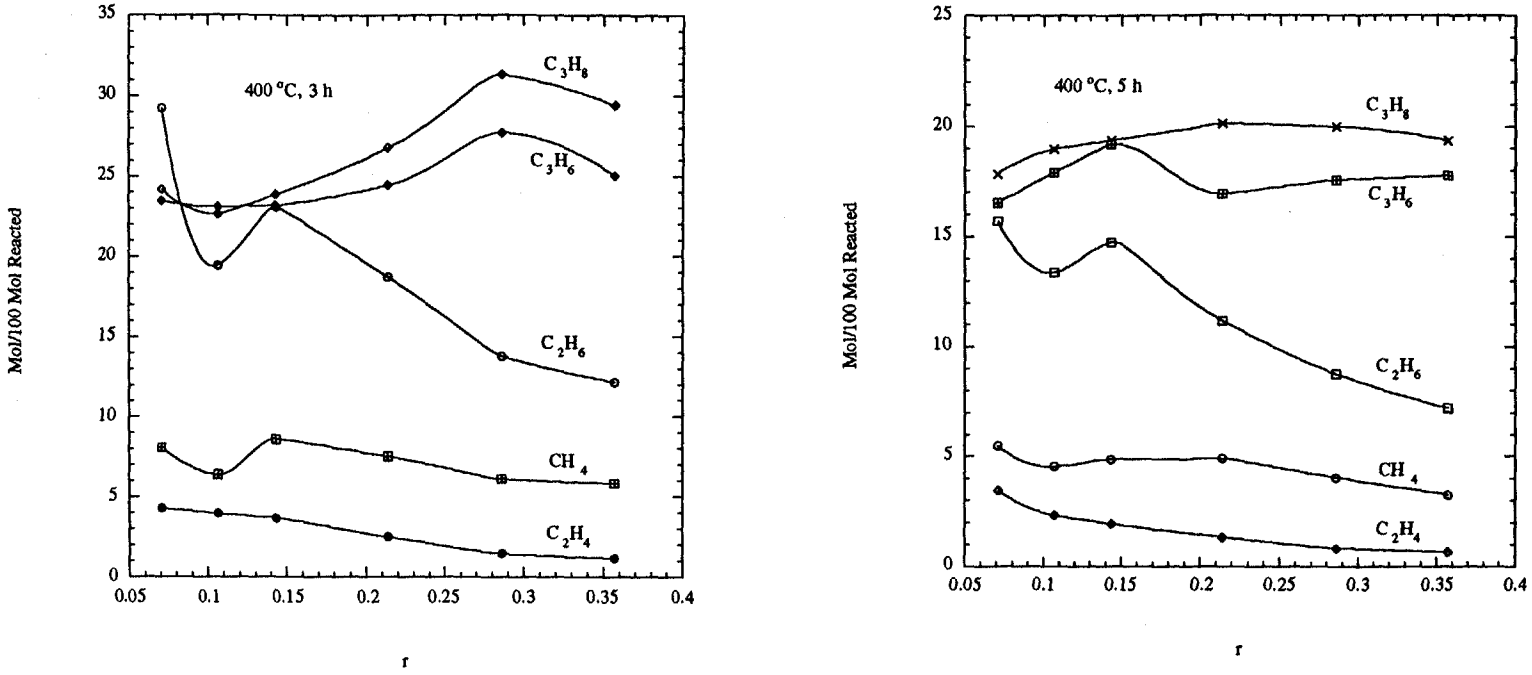

Figure 14. Effects of Loading Ratio (r) on Gas Product Distributions from n-C_{14} Pyrolysis at 400°C for 3 and 5 h.

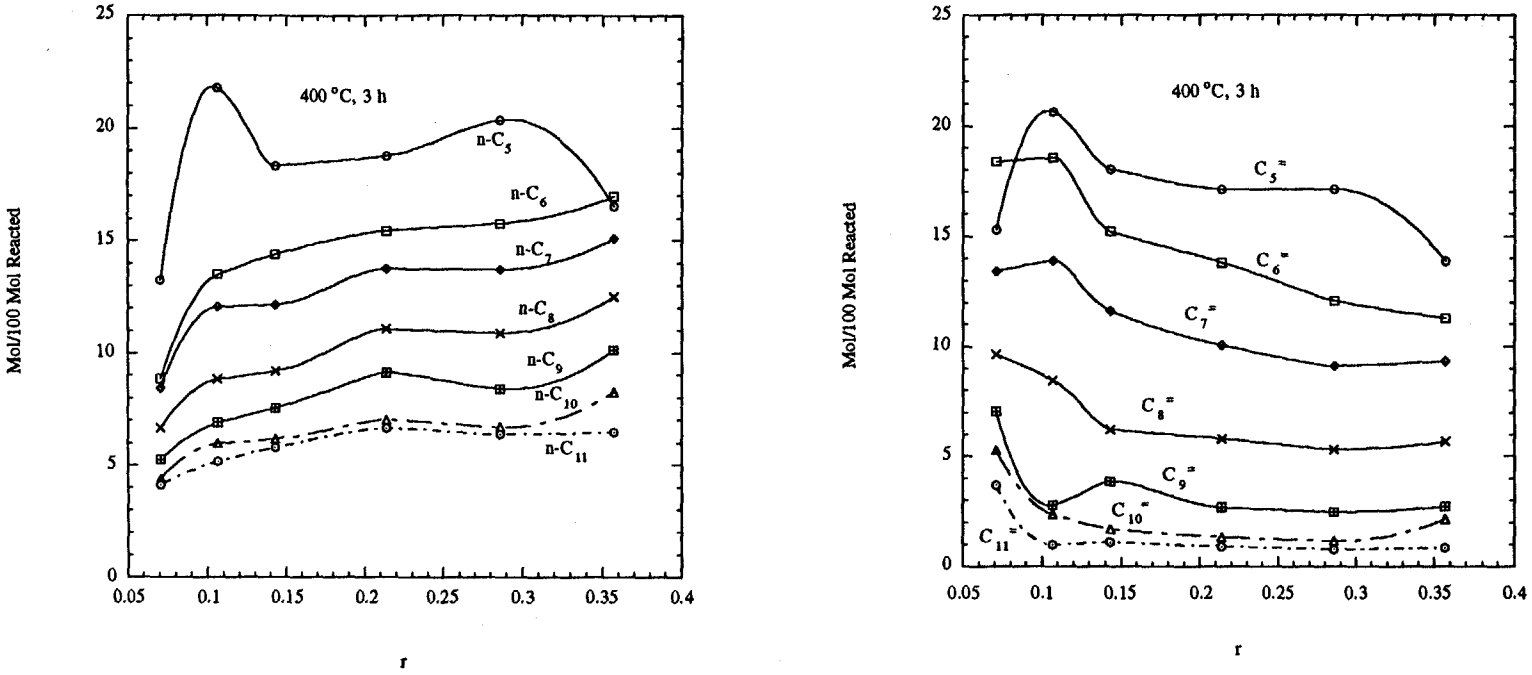

Figure 15. Effects of Loading Ratio (r) on Liquid Product Distributions from n-C_{14} Pyrolysis at 400°C for 3 h.

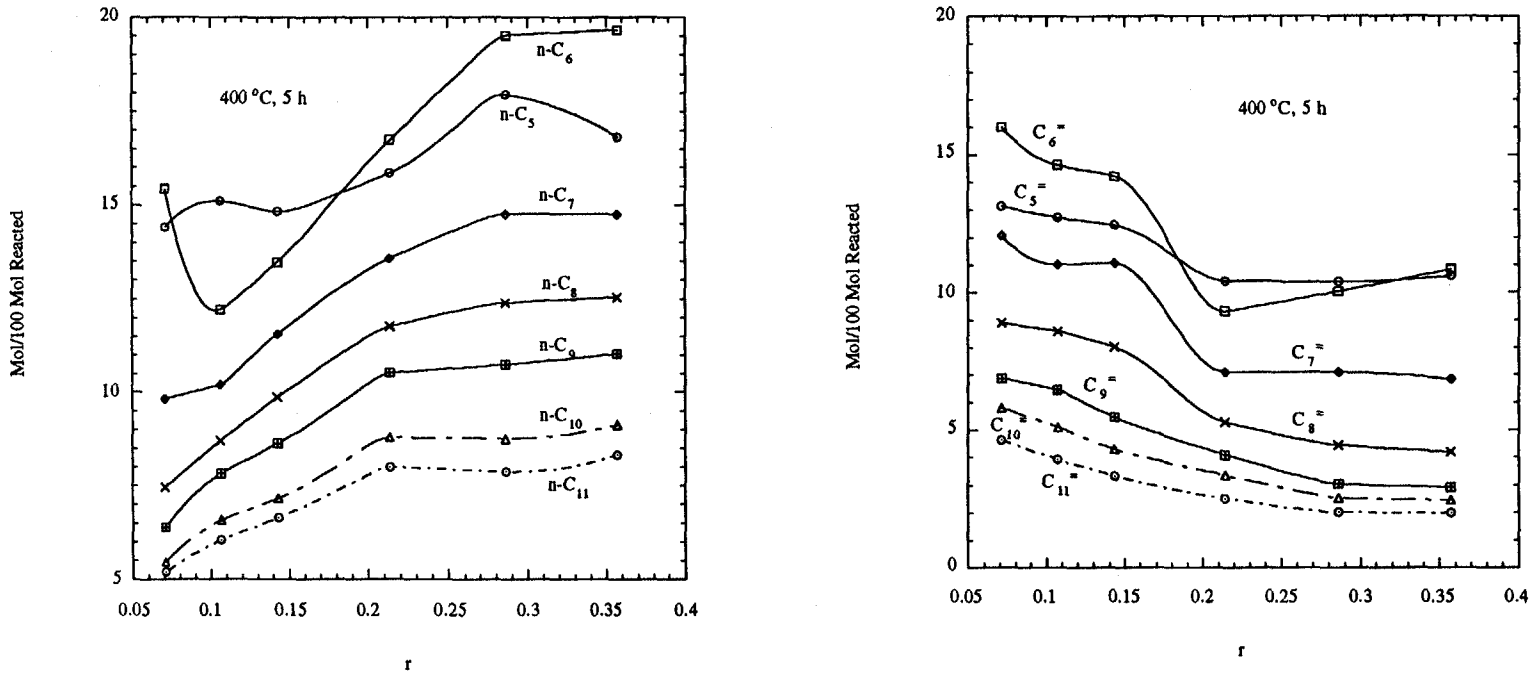

Figure 16. Effects of Loading Ratio (r) on Liquid Product Distributions from n-C_{14} Pyrolysis at 400°C for 5 h.

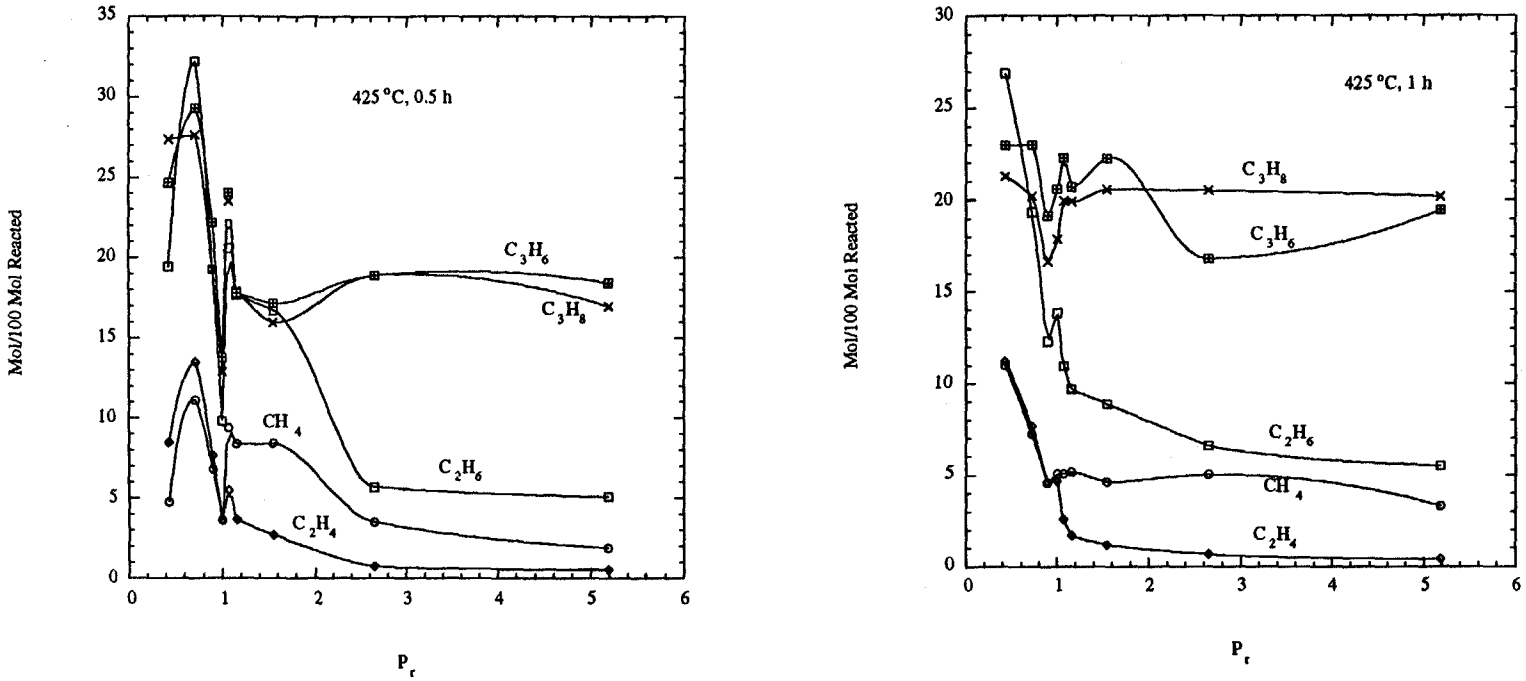

Figure 17. Effects of Initial Reduced Pressure (P_r) on Gas Product Distributions from n-C_{14} Pyrolysis at 425°C for 0.5 and 1 h.

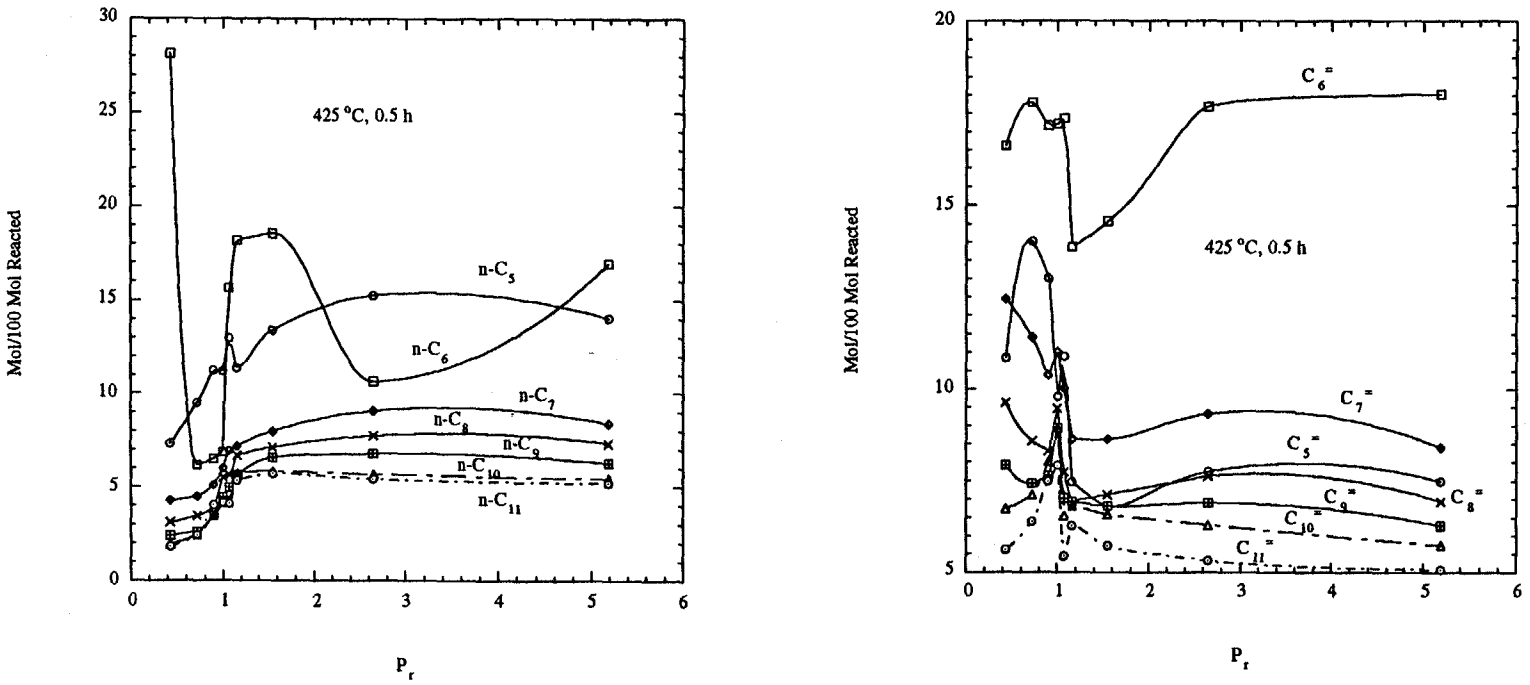

Figure 18. Effects of Initial Reduced Pressure (P_r) on Liquid Product Distributions from n-C_{14} Pyrolysis at 425°C for 0.5 h.

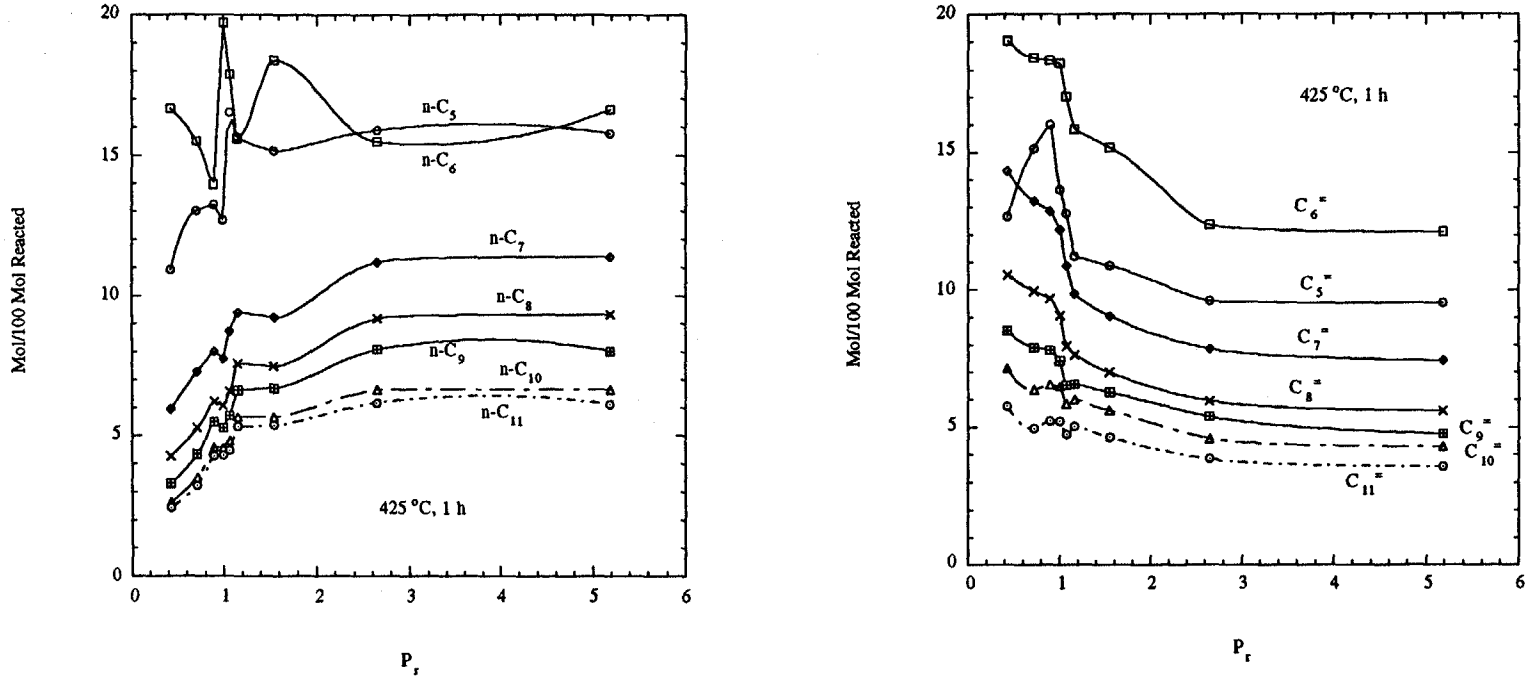

Figure 19. Effects of Initial Reduced Pressure (P_r) on Liquid Product Distributions from n-C_{14} Pyrolysis at 425°C for 1 h.

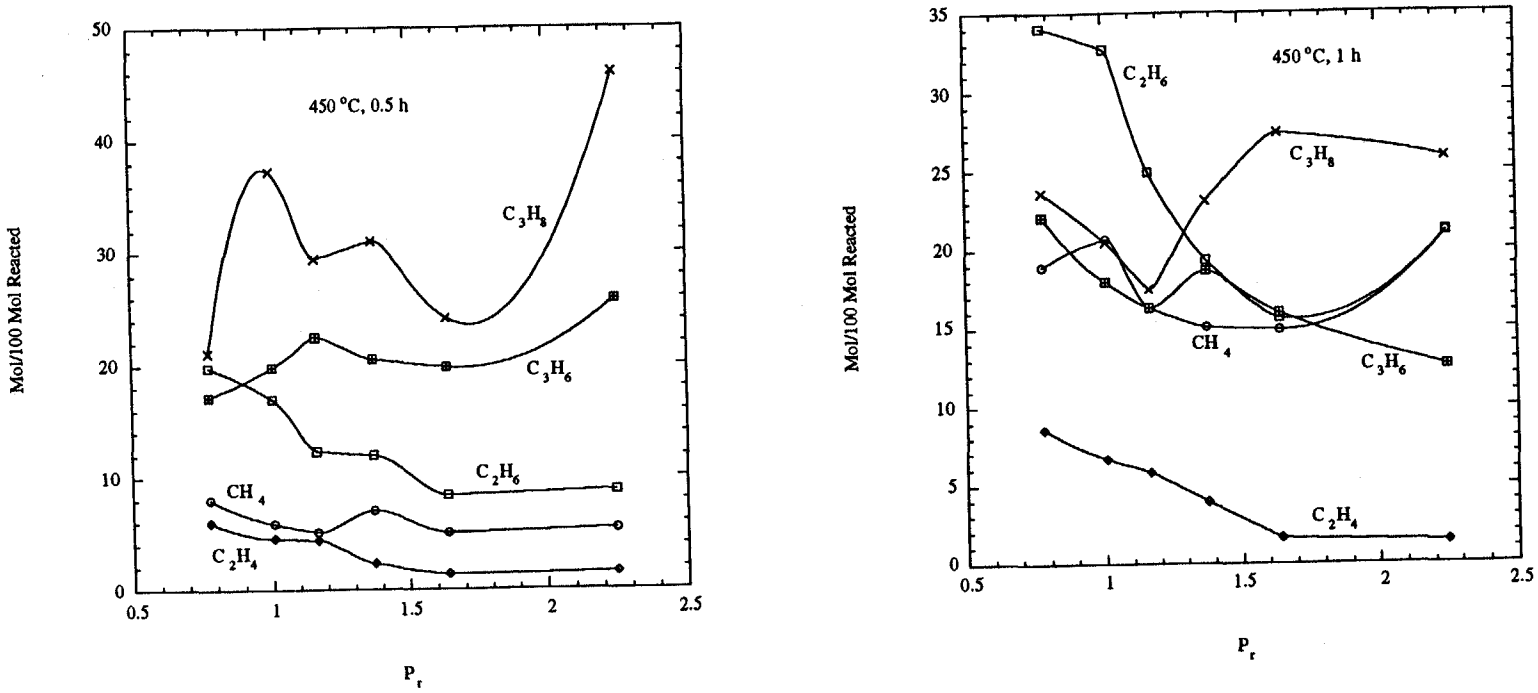

Figure 20. Effects of Initial Reduced Pressure (P_r) on Gas Product Distributions from n-C_{14} Pyrolysis at 450°C for 0.5 h and 1 h.

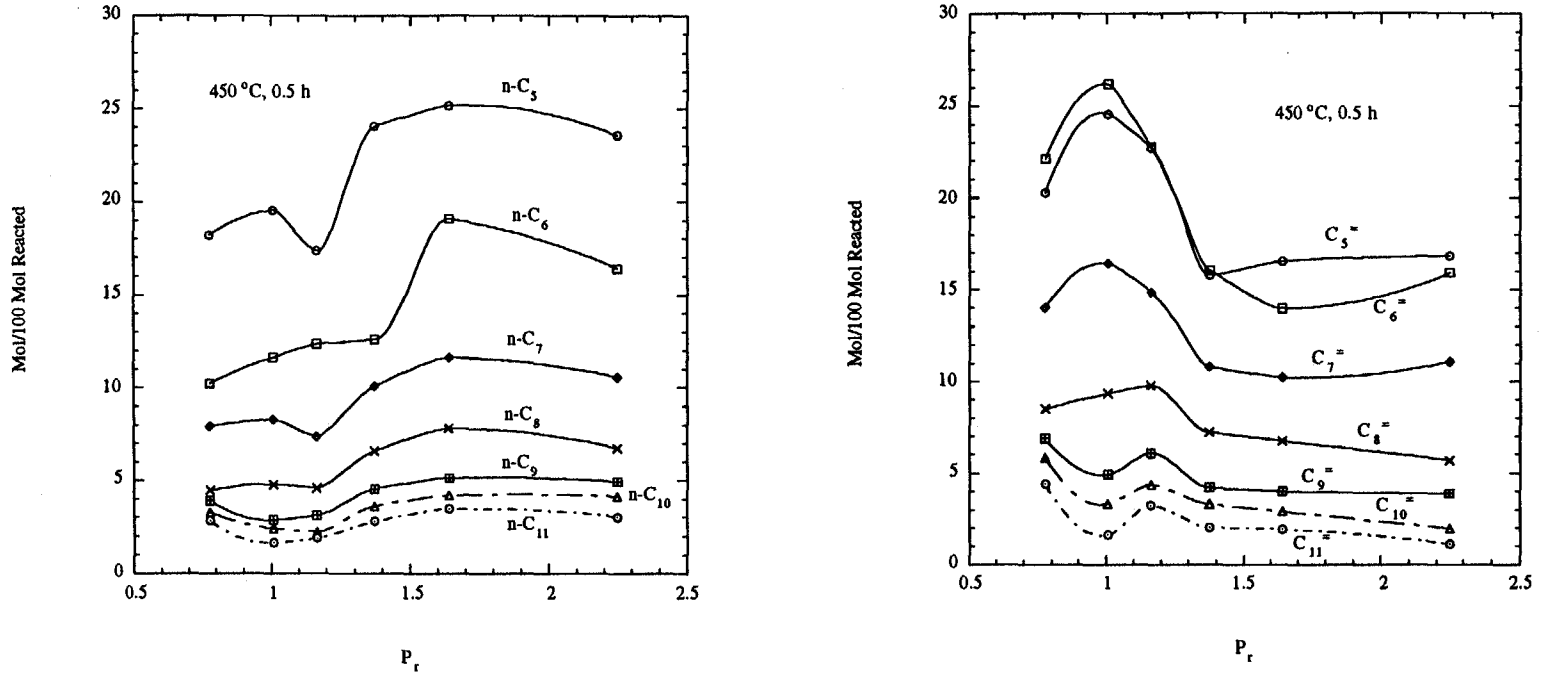

Figure 21. Effects of Initial Reduced Pressure (P_r) on Liquid Product Distributions from n-C_{14} Pyrolysis at 450°C for 0.5 h.

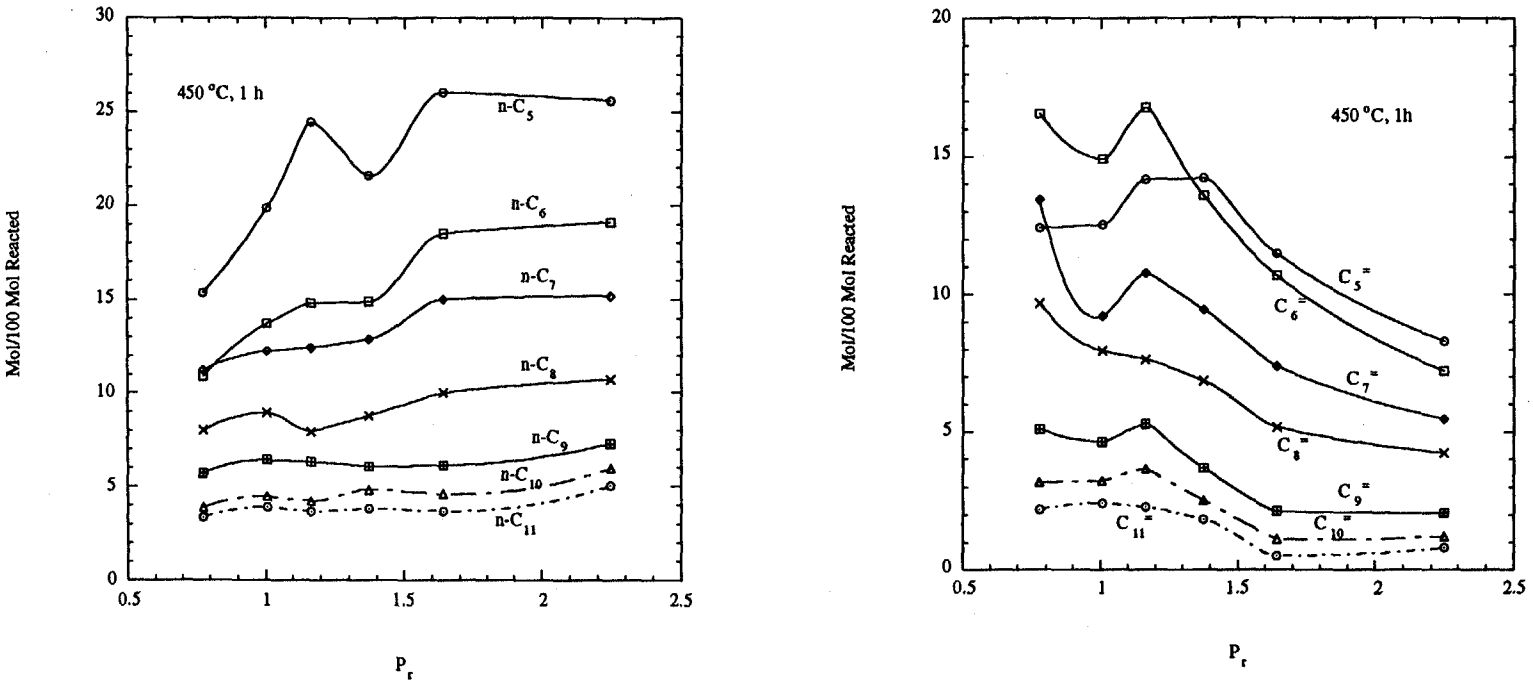

Figure 22. Effects of Initial Reduced Pressure (P_r) on Liquid Product Distributions from n-C_{14} Pyrolysis at 450°C for 1 h.

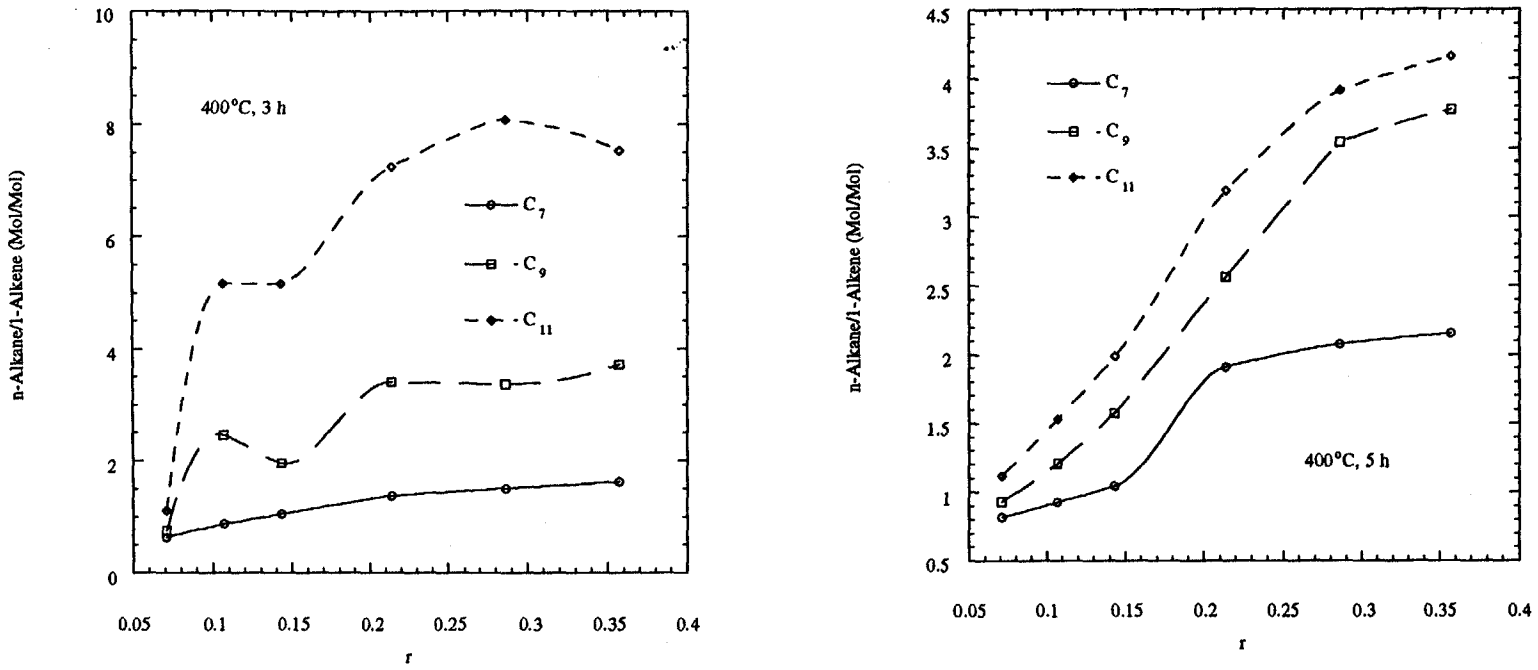

Figure 23. Effects of Loading Ratio (r) on n-Alkane/1-Alkene Ratio (for C_7, C_9, and C_{11}) from n-C_{14} Pyrolysis at 400°C for 3 and 5 h.

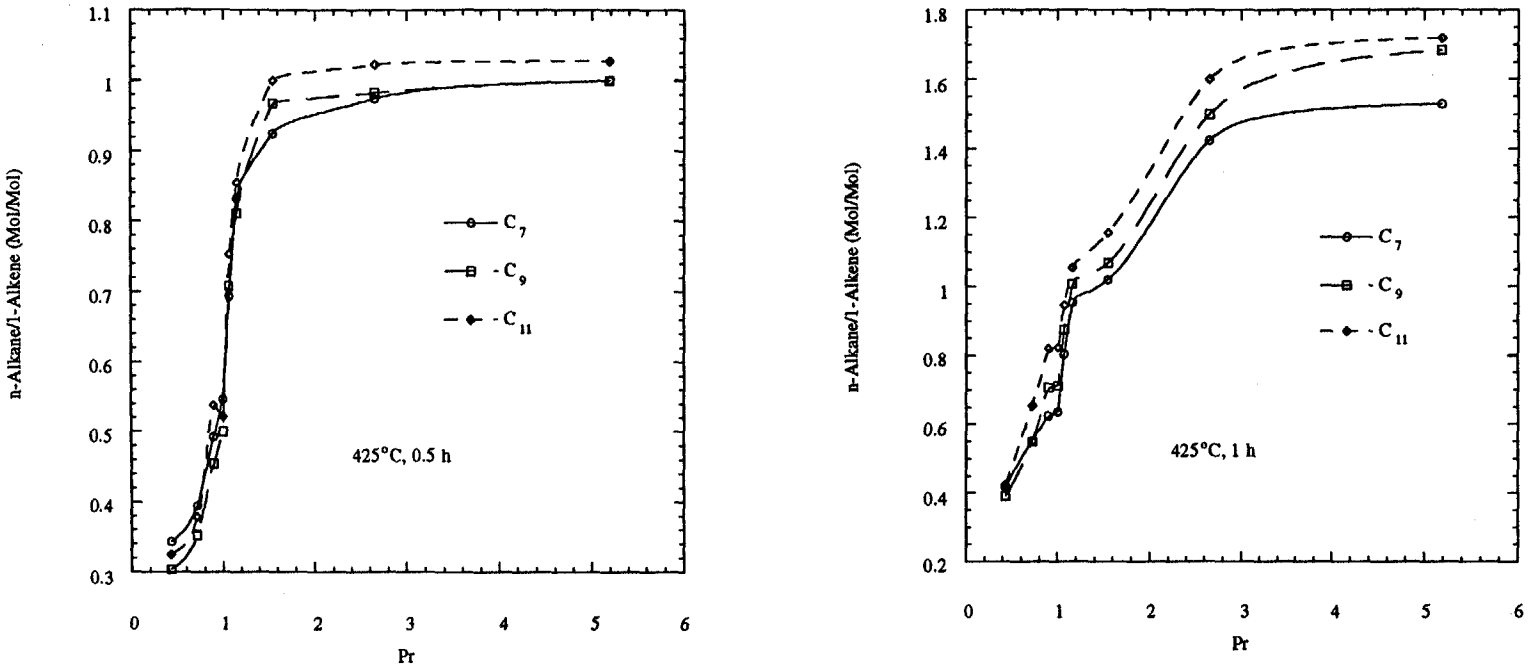

Figure 24. Effects of Initial Reduced Pressure (P_r) on n-Alkane/1-Alkene Ratio (for C_7, C_9, and C_{11}) from n-C_{14} Pyrolysis at 425°C for 0.5 and 1 h.

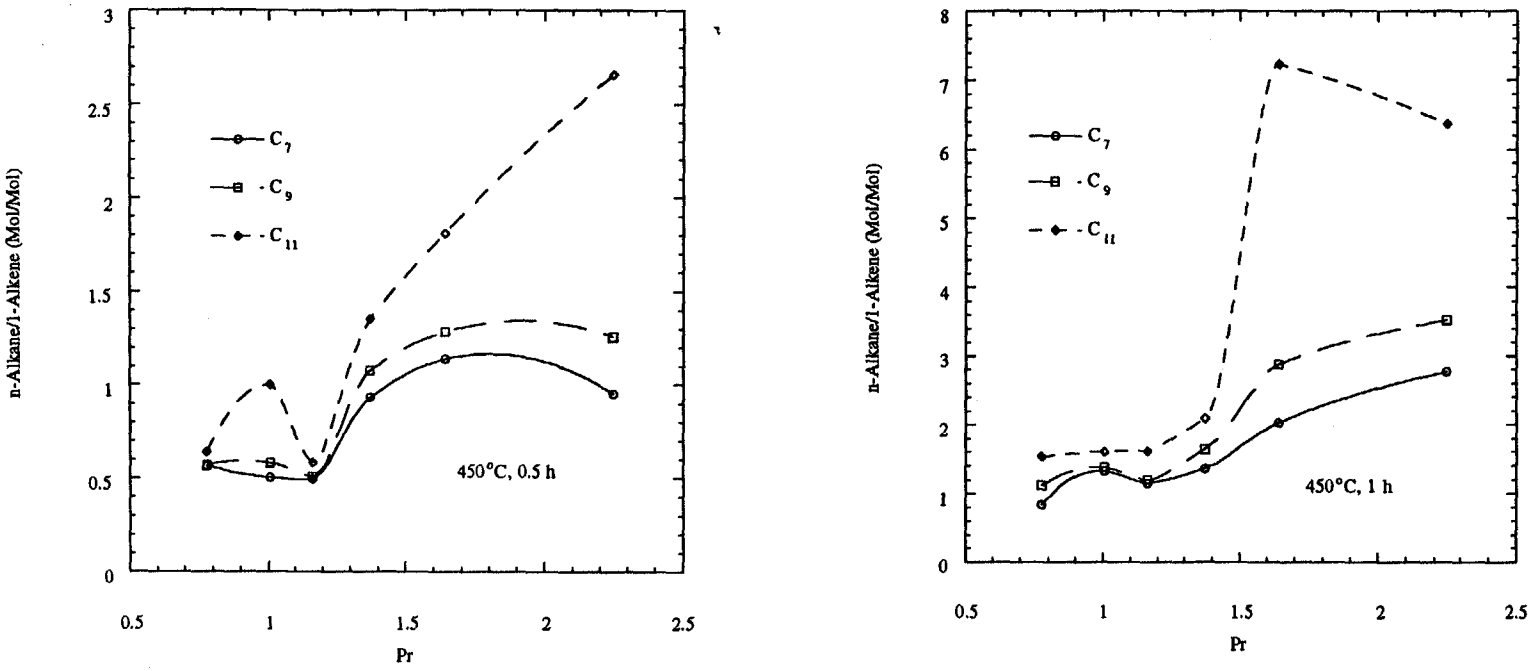

Figure 25. Effects of Initial Reduced Pressure (P_r) on n-Alkane/1-Alkene Ratio (for C_7, C_9, and C_{11}) from n-C_{14} Pyrolysis at 450°C for 0.5 and 1 h.

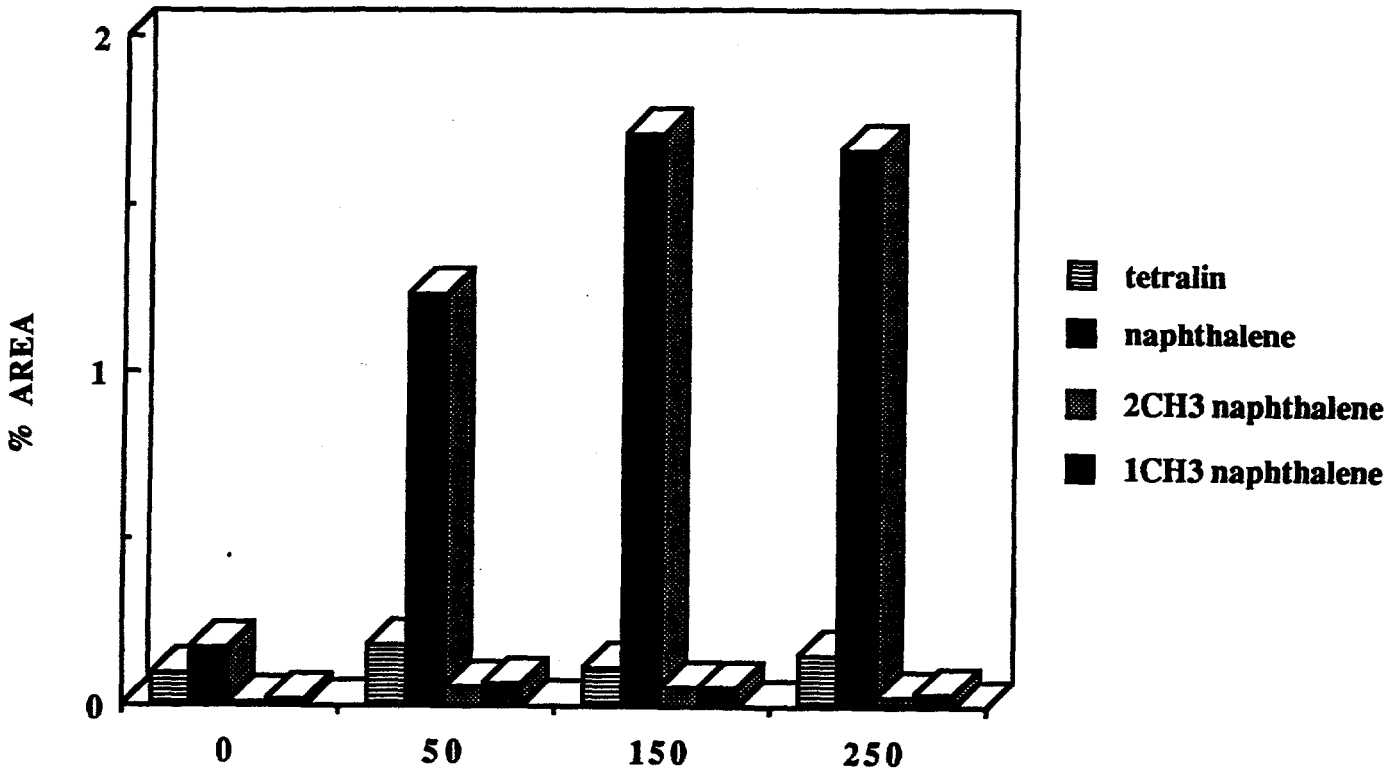

Figure 26. Effect of PX-21 on the naphthalene and tetralin concentration in the liquids obtained from thermal stressing of n octance with decalin.

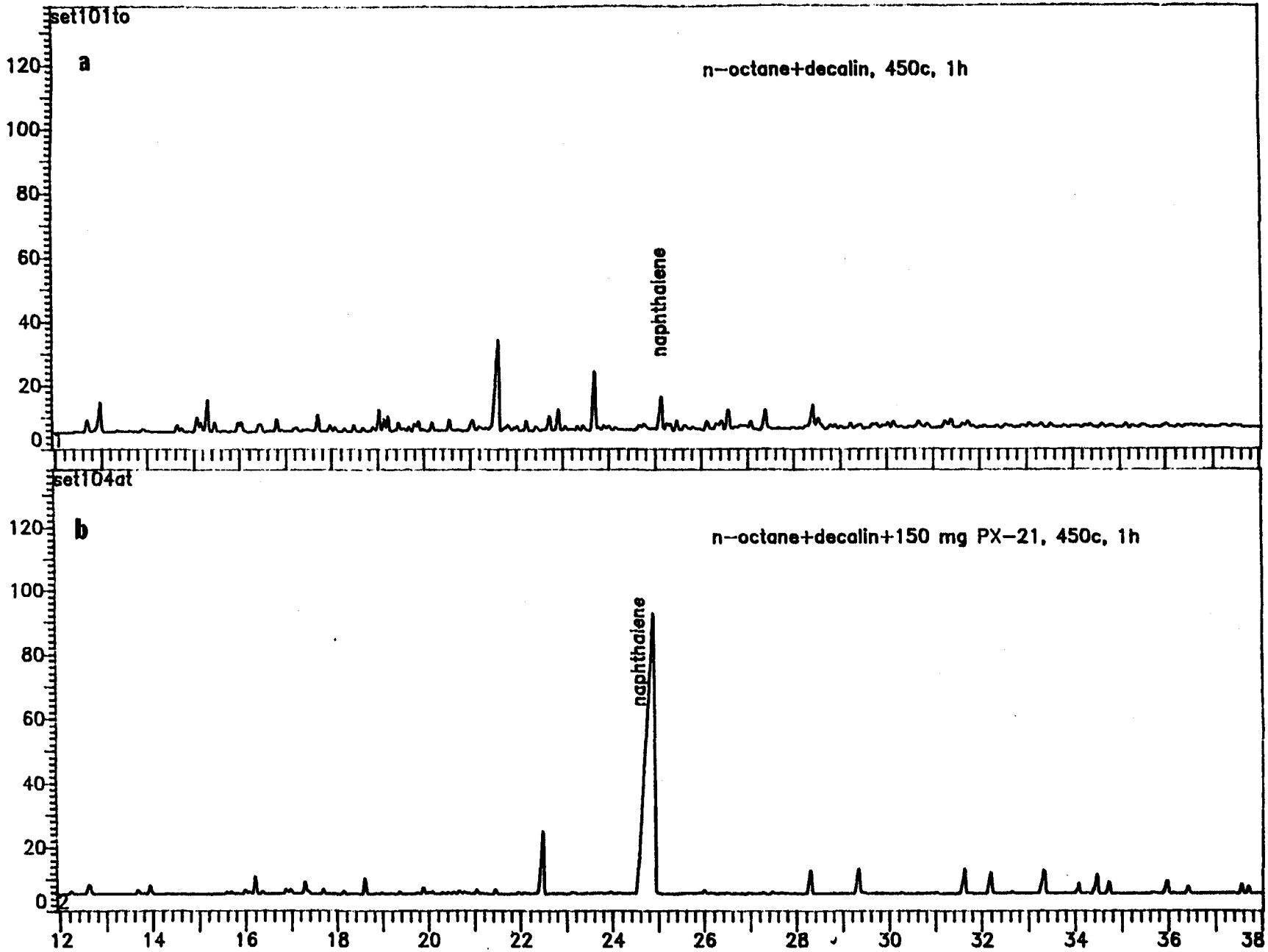

Figure 27. 1Gas chromatograms of toluene+THF fraction of (a) n-octane+decalin and (b) n-octane+declain+150 mg PX-21.

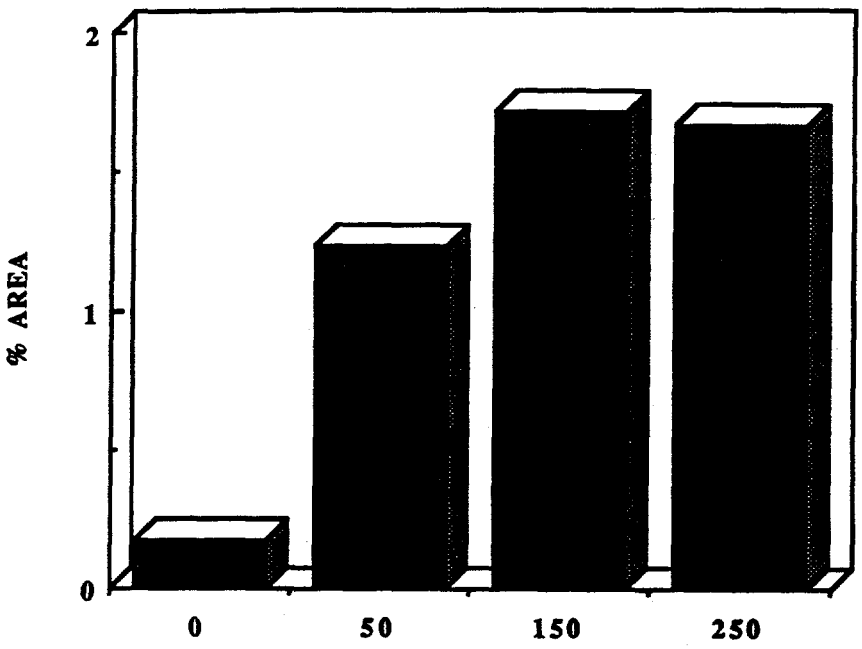

Figure 28. Effect of different amount PX-21 on the naphthalene concentration in the liquids obtained from thermal stressing of n-octane with decalin.

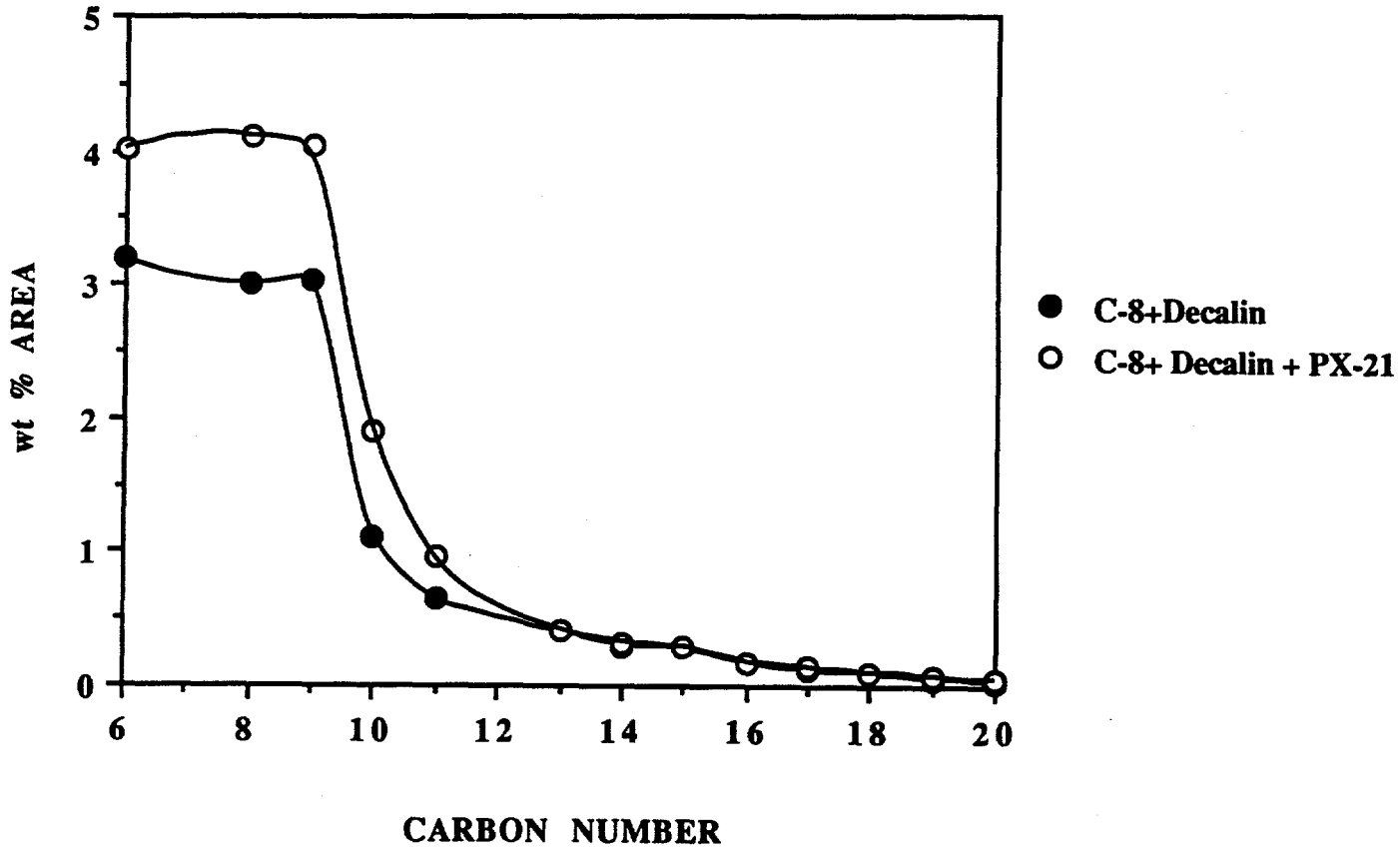

Figure 29. Effects of PX-21 addition on the n alkane distribution of the liquids obtained after stressing of dodecane+tetralin-d_{18}.

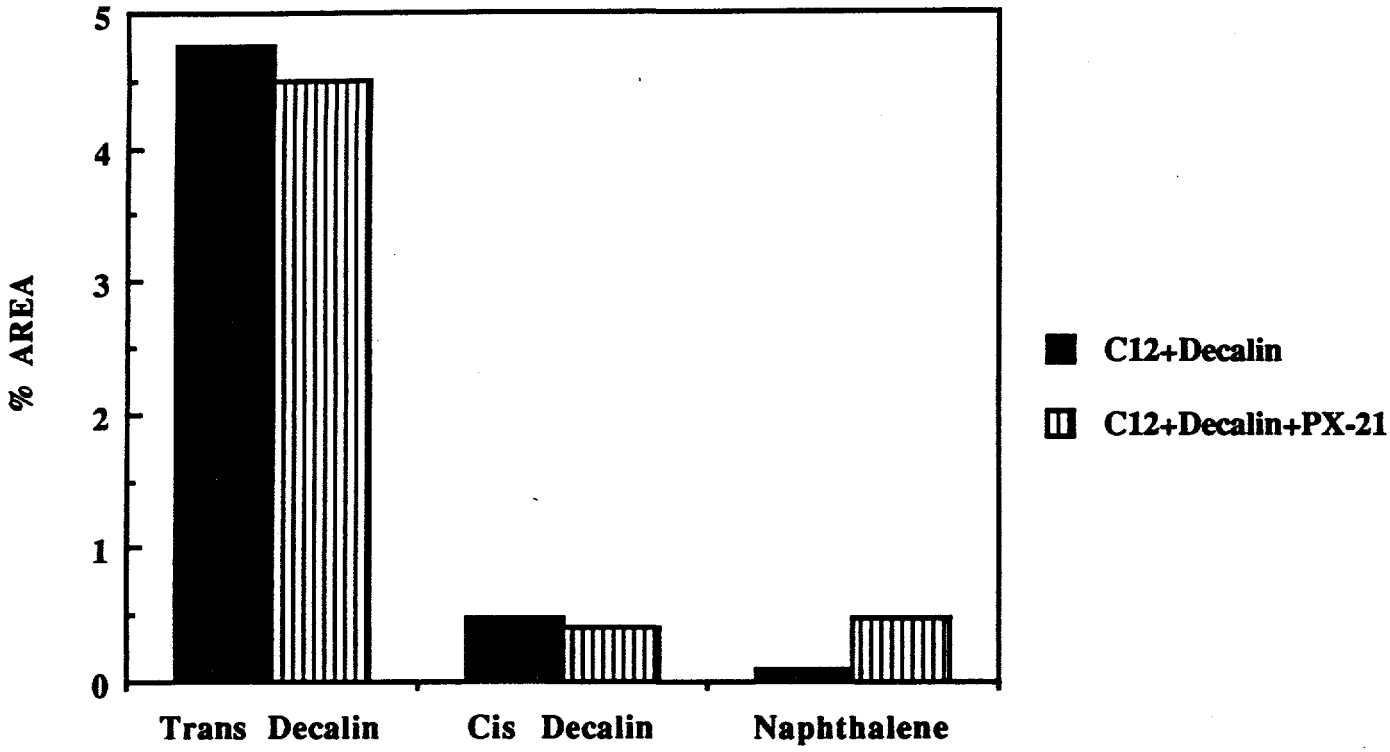

Figure 30. Effects of PX-21 on the naphthalene and decalin concentration of the liquids obtained after stressing of dodecane+decalin d_{18}.

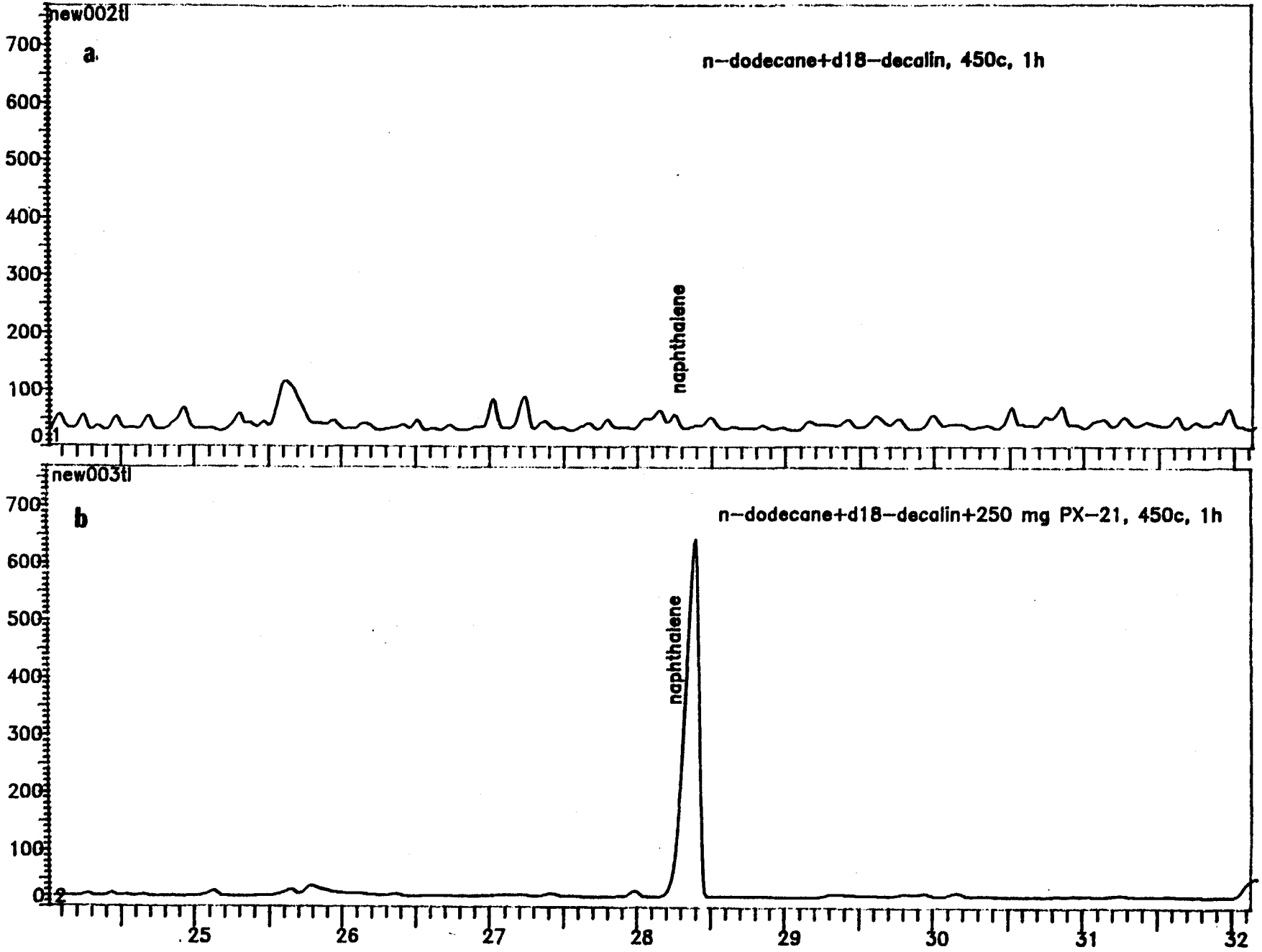

Figure 31. Gas chromotograms of toluene+THF fraction of (a) dodecane+decalin d_{18} and (b) dedecane+decalin d_{18}+250 mb PX-21.

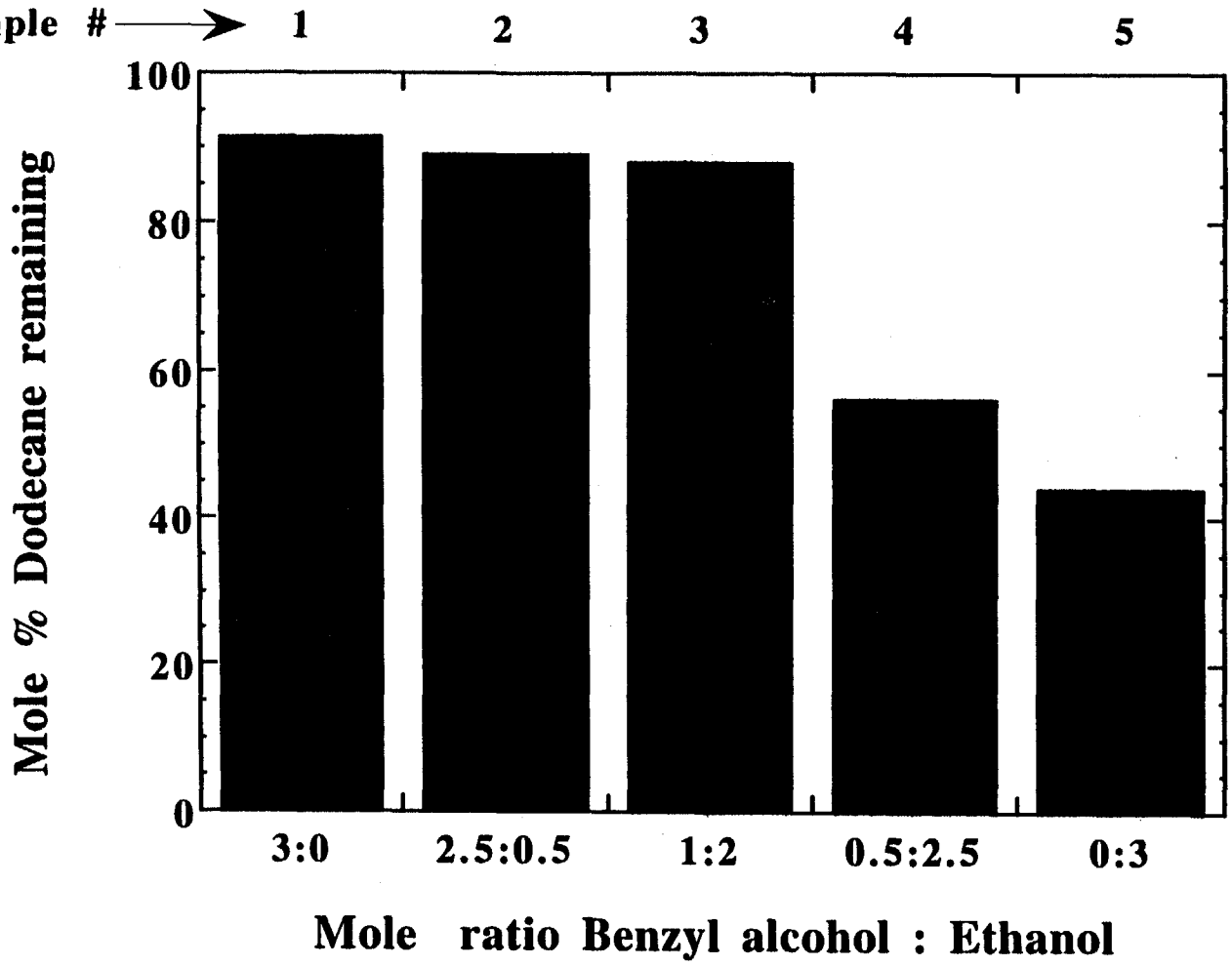

Figure 32. The amount of dodecane remaining as determined by GC analyses samples of dodecane stressed with stabilizer mixtures after thermal stressing at 425°C under 100 psi air for 6h .

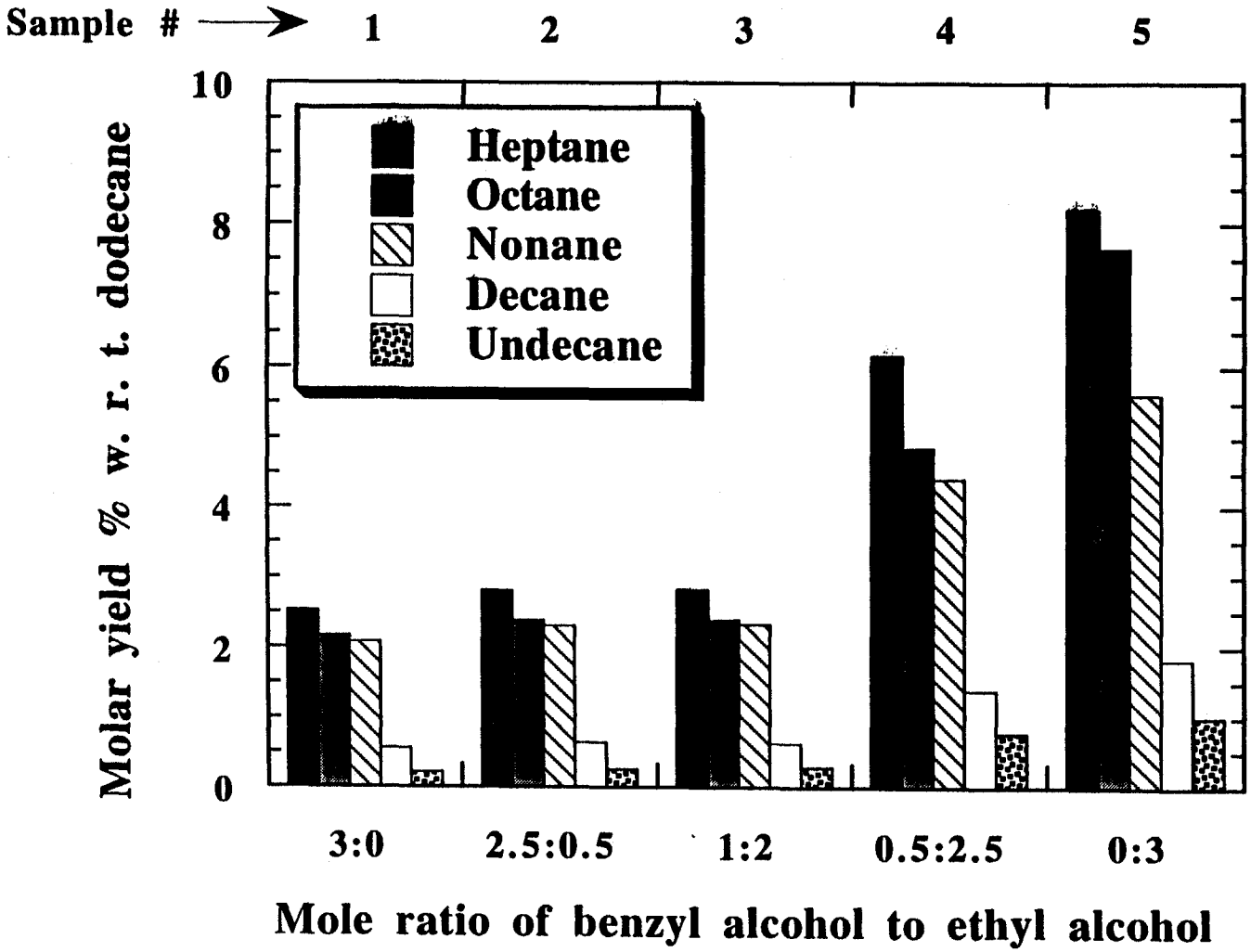

Figure 33. The amount of C7 to C11 alkanes remaining as determined by GC analyses samples of dodecane stressed with stabilizer mixtures after thermal stressing at 425°C under 100 psi air for 6h .

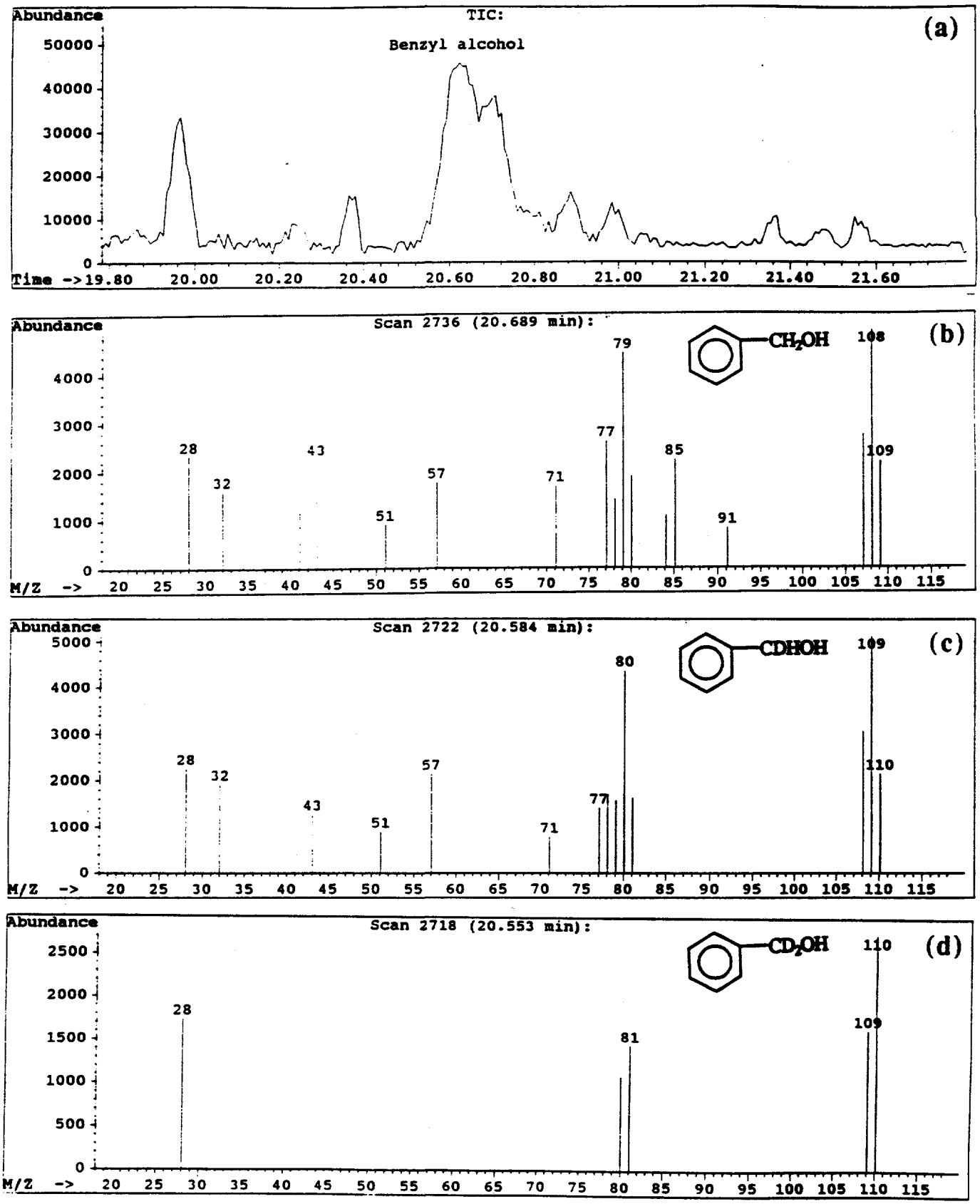

Figure 34. GC/MS analysis of dodecane stressed with benzyl alcohol and deuterated ethanol for 3h at 425°C under 100 psi air. (a) Total ion chromatogram showing benzyl alcohol peak, (b) Fragmentation of $C_6H_5CH_2OH$, (c) Fragmentation of C_6H_5CDHOH and (d) Fragmentation of $C_6H_5CD_2OH$.

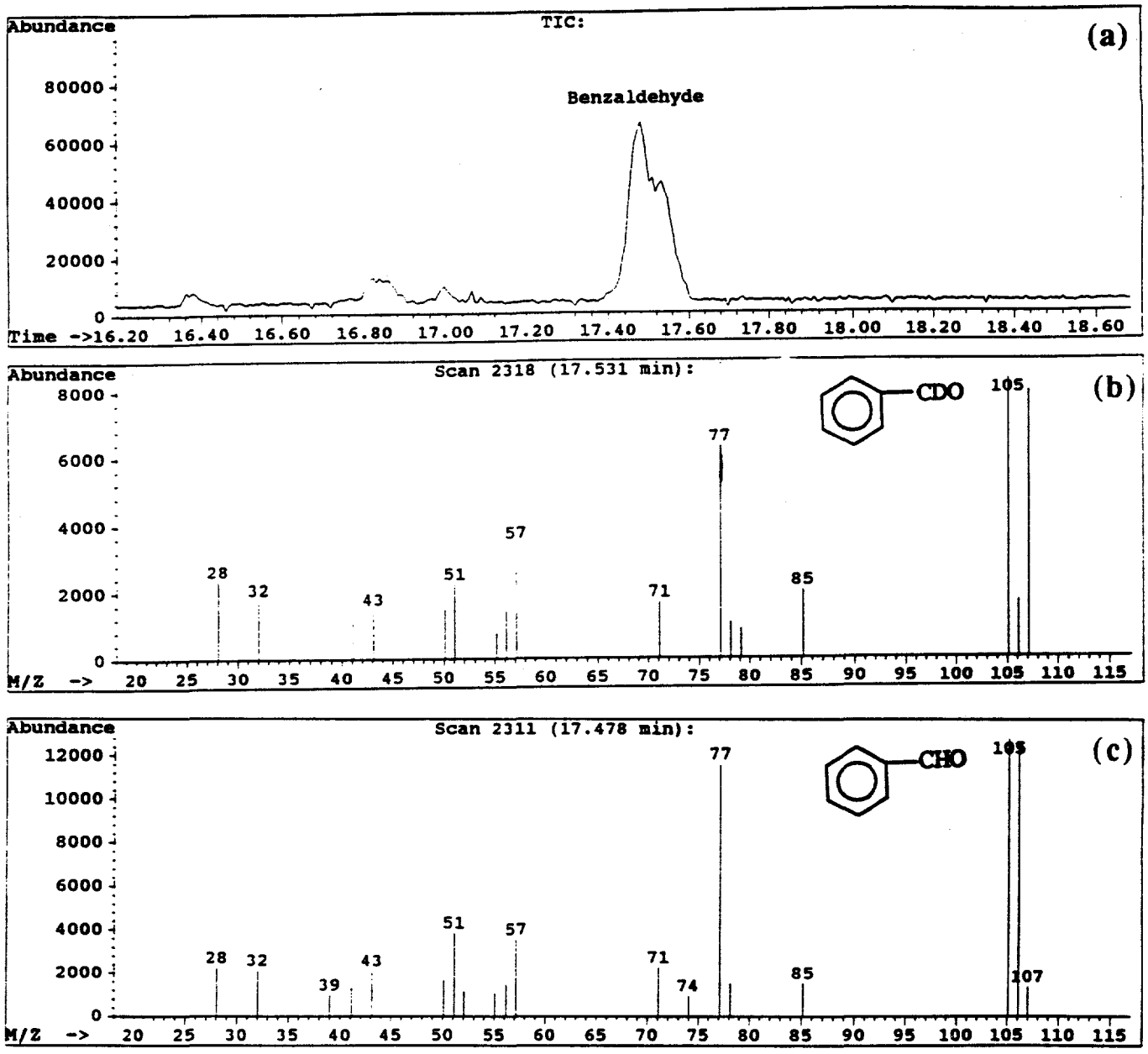

Figure 35. GC/MS analysis of dodecane stressed with benzyl alcohol and deuterated ethanol for 3h at 425°C under 100 psi air. (a) Total ion chromatogram showing benzaldehydepeak, (b) Fragmentation of C_6H_5CDO, and (c) Fragmentation of C_6H_5CHO.

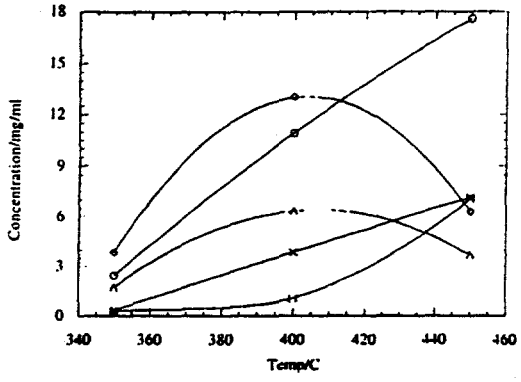

Figure 36. Rosin product distribution vs temperature.

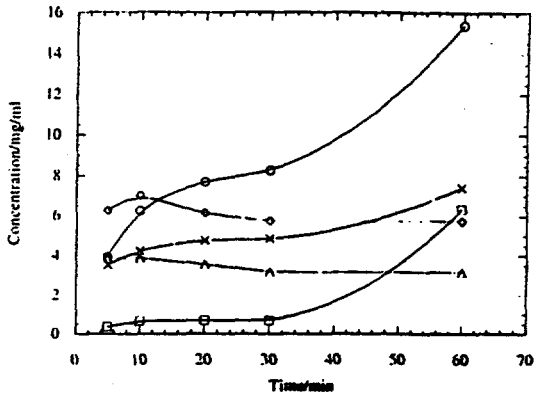

Figure 37. Rosin product distribution vs time - 450°C (no catalyst).

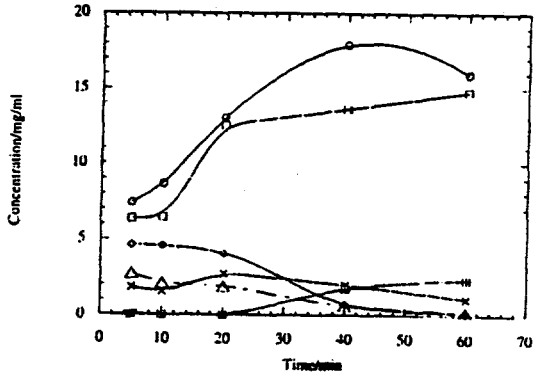

Figure 38. Rosin product distribution vs time - 450°C ($NiMo/Al_2O_3$).

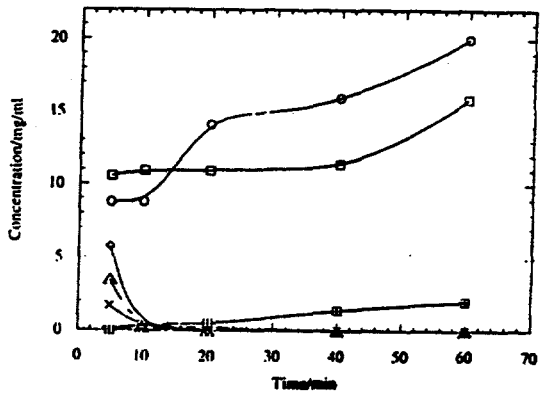

Figure 39. Rosin product distribution vs time - 450°C (Ni-Y zeolite).

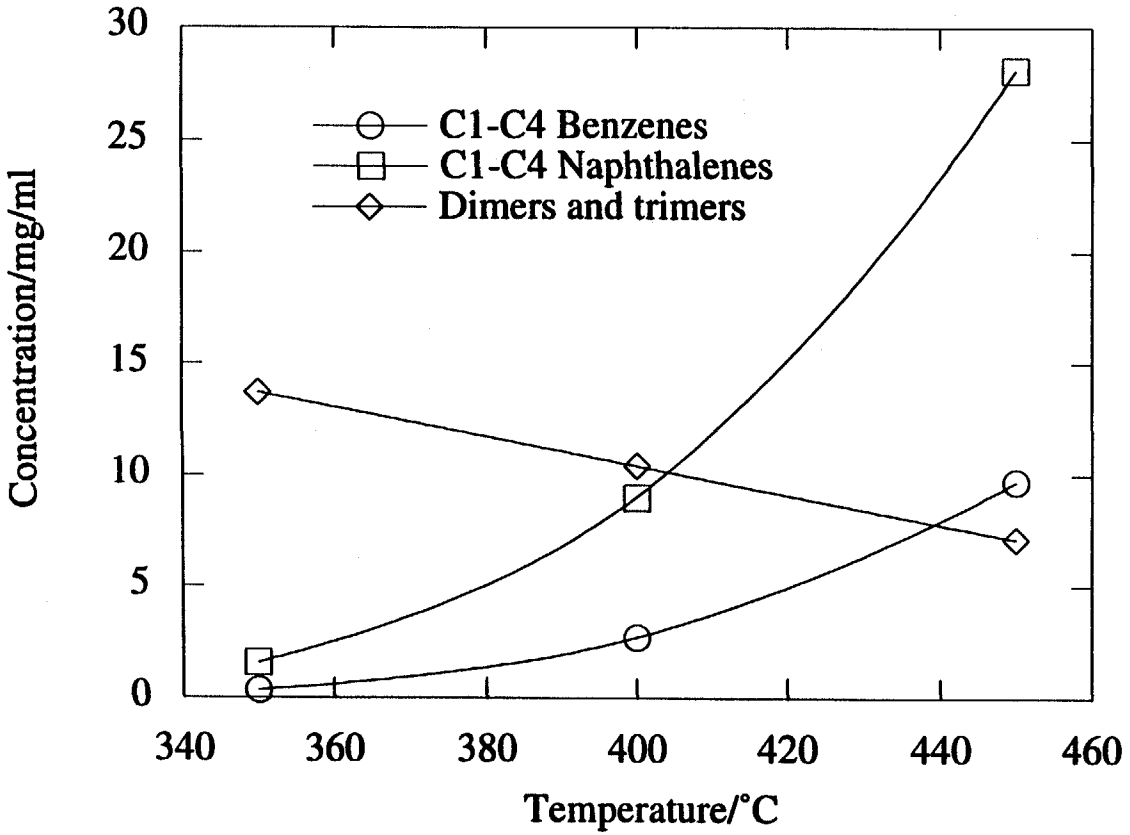

Figure 40. Product distribution of dammar hydrogenation at various temperatuers.

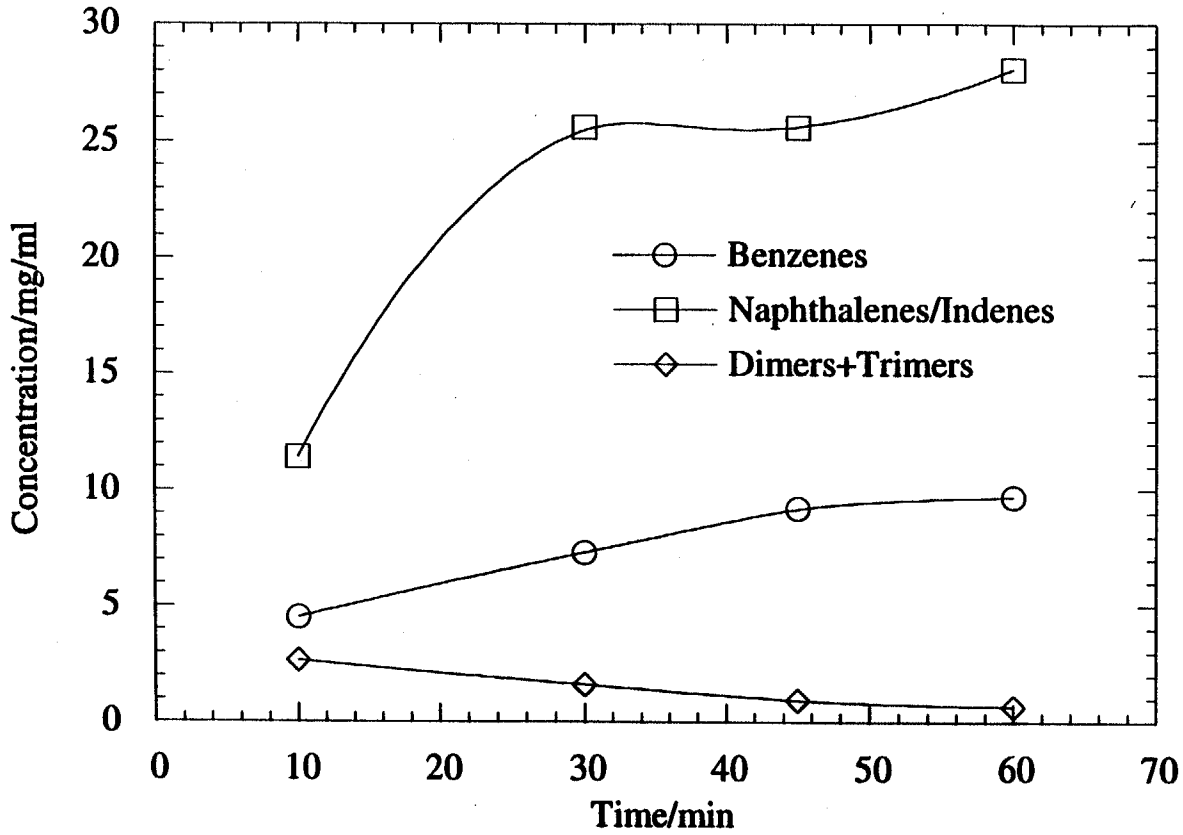

Figure 41. Product distribution vs time - dammar 450°C.

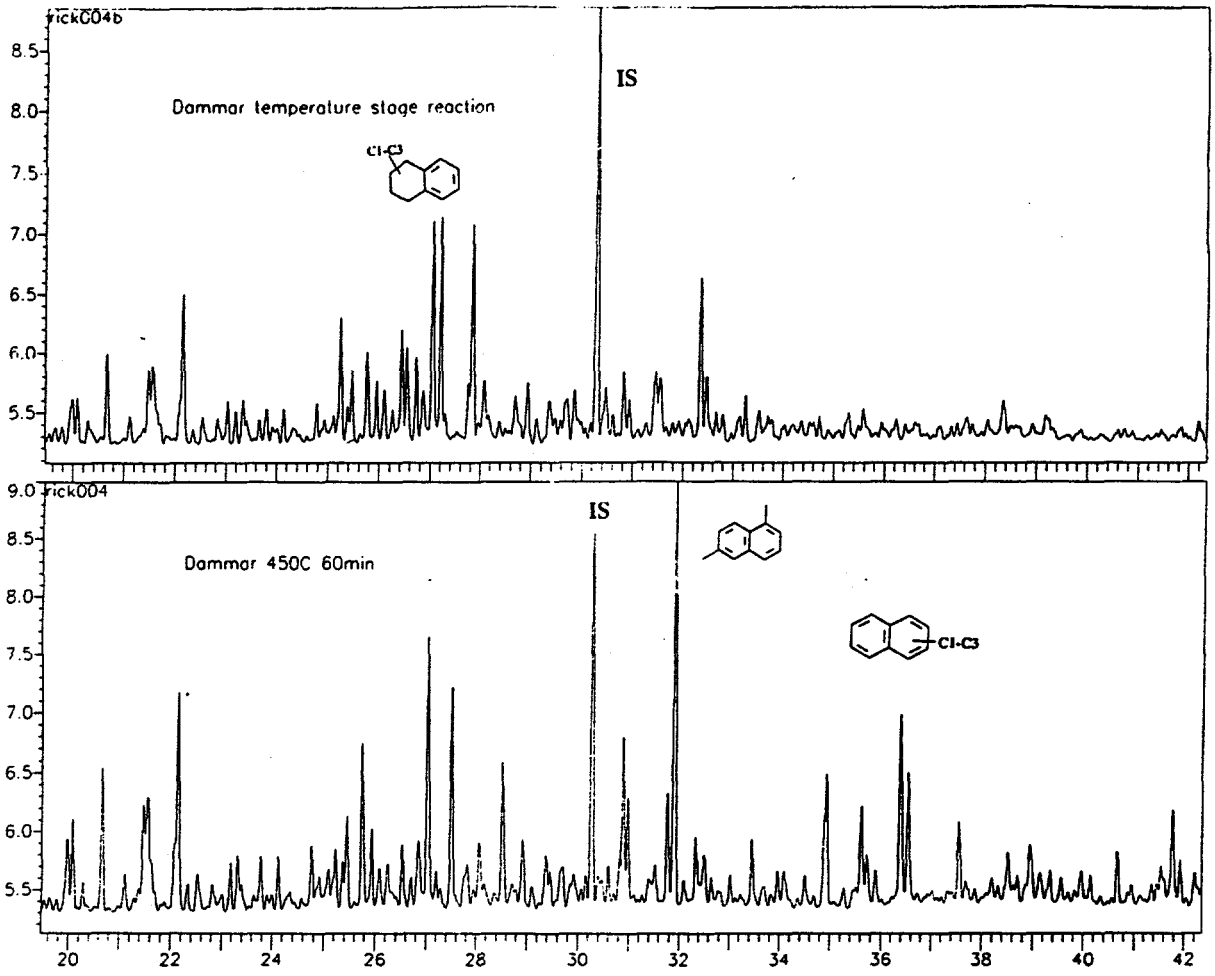

Figure 42. Bicyclic products of reverse temperature stage hydrogenation of drammar.